Remediation of Multicomponent Dense Nonaqueous Phase Liquids in Porous Media

Pamela Schultz Birak

A dissertation submitted to the faculty of the University of North Carolina at Chapel Hill in partial fulfillment of the requirements for the degree of Doctor of Philosophy in the Department of Environmental Sciences and Engineering.

Chapel Hill
2011

Approved by
Dr. Cass T. Miller
Dr. William G. Gray
Dr. Sorin Mitran
Dr. Alberto Scotti
Dr. Jason Surratt

ABSTRACT

PAMELA SCHULTZ BIRAK: Remediation of Multicomponent Dense Nonaqueous Phase Liquids in Porous Media.
(Under the direction of Dr. Cass T. Miller.)

In 2004, the U.S. EPA estimated that as many as 45,000 former manufactured gas plants (FMGPs) required remediation of contaminated soil or groundwater. The primary contaminants at these sites are tars. FMGP tars are complex, dense nonaqueous phase liquids (DNAPLs), containing several thousand compounds including polycyclic aromatic hydrocarbons (PAHs). PAHs are sparingly soluble, but can dissolve from tars into groundwater at concentrations that exceed levels of concern. Tar DNAPLs can also sink below the water table and slowly migrate underground to impact waterbodies directly. Laboratory studies were conducted to investigate in-situ remediation methods that rely on physical and chemical means. Specifically, column studies were used to evaluate cosolvent flushing for removing PAHs from contaminated soil excavated from an FMGP in Salisbury, NC. These experiments were conducted at varying length scales, ranging from 11.9 to 110 cm. PAH effluent concentrations were modeled using a common two-site sorption model. Fitted mass-transfer rates were two to three orders of magnitude lower than predicted values based on published data. Laboratory studies were also conducted to determine how tar density and viscosity vary as a function of composition and temperature. For this work, samples

of tars were obtained from wells at two FMGPs: one in Baltimore, MD and one in Portland, ME. The tar composition varied spatially across both sites. Empirical relationships were developed that can be used in predicting tar recovery during thermal remediation.

To Peanut,
extraordinary friend and companion of 17 years

ACKNOWLEDGMENTS

This achievement would not have been possible without the support of many individuals who have been my mentors, colleagues and friends. I give special thanks to my advisor, Dr. Casey Miller, for his inspired leadership and support. Over the years, he has allowed me to grow as a researcher and as a person. I sincerely thank my committee members for their time, energy and expertise. I have had the honor of making many good friends in the Environmental Sciences and Engineering Program. I am particularly grateful to the students that I have worked with in Dr. Miller's Laboratory. I give special thanks to my collaborators and coauthors: Scott Hauswirth, Arne Newman, Joseph Pedit, and Stephen Richardson. From my years in Chapel Hill, I can say with certainty that "I am a Tar Heel," both in my affection toward the University of North Carolina and the topic of my research. Thanks to my many friends that I have made since living in North Carolina. You have provided me with more support than you know.

My greatest thanks go to my family for their love and support: my father, Stephen; my mother, Patricia; my sister, Rebecca; and my brother, Christopher. In my younger days, I witnessed both of my parents achieving advanced degrees, my father attaining his PhD in Mathematics, and my mother earning a Masters degree in Special Education. They set an example for me of what it means to be a lifetime learner.

TABLE OF CONTENTS

LIST OF TABLES

LIST OF FIGURES

LIST OF ABBREVIATIONS

ACE	Acenaphthene
ACY	Acenaphthylene
ANT	Anthracene
BaA	Benzo[a]anthracene
BaP	Benzo[a]pyrene
BbF	Benzo[b]fluoranthene
BgP	Benzo[ghi]perylene
BkF	Benzo[k]fluoranthene
BEN	Benzene
CHR	Chrysene
DBA	Dibenzo[ah]anthracene
DNAPL	dense nonaqueous phase liquid
ETH	Ethylbenzene
FLN	Fluoranthene
FLR	Fluorene
FMGP	former manufactured gas plant
IFT	interfacial tension
IND	Indeno[123-cd]pyrene
MAH	monocyclic aromatic hydrocarbon
NAP	Naphthalene

PAH polycyclic aromatic hydrocarbon

PCB polycholorinated biphenyl

PCE tetrachloroethylene

PHE Phenanthrene

PYR Pyrene

TCE trichloroethene

TOL Toluene

VPO vapor pressure osmometry

XYL Xylenes

CHAPTER 1

INTRODUCTION

Groundwater is a critical natural resource that is relied upon for drinking water, irrigation, and many industrial uses. In the U.S., an average of 85 billion gallons of groundwater is used daily, amounting to 21% of the total water usage [5]. Of the total groundwater withdrawn, 90% is used for irrigation [6]. Though drinking water usage is small relative to irrigation, groundwater constitutes about one-half the nation's drinking water supply [6]. In certain geographic regions, groundwater is the primary drinking water source [6]. Groundwater also interacts directly with surface water bodies and is an important source of stream flow [5].

In the 1970s, the potential of buried hazardous waste posing a threat to groundwater gained national attention. Before that time, disposal of waste in landfills or via underground injection was an acceptable practice. In the late 1970s, buried waste under a residential community in the Love Canal neighborhood of Niagara Falls, New York received national attention and there was a growing concern across the country about exposure to hazardous materials remaining at old manufacturing sites. In response, the Comprehensive Environmental Response, Compensation, and Liability Act (CERCLA) was enacted by congress. Commonly referred to as Superfund, the program was put into place to provide a means to remediate the most contaminated sites in the country [30].

The first site to receive emergency funding through Superfund was a former gas manufacturing plant (FMGP) in Stroudsburg, PA [94]. The site operated for several decades from 1888 to 1944. During that time, three to eight million gallons of tar were disposed of into the subsurface. In 1980, subsurface tar from this site was found to be leaking into a nearby creek. Groundwater and surface water were both contaminated with chemicals dissolving from the tar. As part of the remedy, the site owner pumped about 9,500 gallons of tar from the subsurface. In addition, contaminated soil was excavated and slurry walls were built underground to limit further contamination to the creek [155].

Though several decades have passed since the discovery of contamination at the Stroudsburg site, considerable work remains to remediate FMGPs around the country. Many of these sites are still owned by gas companies that changed operations from gas manufacture to gas distribution; thus, the urgency to remediate these sites may not exist until tar or dissolved phase contamination is found migrating off-site. The locations of these sites in urban areas can also make them attractive sites for redevelopment, triggering remediation. In 2004, the U.S. EPA estimated that 30,000 to 45,000 sites are in need of remediation. At a particular site, the cost and magnitude can vary considerably. For example, the cost to remediate a single commercial FMGP was estimated to range from $3 to $100 million. The overall cost of cleaning up these sites was estimated from $26 to $128 billion [152].

The overall objective of this work is to conduct research that will lead to more effective and efficient remediation approaches for tars in the subsurface at FMGPs.

The following sections provide an overview of the history of these sites, the type of contamination present at these sites today, and current practices for remediating these sites. Finally, the motivation for various aspects of this study are outlined at the end of this chapter along with specific research objectives.

1.1 The History of Gas Manufacturing

Gas manufacturing was a key industry in the U.S. and Europe for over a century. The gas manufacturing process, or gasification, involved heating a feed stock containing organic compounds in an enclosed chamber. During the process, combustible gases were released and collected, such as methane and hydrogen. In the early 1800s, the first municipal gasification plant was built in the U.S. in Baltimore, MD. Initially, the facility used pine as a feed stock, but eventually switched to coal. Soon after, plants began to open in other cities and towns across the U.S. Initially, these plants primarily provided illumination for streets and homes and later they provided fuel for home heating and cooking. From the opening of the first plant until the demise of the industry in the late 1950s, gas manufacturing plants existed in most cities and towns in the U.S [57, 54, 108].

Tar was a by-product of the gasification process. During gasification, the off-gases were collected and would cool as they traveled away from the heating source. In addition to the lower molecular weight combustible gases, these emissions contained a range of compounds with various molecular weights and boiling points. Some of these compounds would condense as the gas was cooled. This condensate was a black

tarry mixture. The tars were named by referring to the feed stock or manufacturing process used in the gasification process. In addition to coal tar, numerous types of tars were produced such as wood tar, peat tar, shale tar, and even bone tar [2].

The dominant gasification process varied temporally and regionally, given the availability of feed stocks and improvements to the gasification process. The three dominant classes of gas production included: coal gas, oil gas, and carbureted water gas, also known simply as water gas [57, 54, 108]. Oil gas was dominant in the western states where coal was less available. The process of producing water gas was invented in 1873 and it was typically less expensive to generate than coal gas. Not surprisingly, many gas manufacturing plants switched to producing water gas and by the late 1800s this was the dominant process [138].

The tars from each process varied considerably in terms of both composition and properties. All tars contained a complex mixture of organic compounds; however, coal tar and oil-gas tars tended to have a greater percentage of higher molecular weight compounds, compared to water-gas tars. As a result, these tars were denser than water-gas tars. For example, the density of coal tar from coke ovens ranged from 1.13 to 1.24 g/cm^3, while the density of water-gas tar from light oils ranged from 1.02 to 1.15 g/cm^3 [7]. Coal tars also contained acidic compounds, which were generally not present in water-gas and oil-gas tars.

The need for tar disposal varied depending on changes in its market value and the quality of tars produced. During the early years of the coal tar industry, the uses for coal tar were limited to dust suppression on roads and treatment of lumber for

railroad ties. In 1850, the first synthetic dye was discovered by William Perkin in London. This discovery led to a revolution in synthetic chemistry and a vast array of materials were derived from coal tar. After this time, coal tar was a commodity that had a market value, although coal tar disposal still occurred due to excess supplies. Also, the U.S. continued to import coal tar from Europe where the industry was better developed and by-product plants processed raw tars into more useful materials. Similar plants were not built in the U.S. until the early 1900s, when the need was clear for the U.S. to have its own source of these materials for the war effort. Later in the 1900s, petroleum replaced tars as a source material for most synthetic products. The most significant need for tar disposal occurred when water gas became the dominant process since water-gas tars were considered inferior to coal tar [57, 54, 108].

The amount of tars produced also varied as the demand for gas itself varied over-time. In the early 1900s, electricity replaced the need for gas street lamps. The industry responded by inventing and installing gas appliances for cooking and heating. The final blow to the gas manufacturing industry came in the middle of the twentieth century when the distribution of natural gas became widespread. In a short period of time, gas plants were shut down as the industry shifted its mission from gas manufacturing to gas distribution after the construction of natural gas pipelines across the county [54, 108].

1.2 Contamination at FMGPs

The operation and dismantling of FMGPs occurred prior to our modern system of environmental legislation, and the vast majority of sites are believed to have contaminated soils and groundwater. Although the focus of this work is on tars, other types of waste are also often present at FMGPs including: lampblack, ammonia, and cyanide [60]. During facility operation, tars and other wastes could contaminate the environment due to leaking pipes, land filling of excess materials, or disposal into waterways. In particular, the limited market for water-gas tars suggests a strong likelihood that much of the water-gas tar produced was land filled, in many cases, in unlined pits. During the operation of facilities, tars were often stored underground in "tar wells". When facilities closed, these were often left in place with tar remaining in them. Other parts of the facility, such as gas holders, were dismantled on the surface but the underlying structures were covered [60, 54, 108].

Exposure to FMGP tars can occur though both direct and indirect means via contaminated soil, groundwater, and surface water. Direct exposure occurs when tars come into direct contact with human or ecological receptors. Indirect exposure pathways can be important when the contaminants in tars are dissolved in groundwater or surface water, and can be transported from the location of the tar itself, referred to generally as the source zone. For sites where tars are primarily in the vadose zone (e.g., above the water table), rainwater infiltrating through the source zone can dissolve contaminants in tars and subsequently contaminate groundwater, which can then impact surface waters. Tars that migrate below the water table will

continue to sink downward, as they are denser than water and are commonly referred to as dense non-aqueous phase liquids (DNAPLs). Tars can also migrate laterally in the subsurface when contact is made with a confining layer, such as clay. Since many FMGPs are located adjacent to water bodies, migrating tars can also intersect surface water and be a problem for both direct and indirect exposure.

DNAPLs released to the subsurface typically have complex patterns of contamination that are governed by the properties of the fluid phases combined with local geology. When DNAPLs are released to the land, their initial vertical migration through the unsaturated zone, consisting mostly of solid grains and air-filled pore spaces, is governed primarily by gravity and capillary forces [114]. Below the water table, DNAPL migration is a function of gravity, capillary, and viscous forces. The balance of these forces determine the DNAPL morphology and topology along with the rate and extent of migration [114]. As DNAPLs migrate in either the unsaturated or saturated zones, capillary forces can lead to isolated globules of DNAPL trapped in pore spaces between sand grains, referred to as the residual phase.

The properties influencing DNAPL migration and distribution are much different for FMGP tars as compared to other environmentally relevant DNAPLs. The overwhelming majority of research studying DNAPLs in environmental systems has been focused the tetrachloroethylene (PCE) and trichloroethylene (TCE), which are common contaminants at industrial facilities and dry cleaner sites. PCE and TCE have much higher interfacial tension (IFT); thus, systems contaminated with these single-component DNAPLs are more likely to be water-wet, meaning that the DNAPLs exist

as isolated globules in between sand grains. In the case of tars, they contain a complex mixture of compounds including natural surfactants that reduce the IFT. Tars are more likely to coat sand grains, at least partly, resulting in oil-wet systems. Typically, PCE and TCE DNAPL plumes are assumed to be relativity immobile horizontally, and it is the dissolved phase plume that poses the more direct threat to human health and the environment. As demonstrated at the Stroudsburg site, FMGP tars have the potential to migrate vertically and horizontally.

The dissolved phase plume leaving a tar contaminated source zone may contain dozens, if not hundreds of individual compounds. One estimate puts the number of individual compounds in tars at over 10,000 [111]. The compounds that are of most concern in tars are typically the 16 U.S. EPA priority pollutant polycyclic aromatic hydrocarbons (PAHs) [57]. It is important to recognize that the composition of tars changes as they age in the environment, such that the lower molecular weight PAHs are depleted more rapidly than the higher molecular weight compounds. As a result, concentrations in the dissolved phase plume will also vary over time.

1.3 Remediation of FMGPs

Because the size of these sites varies considerably, the remedy for contamination is highly variable. At many sites, excavating contaminated soil is the best and most cost effective option. At larger sites, the extent of subsurface tar contamination can be so great that excavation of the contamination would be nearly impossible. At these sites, remediation of tars in place without excavating the source zone may be the only

choice. This is referred to as in-situ remediation. The extent of contamination, the sinking of tars in the subsurface, and the presence of buildings on top of contaminated areas can all make in-situ methods of remediation the most viable option.

Remediation of many sites containing hazardous materials was initially conducted using an in-situ method referred to as "pump and treat"; however, many years of experience have shown that pump and treat has limited success in completely removing contamination from a source zone. During pump and treat, groundwater is actively pumped through the source zone to remove contamination via dissolution. When pump and treat methods were first used to remediate contaminated subsurface systems, models were used to predict the amount of time required to achieve groundwater standards, such as EPA maximum contaminant levels (MCLs). Over time, it was recognized that these estimates were overly optimistic and significant mass transfer limitations could mean that many decades, if not hundreds of years, could be required to reach groundwater standards at some sites NRC [114].

Modern remediation techniques have sought to actively treat the source of groundwater contamination, often the DNAPL residual. These include methods to increase solubility, mobilize and capture residual, or effectively destroy contaminants [114]. To help minimize solubility limitations, many researchers have used cosolvents and surfactants to enhance the solubility of DNAPLs [90, 141, 71, 67]. Such approaches may reduce the total amount of time required to remediate a particular system; however, mass transfer limitations can still limit the rate of mass removal. Co-solvents and surfactants can also lower the IFT of trapped residual, leading to downward migra-

tion to previously uncontaminated regions of an aquifer [73]. Mobilization approaches take advantage of flushing solutions that reduce the IFT, allowing for migration and subsequent removal [63, 70]. Destructive techniques include chemical means, such as oxidation, and physical means, including thermal methods [143, 98].

Compared to the amount of effort expended to investigate PCE and TCE contaminated systems, much less work has been done to investigate FMGP tars. As discussed, these single component DNAPLs have very different properties when compared to FMGP tars; thus, remediation approaches that have been successful for PCE and TCE contaminated sites may not be successful at remediating tar at FMGP sites.

1.4 Research Objectives

In this work, research has been conducted to improve our understanding of tar composition and properties, as well as, to investigate in-situ remediation methods that use physical or chemicals means to actively remediate source zones. The remainder of this dissertation consists of three chapters that have been written in paper format. A summary and the overall objectives of each paper are described below.

The objective of the first paper was to conduct a critical review of the literature on the composition and properties of FMGP tars that control their distribution and fate, as well as, will influence what remediation technologies will have the most promise. The motivation for this work was driven by the realization that most of the detailed analyses of tar properties such as IFT and contact angle were limited to a small number of tar samples, in particular, tar from the Stroudsburg, PA site. Surveys

of tar composition reveal that the Stroudsburg tar is relatively low in density and viscosity compared to other tars sampled at FMGPs. In addition, tars at FMGPs are often referred to as coal tars yet, historical documents made a clear distinction between tars from different manufacturing processes. A considerable effort was taken for this paper to study published data on tar composition as far back as 1912, to better inform the current understanding of the properties of tars at these sites. This paper was peer reviewed and published in the Journal of Contaminant Hydrology in 2009.

The objective of the second paper was to examine the ability of cosolvent flushing to remediate an aged soil from a FMGP in Salisbury, N.C. Prior to this work, several studies had been conducted to investigate cosolvent flushing of PAH contaminated media; however, this work was limited to using single-solute systems of artificially contaminated sands in 5 cm columns. In this work, a field sample was used and column experiments were conducted at varying lengths from 15 to 100 cm. A version of this paper was submitted to the Journal of Contaminant Hydrology in late 2009. Based on the peer review comments, additional experiments were conducted and a revised version of the manuscript was resubmitted in April 2011.

The objective of the third paper was to develop relationships for predicting the viscosity of FMGP tars as a function of temperature. This work was motivated in part by viscosity data gathered during the writing of the first paper that was only available at 35°C. There was no way to convert these data to a temperature more likely to be encountered in subsurface environments (i.e., 15°C). Such a relationship

is also needed for modeling the removal of tars using thermal treatment, which has become increasingly popular for the remediation of subsurface tars. An additional objective of this paper is to examine the heterogeneity of tars across FMGPs, which is likely to be an issue, given the changes in tar manufacturing over time. For this paper, tar samples were obtained from several wells at two FMGPs: one in Baltimore, MD and one in Portland, ME. This paper has recently been submitted to Environmental Science and Technology.

CHAPTER 2

DENSE NON-AQUEOUS PHASE LIQUIDS AT FORMER MANUFACTURED GAS PLANTS: CHALLENGES TO MODELING AND REMEDIATION[1]

Pamela S. Birak and Cass T. Miller

2.1 Abstract

The remediation of dense non-aqueous phase liquids (DNAPLs) in porous media continues to be one of the most challenging problems facing environmental scientists and engineers. Of all the environmentally relevant DNAPLs, tars in the subsurface at former manufactured gas plants (FMGPs) pose one of the biggest challenges due to their complex chemical composition and tendency to alter wettability. To further our understanding of these complex materials, we consulted historic documentation to evaluate the impact of gas manufacturing on the composition and physicochemical nature of the resulting tars. In the recent literature, most work to date has been focused in a relatively narrow portion of the expected range of tar materials, which has yielded a bias toward samples of relatively low viscosity and density. In this work, we consider the dissolution and movement of tars in the subsurface, models used to predict these phenomena, and approaches used for remediation. We also explore the open issues and detail important gaps in our fundamental understanding of these

[1]Reprinted from *Journal of Contaminant Hydrology*, 105(3–4), 81–98 (2009), with permission from Elsevier.

extraordinarily complex systems that must be resolved to reach a mature level of understanding.

2.2 Introduction

Prior to the widespread use of natural gas, cities and towns throughout the U.S. and Europe relied upon gas manufactured from coal and oil. In the U.S. alone, several thousand manufactured gas plants existed between the early 1800s to the 1950s [153]. During this time, there were numerous documented examples of groundwater contamination, though its persistence and the potential for further migration was not well understood [57]. In the present day, many of these sites are located in the heart of urban areas and are attractive sites for redevelopment. Wastes at FMGPs have led to contaminated soils, groundwater, and sediments, which can hinder redevelopment efforts and may pose a risk to human health and the environment.

One of the primary waste streams from gas production is tar, an opaque viscous liquid that is enriched in high molecular weight compounds. Large volumes of tar were often disposed of in pits or landfilled on-site, after mixing with subsurface materials [108]. Over the many decades since these wastes were generated, tar can migrate from these primary source zones [57]. Because tars are DNAPLs, they tend to migrate downward and have the potential to act as long-term sources of dissolved phase contaminants. The specific contaminants of concern in tars can vary depending on the gas manufacturing process; however, all tars contain polycyclic aromatic hydrocarbons (PAHs) [57]. PAHs are a class of compounds containing several known

carcinogens [153].

Despite the large number of sites and documented cases of groundwater contamination, tars are not as widely studied when compared to other environmentally relevant DNAPLs such as chlorinated solvents. One obvious limitation is access to tar DNAPLs. Whereas chlorinated solvents can be purchased commercially, samples of tar are obtained from former disposal pits or retrieved from groundwater wells. Tars are also difficult to work with in a laboratory setting. They can be highly viscous and contain hundreds of compounds making them physically and analytically challenging.

The physicochemical properties of tars are also very different from single component DNAPLs such as tetrachloroethylene (PCE) and trichloroethene (TCE). The movement and dissolution of these chlorinated solvents is governed largely by their high values of interfacial tension (IFT) and intermediate solubilities. In contrast, tars have a relatively low IFT, but they are prone to alter system wettability [15]. Thus, remediation technologies that have been successful for PCE and TCE contaminated media, may not be applicable to tar contaminated media.

Though much of the recent literature refers to tars from FMGPs as "coal tar," historical documents make distinctions between tars to reflect the underlying manufacturing process (e.g., coal tar, water-gas tar, and oil-gas tar) [137, 138]. These distinctions are important to understand because the manufacturing process can have a significant impact on tar composition [137, 138, 57, 108, 54]. As an example, one of the most studied tars is from a FMGP in Stroudsburg, PA. This was the first site in the U.S. to receive emergency funding through the U.S. Environmental Protection

Agency's Superfund Program [156]. In the literature, tars from this site are referred to as coal tars. In fact, the Stroudsburg FMGP used a process resulting in what is historically referred to as water-gas tars, explaining their low density and viscosity [57].

The overall objective of this work is to identify gaps in our fundamental understanding of tar DNAPLs, limiting our ability to predict tar behavior and to design more effective in-situ remediation approaches. We believe these wastes pose a more difficult remediation challenge when compared to contaminated soils, which, in many cases, can be excavated for ex-situ treatment. Slow moving tar DNAPL plumes can also be the underlying source of sediment contamination. Specific objectives of this work are: (1) to review data on tar chemical composition, (2) to evaluate how composition affects tar behavior, (3) to critique modeling efforts for predicting the impact of tar in the subsurface, and (4) to outline the most pressing open issues. The focus of this work is the peer-reviewed scientific literature, rather than the gray literature, consisting of site-specific technical reports and industry documents. We also specifically focus on the U.S. manufactured gas industry, though major differences between the U.S. and European industries are noted along with differences in tar composition.

2.3 Sources

Manufactured gas plants were used extensively in the early part of the 20th century to produce gas from coal or oil. In 1812, the first commercial gas works was established in London to provide street lighting [136]. The establishment of gas works throughout

cities in Europe and the U.S. soon followed. In the U.S., the first commercial gas works was established in Baltimore in 1816 [27]. By the 1900s, electricity filled most lighting needs while manufactured gas became widely used for home heating and cooking. After World War II, the market for manufactured gas began to decline with the increasing availability of natural gas. By the 1960s, extensive natural gas pipelines were constructed in the U.S.; consequently, manufactured gas became obsolete [27]. Across Europe, similar pressures from natural gas and competing petroleum products led to a significant decline in manufactured gas use after the late 1950s [136].

The three predominant types of gases manufactured for distribution included: coal gas, carburetted water gas, and oil gas [57]. Coal gas is a by-product of carbonization, also referred to as gasification. In this process, bituminous coal is heated in a sealed chamber and the volatiles are collected [127]. The coal is also converted to high carbon coke [127]. Two types of plants used coal carbonization. These include plants that were primarily in the business of making coke and plants that were operated for the purpose of gas production. Though the process was similar at both facilitates, coke plants tended to be larger and sold the coal gas to gas companies for distribution [57].

Carburetted water gas and oil gas both relied on oil for their illuminating power. The production of carburetted water gas took place in two steps. First, either coke or coal, preferably coke, was heated in the presence of steam to produce a stream of hydrogen and carbon monoxide, known as water gas. Next, oil was sprayed into this gaseous mixture, increasing the BTU capacity of the gas and creating carburetted

water gas. In the production of oil gas, oils alone were heated and cracked to produce a mixture of mostly hydrogen and methane, along with other illuminates [138].

The predominant type of gas manufactured varied over time and by region. During most of the 1800s, gas works produced primarily coal gas. Coke production was accomplished using beehive ovens, such that gas was not collected. By the late 1800s, many U.S. gas works switched to producing carburetted water gas because it was cheaper and easier to produce [138]. While in Europe, especially in Germany, the by-product coke oven was rapidly replacing beehive ovens, generating more coal gas and tar. By 1914, 100% of all German beehive ovens were replaced with by-product coke ovens, while in the U.S only 5% were replaced [138]. After the beginning of World War I, the U.S. began to aggressively build by-product coke ovens, increasing U.S. coal gas production [127]. In 1902, the first oil gas plant was established in Oakland, California [138]. Oil gas was important in regions where coal was not easy to come by, especially the Pacific Coast region [54]. By 1926, the percentage of total U.S. gas manufactured from carburetted water gas plants was 58%; from coal gas plants, 35%; and from oil gas plants, 7% [138]. In Europe, carburetted water gas did not achieve the same popularity, and its used was limited primary to enriching coal gas [150].

The specific wastes generated from gas manufacturing varied depending on the type of gas produced; however, tars were one of the primary waste streams from all types of gas manufacturing. In general, tar is an opaque viscous liquid, enriched in high molecular weight compounds. The tars from coal gas manufacturing are referred to as coal tars; from carburetted water gas, as water-gas tars; and from oil gas, as

oil-gas tars. All of these tars contain significant quantities of aromatic compounds [57]. Coal tar is also enriched in phenolic acids, nitrogenous bases, and ammonia [138]. Water-gas and oil-gas tars share similar characteristics. These tars are mostly absent of the acids and bases in coal tars and contain more sulfur [138].

Tars from the same process also varied over time as technologies changed and optimal feedstocks became scarce or too expensive. Details of these changes and the implications on tar composition are provided in Table 2.1 for the U.S. industry. From coal gas manufacturing, tar varied somewhat predictably based on the operating temperature of the process. A lower operating temperature resulted in tars containing relatively more acids and heterocyclic compounds [3]. Higher operating temperatures resulted in tars containing more unsubstituted aromatic compounds [3]. Tars produced from oils were most affected by changes in the feedstock. Over time, manufacturers were forced to switch to lower quality oils based on availability and competition from other petroleum based products, resulting in heavier, lower quality tars [138]. Changes in tar quality and composition were most dramatic in water-gas tars [138]. In Germany and other parts of Europe, large quantities of brown coal were available. This type of coal was generally carbonized by low temperature methods not used in the U.S., producing a relatively low density coal tar with more tar acids and bases [136].

The ultimate fate of these tars was highly dependent upon the market conditions and the quality of the tar. Initially, coal tar use was limited primarily to wood preservation (i.e., creosote) [57]. By the late 1800s, coal tar became an important

Table 2.1: Impact of manufactured gas process on tars produced in the U.S.

Product	Time Period	Process	Tar Properties & Composition
Coal gas (coke plants)	1800s–1918	Bituminous coal was heated in beehive ovens to create coke. Coal gas was not captured.	Negligible tar production.
	1892–1918	Facilities upgraded to by-product coke ovens, allowing the capture of off-gases and operating from 850–900°C.	Primarily unsubstituted aromatic compounds. Contain tar acids, tar bases. Water content 3–7%.
Coal gas (gas plants)	Before 1850	Bituminous coal was heated in cast iron horizontal retorts from 600–800°C.	Similar to coal tar from carbonization. Lower temperatures resulted in more heterocyclics and tar acids.
	After 1850	Facilities switched to clay retorts allowing temperatures >900°C.	Higher temperatures resulted in more aromatics and less acids.
	After 1910	Facilities switched to vertical retorts. Operating temperatures lower than horizontal retorts.	More heterocylics. Tar acids 5-10%.
Carburetted water gas	Before 1910	Coke or anthracite coal was heated in the presence of steam. Oil was sprayed into emissions to crack the oil. Oil was predominantly paraffinic.	Primarily aromatics. Absent of tar acids and bases. Water content 50–90% but easily separated.
	After 1910	Most facilities switched to heavier, asphaltic oils mostly from Texas.	Higher density. 68% of these facilites reported problems separating emulsions.
	1910–1930	Many facilities switched to bituminous coal.	Higher density. 100% of these facilites reported problems separating emulsions. Composition more closely resembled coal tar.
	After 1940	Many facilities forced to use heavy fuel oil fractions.	Higher density and continued difficulty separating emulsions.
Oil gas	Before 1919	Oils were heated to crack hydrocarbons into smaller molecules. Mostly used in the West. Used raw crude.	Primarily aromatics. Almost no tar acids and bases. Some problems with emulsions.
	After 1919	Facilities forced to use heavier residual oil.	Increased emulsions. More difficult to break.

Sources: Adam [3], Harkins et al. [57], Hatheway [60], Murphy et al. [108], and Hamper [54].

commodity, used in the synthesis of an incredible array of materials, including: dyes, perfumes, explosives, pharmaceuticals, and many more [138]. Since water-gas and oil-gas tars typically did not contain large amounts of anthracene, their usefulness was more limited [57]. Light water-gas tars were used mostly for fuel and road construction. Heavy water-gas and oil-gas tars were more difficult to use in these applications due to variable chemical compositions and higher viscosities [138]. Tars that were not sold to refiners were either landfilled or disposed of in open pits [108].

One of the most significant hurdles to using tars was the presence of difficult to break tar-water emulsions. Refiners would only purchase tars with <3% water [54]. For coal tar, this was typically not a significant issue as it contained very low amounts of water that could easily be removed. As described in Table 2.1, carburetted water gas and oil gas producers had considerable problems with emulsions, especially after switching to heavier, lower quality oils [54, 108]. These emulsions were intractable, and attempts to dewater them were expensive. There were also many years after World War II when the demand for tar was low, leaving large volumes unused [108].

Estimates for the number of specific U.S. FMGP sites vary widely from 1,500 to 50,000 and are a function of the type of facilities considered [57, 152]. The first survey conducted by EPA identified approximately 1,500 sites, which mostly included facilities that were members of gas associations [40, 108]. Higher estimates are obtained by considering the wide variety of facilities that used coal or coal tar. [59, 152]. Regardless of the exact number of sites, a large amount of tar was produced from gas manufacturing. Eng [40] estimated 11.5 billion gallons of tar were produced in the

U.S. from 1820 to 1950.

Given the materials and waste handling in use while these sites were in operation, U.S. EPA [152] concluded that releases of tar and other wastes to the environment occurred at over 90% of sites. Many sites operated for over 50 years before tar was widely utilized for other products. Waste tars and tar emulsions were often mixed with subsurface materials and landfilled [108] or disposed of in large pits [57]. Even when tars were recycled for other uses, they were typically stored in underground enclosures made of either wood, masonry, or concrete, known as tar wells [57, 108]. Over time, even a small percentage of tar leaking from a tar well could result in many thousands of gallons released to the subsurface. Upon decommissioning, wastes in tanks and holding pits were often left in place and covered with fill [108].

2.4 Composition

Tars are a complex mixture of a large number of mostly organic aromatic compounds. During the late 1800s and early 1900s, a considerable amount of work was done to isolate and identify the components of tars, especially coal tars. This interest was driven by a desire to find compounds of economic value, along with an optimism that any compound could be found in tar [158]. According to Weiss and Downs [158], the authoritative work by George Lunge, entitled *Coal Tar and Ammonia*, details some 200 substances isolated from coal tar [92]. Rhodes [136] published a list of 348 compounds in coal tar.

Early efforts to quantify individual constituents in tar demonstrated that most

were not present at appreciable concentrations. Weiss and Downs [158] conducted a large-scale distillation of 10,000 gallons of coal tar. As was generally accepted, this work confirmed that naphthalene was the most abundant compound, an aromatic hydrocarbon consisting of two fused benzene rings. Despite their efforts, only one compound was identified that was not previously recognized for its abundance in tar, phenanthrene. In Table 2.2, their results are presented along with some limited data for water-gas tars. Historically, less effort was expended to determine the composition of water-gas and oil-gas tars; however, they are expected to contain a similar list of compounds as coal tars, absent the tar acids and bases [57].

Most of the early characterization of tars used tests to infer the chemical composition, rather than quantification of individual compounds. Based on its commercial value and abundance in tar, the only compound typically quantified was naphthalene. Other common analyses included: distillation tests, used to determine the percentage of mass in certain boiling point ranges; solubility tests, used to determine the percent mass that is either soluble or insoluble in a particular solvent; and chemical reactivity tests, used to determine the concentration of various chemical classes, such as tar acids and bases [1]. In Table 2.3, data on the characterization of U.S. tars are presented using some of the typical analyses conducted in the early to mid 1900s.

As discussed in §2.3, the composition of tars is a function of the gas manufacturing process from which they were produced. The data in Table 2.3 further illustrates the differences between various coal, water-gas, and oil-gas tars. For example, the percentage of naphthalene is greater in the coal tars produced at the greatest tem-

peratures, namely horizontal retort and coke oven coal tar. Based on the distillation data, these tars are composed mostly of compounds with boiling points above 355°C. This fraction is the solid residue remaining after distillation and is commonly referred to as pitch [101]. The water-gas and oil-gas tars are almost completely absent of tar acids. In comparison, low-temperature tars produced in Germany contained from 20–50% tar acids [2]. There is also an interesting similarity between the tars. The sulfonation residue, which is a measure of saturated hydrocarbons [1], indicates that $> 90\%$ of the mass in all the tars is of an aromatic nature. This is also true of low

Table 2.2: Historic percent composition data for manufactured gas tars

Fraction	Component	Coal tar[a]	Water-gas tar
Light oil (0–170°C)	Crude benzene and toluene	0.3	1.2[b]
	Coumarone, indene, etc.	0.6	2.6[c]
	Xylenes, cumenes, and isomers	1.1	1.2[b]
	Total light oil	2.0	
Middle and heavy oils (170–270°C)	Naphthalene	10.9	8.0[b]
	Unidentified oils in range of naphthalene and methylnaphthalenes	1.7	
	α-Monomethylnaphthalene	1.0	
	β-Monomethylnaphthalene	1.5	
	Dimethylnaphthalenes	3.4	
	Acenaphthene	1.4	
	Unidentified oil in range of acenaphthene	1.0	
	Fluorene	1.6	
	Unidentified oil in range of fluorene	1.2	
	Total middle and heavy oils	23.7	
Anthracene oil (270–350°C)	Phenanthrene	4.0	
	Anthracene	1.1	0.29[b]
	Carbozole and kindred nonbasic nitrogen-containing bodies	2.3	
	Unidentified oils in anthracene range	5.4	
	Total anthracene oil	12.8	
Other	Phenol	0.7	
	Phenol homologs (largely cresols and xylenols)	1.5	
	Tar bases (mostly pyridine, picolines, lutidines, quinolines, and acridine)	2.3	
	Yellow solids and pitch oils	0.6	
	Pitch greases	6.4	
	Resinous bodies	5.3	
	Pitch (238°C melting point)	44.7	

Temperature ranges from Porter [127]; pg 323.

[a] Weiss and Downs [158]

[b] Downs and Dean [34]

[c] Brown and Howard [24]

Table 2.3: Typical analyses of U.S. tars in the early to mid 1900s

Analyses	Coal tars			Water-gas tars		Oil-gas tar
	HR	*CO*	*VR*	*LG*	*HG*	*FG*
Naphthalene, % by vol.[a]	5.31	7.45	0.55	–	7.8	11.4
Tar acids, % by vol.[b]	2.6	3.6	10.5	0.0	0.0	0.5
Sulfonation residue, % by vol.[b]	0.5	0.1	2.1	3.3	2.1	0.5
Distillation, % by wt.[b]						
up to 170°C	0.0	0.3	1.8	2.0	0.2	0.8
up to 235°C	6.0	9.9	14.6	17.7	11.6	4.0
up to 270°C	13.8	17.4	25.2	34.2	29.0	12.7
up to 300°C	20.0	25.0	32.0	45.0	37.8	21.6
up to 335°C	23.1	32.1	40.3	62.8	48.8	29.0
up to 355°C	27.4	38.0	50.0	69.3	57.3	35.8
Residue	72.6	62.0	50.0	30.7	42.7	64.2

HR=horizontal retort; *CO*=coke oven; *VR*=vertical retort; *LG*=light gas oil; *HG*=heavy gas oil; *FG*=fuel gas oil

[a] Rhodes [136] for coal tars, Rhodes [138] for water-gas and oil-gas tars

[b] Phelan and Rhodes [126]

temperature tar [2].

Using modern analytical techniques, we are still limited in our ability to fully characterize tars, in which the total number of compounds has been estimated as high as 10,000 [111]. This is especially true of the pitch fraction, which can account for as much as 70% of tar mass (See Table 2.3). The routine state of the science of gas chromatographic analyses of PAHs typically quantifies compounds with boiling points up to approximately 500°C and as many as six aromatic rings [128]. Recently, more sophisticated methods have indicated the presence of compounds with as many as 210 rings in the pitch fraction [104]. One significant limitation in analyzing these complex compounds is the lack of reference standards [44].

Despite limitations, modern analytical techniques allow for considerably more detailed analysis compared to the era of gas manufacturing. Given that the coal carbonization industry continues today, the recent literature includes analyses of fresh coal tars. Some of this work continues the search for identifying chemical constituents in tars [165, 166]. A fresh coke oven coal tar has also been used to study the fate

of tar constituents in groundwater [37]. Newly produced high temperature coal tars are likely to be similar in composition to those produced at U.S. FMGPs, which were virtually all high temperature tars [136]. Even in the early 1900s, it was well documented that the composition of high temperature tar was mostly independent of the original coal [127]. A relatively recent analysis of eight U.S. high temperature coal tars confirmed this observation [113]. Conversely, the composition of tars produced at low temperatures is highly influenced by the composition of the original coal [136].

Regardless of the improvement in analytical methods, there are few analyses of FMGP tars reported in the recent literature. Most site investigations of FMGPs are driven primarily by the desire to determine the extent of contamination, and tar samples are not typically analyzed [52]. The most detailed survey of tar samples was conducted by the Electric Power Research Institute (EPRI) and included tars from eight FMGP sites [41]. A more recent survey analyzed 11 tars from 10 FMGP sites [22]; however, this data is somewhat less useful for evaluating the impact of aging because the gas manufacturing history of the sites and the nature of the sample location is not provided (e.g., near ground surface versus well samples).

Several other tar samples have been recovered from U.S. FMGPs in order to study phenomena that influence the fate of tars in the subsurface, such as mass transfer and wettability. A number of researchers have studied two samples of flowing tars obtained from wells at FMGPs in Stroudsburg, PA and Baltimore, MD [118, 93, 132, 133, 134, 48, 110, 130, 15]. An additional well sample was obtained from an unspecified mid-Altantic FMGP [97]. Samples have also been studied that were

obtained from holding tanks at FMGPs in Connecticut, Pennsylvania, and New York [130, 168, 169, 170, 65]. Only the three tars obtained from wells were analyzed for chemical constituents [118, 48, 97].

In Table 2.4, compositional data from fresh coal tars is compared to tars recovered from FMGPs. The samples from the EPRI survey include liquid samples from free flowing tar plumes and holding tanks. Though the focus of this review is on the behavior and fate of tar DNAPLs in the saturated zone, data for solid tar samples collected from at or near ground surface are provided in Table 2.5, to give some perspective on tar aging. Though in some cases other compounds were quantified, the tables were limited to include U.S. EPA priority pollutant monocyclic aromatic hydrocarbons (MAHs) and PAHs. Two branched naphthalenes were also included, which are not on U.S. EPA's list of 16 priority pollutant PAHs but are often quantified due to their relatively high concentrations. Heterocyclic compounds and metals were limited to those detected at the highest concentrations.

The type of tar is also provided in Tables 2.4 and 2.5, which is based on historic manufacturing data. For sites in the EPRI survey with more than one type of manufacturing, the primary method is provided. As noted in §2.2 the tar from Stroudsburg is a water-gas tar, despite often being referred to as coal tar. The tar from Baltimore is also referred to in the literature as a coal tar [15]; however, data compiled by Eng [40] indicates that this site produced primarily water-gas from 1890–1950.

Table 2.4: Composition of unweathered and weathered tar DNAPLs

Type	Constituent	Fresh tars		FMGP tars						
				Well samples					Holding tanks	
				Site 1[e]	Site 4[e]	Site 5[e]	Str., PA[c]	Balt, MD[d]	Site 7[e]	Site 9[e]
		Coal[a]	Coal[b]	Water	Water	Coal	Water	Water	Coal	Coal
Total as % wt.	Quantified MAHs	–	.34	0.97	0.38	2.5	1.2	0.73	0.37	0.36
	PP MAHs	–	0.21	0.45	0.036	1.5	0.14	0.44	0.25	0.17
	Quantified PAHs	54	38	25	18	33	46	28	2.5	6.2
	PP PAHs	46	37	24	18	32	17	28	2.4	6.0
PP MAH	Benzene	–	950	550	4	4 970	500	1 000	790	450
mg/kg	Toluene	–	1 074	2 120	53	7 000	940	–	1 310	1 060
	Ethylbenzene	–	44	1 860	300	2 700	–	3 400	400	170
PP PAH	Naphthalene	148 000	140 900	70 000	52 000	135 000	21 600	100 000	6 540	21 400
mg/kg	2-Methylnaphthalene	13 700	16 100	33 400	37 400	34 100	37 500	53 000	2 080	5 770
	1-Methylnaphthalene	6 310	6 900	23 500	21 500	19 600	38 000	–	1 170	3 320
	Acenaphthylene	37 800	19 900	610	12 100	17 800	6 800	3 700	1 180	530
	Acenaphthene	1 100	3 100	11 900	900	1 650	15 200	13 000	270	500
	Fluorene	20 800	16 900	11 600	6 870	1 150	14 000	1 800	1 080	2 100
	Phenanthrene	65 300	55 100	32 600	17 000	34 600	21 200	1 600	3 130	7 000
	Anthracene	15 400	13 500	8 570	5 420	7 670	5 900	20 000	980	1 080
	Fluoranthene	47 000	29 500	13 400	4 760	12 600	3 000	5 500	1 900	4 150
	Pyrene	34 500	21 300	13 200	6 890	17 900	5 000	3 200	1 000	3 080
	Benzo[a]anthracene	14 100	10 800	4 900	2 340	5 130	3 100	10 000	610	1 470
	Chrysene	9 520	7 600	5 100	2 340	6 470	2 700	3 600	620	1 880
	Benzo[b]fluoranthene	9 500	11 700	2 150	1 350	3 130	–	4 000	490	1 150
	Benzo[k]fluoranthene	5 920	–	2 950	610	2 850	–	1 600	360	850
	Benzo[a]pyrene	13 400	7 400	3 900	1 560	6 420	–	3 600	500	1 330
	Indeno[123-cd]pyrene	7 980	4 000	2 610	1 080	4 890	–	–	790	1 720
	Dibenzo[ah]anthracene	996	700	490	140	640	–	400	180	350
	Benzo[ghi]perylene	7 260	2 700	3 110	1 270	7 090	–	–	960	2 290
Heterocyclic	Quinoline	–	–	2.7	0.9	5.2	–	–	3.3	560
mg/kg	Acridine	–	–	4.7	25	14	–	–	42	33
	Carbazole	–	–	1100	200	160	–	–	140	620
	Dibenzothiophene	–	–	–	2 020	3 230	–	–	1 600	ND
Inorganic	Arsenic	–	–	20	9.3	23	–	–	3.0	3.6
mg/kg	Chromium	–	–	1.1	<1	1.8	–	–	36	2.4
	Lead	–	–	1.0	6.5	1.4	–	–	8.1	37
	Cyanide, Method 4500	–	–	<1	<1	2.3	–	–	5.4	360
Misc.	% Ash	–	–	0.02	0.01	0.2	Low	–	20	4.0
	% Moisture	–	–	0.03	0.10	1.7	Low	–	15	28

PP=priority pollutant plus two branched naphthalenes. Coal = coal tar; Water=water-gas tar; ND = not detected.
[a] NIST [112]; [b] Eberhardt and Grathwohl [37]; [c] EPRI [41]; [d] Peters and Luthy [118]; [e] Ghoshal et al. [48]

Table 2.5: Composition of solid tars recovered from at or near the ground surface at FMGPs

Type	Constituent	Site 2[a]	Site 3[a]	Site 6[a]
		Coal	Coal	Coal
Total as % wt.	Quantified MAHs	0.35	0.028	<0.01
	PP MAHs	0.20	0.006	<0.01
	Quantified PAHs	4.8	2.4	5.2
	PP PAHs	4.6	2.3	5.0
PP MAH	Benzene	460	14	11
mg/kg	Toluene	1 050	9	<1
	Ethylbenzene	450	37	<1
PP PAH	Naphthalene	13 300	4 030	970
mg/kg	2-Methylnaphthalene	7 450	3 080	700
	1-Methylnaphthalene	4 900	2 350	640
	Acenaphthylene	260	300	890
	Acenaphthene	340	1 150	460
	Fluorene	1 350	1 110	1 420
	Phenanthrene	5 210	3 470	11 300
	Anthracene	390	690	2 980
	Fluoranthene	1 500	1 360	8 520
	Pyrene	2 410	2 070	6 170
	Benzo[a]anthracene	750	450	1 920
	Chrysene	1 050	750	2 360
	Benzo[b]fluoranthene	1 240	270	1 540
	Benzo[k]fluoranthene	1 050	130	830
	Benzo[a]pyrene	1 820	390	1 410
	Indeno[123-cd]pyrene	1 400	690	3 500
	Dibenzo[ah]anthracene	ND	250	450
	Benzo[ghi]perylene	1 640	940	4 150
Heterocyclic	Quinoline	3.5	0.9	30
mg/kg	Acridine	4.7	1	71
	Carbazole	49	20	580
	Dibenzothiophene	620	580	ND
Inorganic	Arsenic	6.4	7.8	4.7
	Chromium	11	28	36
	Lead	50	44	930
	Cyanide, Method 4500	2.6	5.7	69
Misc.	% Ash	9.6	54	49
	% Moisture	5.6	7.4	5.2

PP=priority pollutant plus two branched naphthalenes. Coal = coal tar; ND = not detected

[a] EPRI [41]

2.4.1 Organic Compounds

In general, the concentrations reported in the fresh coal tar samples are similar to those reported in the historic literature. Specifically, the concentrations of the priority pollutant MAHs and PAHs reported in the fresh samples are all within two times the values reported in the historical data in Table 2.2. Assuming that lower MAH or PAH concentrations are indicative of tar weathering, the well samples appear to be the least weathered, while the samples taken at the ground surface are generally the most weathered. Though coal tars produced in vertical retorts would have lower concentrations of aromatic compounds regardless of weathering, they would also have a relatively low viscosity. Since the holding tank samples are viscous liquids and the surface samples are all solids, we can rule out these samples originating from vertical retorts.

Weathering of tar samples is also expected to change relative the composition of tar samples, as lower molecular weight compounds are lost first to either dissolution or volatilization and higher molecular weight compounds would actually increase in concentration. Interestingly, in all but two of the samples, naphthalene remains the most dominant compound. In the Stroudsburg sample, the branched naphthalenes are the most dominant and the distribution of the remaining compounds is similar to the other well samples. In one sample taken from the ground surface, not only is phenanthrene the most dominant compound, but other high molecular weight compounds are also seemingly enriched, such as benzo(a)pyrene. In the tar samples analyzed by Brown et al. [22], naphthalene has the highest concentration in every

sample.

Also shown in Tables 2.4 and 2.5 are several heterocyclic compounds. Heterocyclic compounds consist of ring structures in which a carbon atom has been substituted with nitrogen, sulfur or oxygen. Historically, these compounds were considered major components of low temperature coal tars, like those produced in Germany. Thus, it is somewhat surprising that these compounds are detected in U.S. coal tars and water-gas tars, albeit at concentrations one to two orders of magnitude lower than naphthalene. Compared to MAHs and PAHs, these compounds are more difficult to determine analytically [69], but, according to some authors, are a concern in groundwater at FMGPs due to their high water solubility and toxicity [117, 164]. Unlike the MAHs and PAHs, the heterocyclic compounds do not appear to have any trends in concentration related to the degree of weathering.

2.4.2 Inorganic Compounds

Tars also contain a number of inorganic compounds. A number of trace metals, along with cyanide, were measured as part of the EPRI survey [41]. Samples were digested into acid prior to trace metal analysis using inductively coupled plasma emission spectroscopy. This is necessary in order to determine the metal concentration; however, these data do not reveal any information about the possible form of the metal (e.g., elemental vs. metal–organic complexes). The three metals with the highest concentrations are shown in Tables 2.4 and 2.5 . There appears to be a slight decrease in arsenic in the holding tank and surface samples, while chromium and lead

have much higher concentrations. Assuming that the holding tank and the surface samples are relatively more weathered, these data suggest that arsenic is present in a water-soluble form, while chromium and lead are present in relatively insoluble forms. Cyanide concentrations were also highest in the holding tank and surface samples.

From historical data, all tars generally contained some amount of water, which was removed mostly by gravity separation [57]. In water-gas tars, the amount of water could be as high as 90% [57]. Coal tars were most easily dehydrated, resulting in 0–5% remaining water [57]. As noted in Table 2.1, intractable emulsions were common in water-gas and oil-gas tars when heavier oils were used in gas manufacturing. Thus, it is not surprising that both Brown et al. [23] and the EPRI survey reported that several samples of tar contained high concentrations of water. In Brown et al. [23], the water contents of three tars were less than 1%, while the remaining eight tars contained from 22−55% water. One study suspected the water content was a sampling artifact [41], while the other speculated it was the result of tar aging [23]. Given the significant problems the gas industry experienced with tar-water emulsions, combined with the lack of market value for these materials, these samples could also be emulsions.

2.4.3 Saturates, Aromatics, Resins, and Asphaltenes

Characterization of tars using solubility tests has been practiced since the early days of gas manufacturing. As early as 1837, the solubility in light petroleum naphtha was used to separate asphaltenes, the insoluble fraction, from malthenes, the soluble fraction [2]. Historic data for coal tars indicate that the asphaltene content is

highest in higher temperature tars. Specifically, the percentage of asphaltenes in coal tar produced in vertical retorts ranged from 20-40%; in coke ovens, 25-40%; and in horizontal retorts, 60-80% [2].

SARA analysis is a more modern technique, related to the petroleum naphtha solubility test, which is used to separate mixtures into four general classes, including: saturates, aromatics, resins, and asphaltenes [74]. Asphaltenes have more recently been defined as the fraction insoluble in either n-pentane or n-heptane [55], a definition which continues to be used today [74]. The remaining fractions are separated using column chromatography based on increasing polarity, resins being the most polar. The exact composition of resins and asphaltenes is not known, but it is a topic of considerable research in the petroleum literature. These high molecular weight compounds are believed to play an important role in changing wettability, which affects petroleum recovery. [147, 26, 161, 35].

In Table 2.6, the composition of crude oil is compared to that of several FMGP tars. The asphaltene content of three FMGP tars was over twice as much as an average heavy crude oil. These high asphaltene contents are consistent with the historic data; however, given that accurate and reproducible determination of asphaltenes depends on the quality of the solvent [42], comparing these results to data from several decades ago must be done with caution. Even in the recent literature, the methods used to isolate these fractions often vary. For example, Haeseler et al. [53] isolated saturates, aromatics, and resins by extracting with cyclopentane, possibly biasing their results.

Table 2.6: SARA analysis for crude oils compared to FMGP tars

Fraction	Percent composition								
	Crude oils[a]			FMGP tars					
				Well samples		Holding tanks			
	light	med.	heavy	Str. PA[b]	Balt. MD[c]	PA[d]	NY[d]	US[e]	US[e]
Saturates	53	37	31	8	–	–	–	0.1	0.0
Aromatics	37	44	36	41	98.4	–	–	22.6	27.0
Resins	9	16	22	15	0.4	–	–	3.3	7.2
Asphaltenes	0.8	3	7	34	1.1	20.9	36.4	–	–

[a] Mean values calculated from Hemmingsen et al. [61]

[b] Peters and Luthy [118]

[c] Barranco and Dawson [15]

[d] Zheng and Powers [169]

[e] Haeseler et al. [53]

2.5 Physicochemical Properties

The physicochemical properties of complex mixtures are a function of their chemical composition. Historical tests of tar properties include specific gravity and the viscosity [1]. More current analyses also typically include the average molecular weight ($\overline{Mw}$), which is required for estimating equilibrium concentrations using Raoult's law (See §2.6.1). In order to determine the distribution and movement of NAPLs in porous medium systems, it is also critical to have an understanding of interfacial phenomena, which are a function of IFT, wettability, and the capillary pressure history of the system.

2.5.1 Specific Gravity and Viscosity

In Table 2.7, historic specific gravity and viscosity data are provided for several tar samples from each major category of gas manufacturing in the U.S. In the early 1900s the standard temperature for determining specific gravity was 15.5°C [157]. As noted

in Table 2.7, data at 25°C were converted to the standard temperature using the method of Weiss [157], resulting in <1% increase in the specific gravity. Viscosity of tars is considerably more sensitive to temperature changes [151, 23]. Besides the influence of temperature, comparing tar viscosity reported in the early 1900s is further complicated by methods that often used arbitrary units of measure [151]. During the mid 1900s, numerous consistency relationships were developed to allow for the comparison between various methods [151]. A set of relationships, developed based on coal tars, was used to estimate the dynamic viscosity at 35°C in Table 2.7 [126]. Due to the complexity of tar, no methods are available to convert tar viscosities to values corresponding to typical subsurface temperatures (e.g., 10°C).

Table 2.7: Historic specific gravity and viscosity data for manufactured gas tars

Tar	Type	Specific gravity	Kinematic viscosity	Engler viscosity	Float test seconds		Softening point	Dynamic viscosity
		15.5/15.5°C	35°C cSt	40°C	50°C	32°C	°C	35°C cP
Coal	VR[a]	1.103	237					$2.6 \cdot 10^2$
	CO[a]	1.180	316					$3.7 \cdot 10^2$
	CO[b]	1.196		163	26[e]			$2.0 \cdot 10^3$
	CO[b]	1.198				38		$1.4 \cdot 10^3$
	CO[a]	1.226	2 850					$3.5 \cdot 10^3$
	HR[b]	1.240			24			$1.6 \cdot 10^3$
	HR[a]	1.249	14 090					$1.8 \cdot 10^4$
Water-gas	L[b]	1.061		1.7				$9.1 \cdot 10^0$
	L[b]	1.089		2.0				$1.5 \cdot 10^1$
	L[b]	1.125		11.8				$1.8 \cdot 10^2$
	H[b]	1.212				74		$5.0 \cdot 10^3$
	FO[b,d]	1.227				123		$2.1 \cdot 10^4$
Oil-gas	MT[c]	1.206		13.2				$2.0 \cdot 10^2$
	FO[b,d]	1.256				100		$1.2 \cdot 10^4$
	HT[c]	1.297				247		$7.6 \cdot 10^4$
	FO[c]	1.317					32.6	$5.0 \cdot 10^5$
	HT[c]	1.334					33.8	$6.6 \cdot 10^5$

Viscosity related data were converted to Dynamic viscosity using a linear interpolation of data in Phelan and Rhodes [126] Table 15-13. VR=vertical retort; CO=coke oven; HR=horizontal retort; L=light; H=heavy; FO=fuel oil; MT=medium temperature; HT=high temperature

[a] Rhodes [136]

[b] Rhodes [138]

[c] Pacific Coast Gas Association (1926) cited in Harkins et al. [57]

[d] Density converted from 25/25°C to 15/15°C based on Weiss [157]

[e] Used to estimate dynamic viscosity

These data further illustrate variations in tar properties with changes in the gas manufacturing process. Overall, the specific gravity varies from 1.061 to 1.334. There is considerable overlap among each major category of tar; however, the specific gravity is generally lowest in the water-gas tars and highest in the oil-gas tars. For coal tars, increases in the specific gravity are positively correlated to the temperature of the specific process. For water-gas tars, there is a significant increase in the specific gravity for tars produced using heavy oils. For oil-gas tars, the data illustrate changes in specific gravity due to both temperature and feedstock changes. As shown in Figure 2.1, viscosity is positively correlated with specific gravity and varies widely from ∼10–1,000,000 cP.

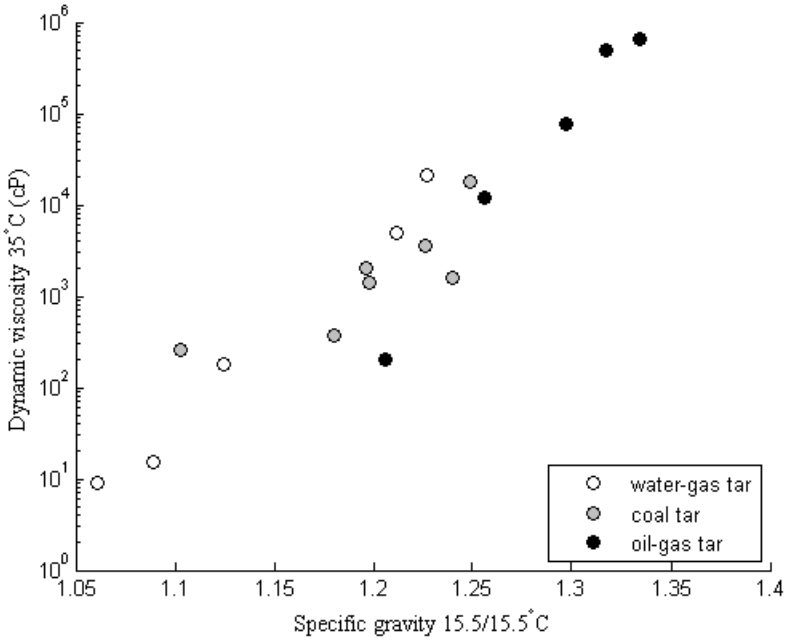

Figure 2.1: Relationship Between Tar Viscosity and Specific Gravity. Data are from Table 2.7.

In Table 2.8, the $\overline{Mw}$, specific gravity, and dynamic viscosity, are provided for several coal tars recovered from FMGPs and one fresh coal tar. In general, the tars with the lowest amount of quantified PAHs have the highest specific gravity and viscosity. Along with the data for $\overline{Mw}$, this trend is consistent with the understanding that the fraction we are unable to quantify is composed of high molecular weight compounds.

Table 2.8: Bulk properties of FMGP tars

Sample	Location	Form	$\overline{Mw}$ (g/mol)	Specific Gravity[a]		Dynamic viscosity[a] (cP)	
Fresh Coal Tar[b]		liquid	248	1.198	(-)	-	
Well samples	Str. Pa[c]	liquid	210	1.005	(30)	9.9	(30)
	Balt. MD[d]	liquid	226	1.047	(25)	9.9	(37)
	Site 1[e]	liquid	250	1.083	(24)	67	(40)
	Site 4[e]	liquid	230	1.064	(24)	34	(40)
	Site 5[e]	liquid	250	1.133	(24)	140	(40)
Holding tanks	PA[f]	liquid	-	1.051	(-)	19	(25)
	Site 7[e]	viscous liquid	780	1.251	(24)	-	
	Site 9[e]	viscous liquid	480	1.107	(24)	6 600	(40)
Surface samples	Site 2[e]	pliable solid	700	1.366	(24)	-	
	Site 3[e]	pliable solid	440	1.423	(24)	-	
	Site 6[e]	solid	1 600	1.424	(24)	-	

[a] Temperature °C in parentheses. When temperature is not noted, data are for density in g/ml.

[b] Eberhardt and Grathwohl [37]

[c] Peters and Luthy [118] and Peters and Luthy [120]

[d] Barranco and Dawson [15]

[e] EPRI [41]

[f] Hugaboom and Powers [65]

For the most part, the property data in Table 2.8 are consistent with the type of gas manufactured. For example, the tars from Stroudsburg and Baltimore both have low density and viscosity, which are consistent with water-gas tars, as shown in Figure 2.1. The tar from Pennsylvania also appears to be a water-gas tar. For the liquid samples in the EPRI survey, the property data are also consistent with the predominant type of gas manufactured. For the weathered solid samples, the specific gravities are higher than any reported in the historic data provided in Table 2.7.

Another consideration in the measurement of viscosities is the possibility that these materials could exhibit non-Newtonian behavior, such that viscosity is also a function of the applied shear stress. Non-Newtonian behavior has been documented for coal tar pitches [163, 87]. For coal tars, studies of rheological behavior have generally revealed Newtonian flow, but they have been conducted at temperatures $> 100°C$ [151]. The behavior of these materials has not been assessed at lower temperatures and sheer stresses where non-Newtonian behavior is more likely [151].

2.5.2 Interfacial Tension

The IFT between tar and water is generally considered low when compared to other DNAPLs; however, it has only been measured for a small number of samples. In Table 2.9, IFTs are listed along with the corresponding pH. The data show that IFTs at neutral and acid pH vary from 20–25 dynes per centimeter. At higher pH, the IFT decreases to near zero. The dependence of IFT on pH is believed to be controlled by the acid functional groups contained in asphaltenes [15, 169]. As noted, the bulk properties of the Stroudsburg, Baltimore, and Pennsylvania tars are at the low end of the reported range. Given the variable composition and wide range of properties for FMGPs tars, it is possible that the range of IFTs could be much broader than what is listed here.

Table 2.9: Interfacial tension of tar samples as a function of pH

Sample	pH	γ^{nw} (dynes/cm)
Stroudsburg, PA[a]	NP	22
Baltimore, MD[b]	<9.1	23.5
	12.4	0.6
Pennsylvania[c]	7	∼20
New York[c]	7	∼25

NP=not provided; nw= NAPL and water interface
[a] Villaume [156]
[b] Barranco and Dawson [15]
[c] Zheng and Powers [169]

2.5.3 Wettability

In NAPL contaminated porous media, it is important to understand the wetting behavior of liquid phases. The wetting phase coats the solid medium while the non-wetting phase tends to exist as isolated globules at residual saturation occupying the largest pore openings. Wettability is defined as the attraction of a liquid phase to solid surface, and it is typically quantified using a contact angle with the solid phase. NAPL contaminated systems can be water wet, oil wet, or exhibit mixed wettability. Changes in wettability from water to oil wet have significant impacts on the pressure-saturation relationship and make remediation particularly challenging.

The ability of coal tar to alter the wettability of solid media has been verified using bottle tests. Bottle tests were originally developed to test the wetting behavior of crude oil-water systems [36]. Crude oils are well documented for altering wettability. The bottle test is a qualitative way to assess system wettability. It involves shaking a mixture of water, NAPL, and unconsolidated media over a period of time to observe the distribution of phases. Powers et al. [130] used the bottle test to compare the wettability for a variety of NAPLs including neat solvents, which remained water wet (e.g., TCE); petroleum products, which were mostly weakly-water wet or mixed

wetting (e.g., gasoline and crude oil); and coal-derived creosote and tar, which were both oil wet.

Asphaltenes contain organic bases that are believed to cause these wettability shifts [15, 170]. In bottle tests, Powers et al. [130] used dodecylamine as a surrogate compound to illustrate how increasing the amount of an organic base in a NAPL changes wettability from strongly water wet to oil wet. At low pH, these organic bases become positively charged and have an even stronger attraction to solid grains, which are typically negatively charged. Zheng and Powers [168] conducted bottle tests with four tars and four creosote samples at pH of 7.2 and 4.7. At neutral pH, only one tar and one creosote were wetting. At the lower pH, all the creosotes and half the tars were wetting. Zheng and Powers [168] also showed that NAPLs with higher base numbers were more likely to be the wetting phase. Base numbers were determined using non-aqueous titrations and correspond to the milligrams of acid required to neutralize one gram of tar. Of the four tar samples analyzed, the one with the highest base number exhibited oil wetting behavior regardless of pH.

A more quantitative measure of wettability is the contact angle. Contact angles are measured by placing a drop of a liquid, though a syringe, on a flat, clean surface and measuring the angle between the two. For NAPLs in porous medium systems, researchers typically immerse a drop of NAPL in an aqueous phase on a solid media (e.g., quartz slides) and measure the angle through the water phase [99]. Contact angles can be determined as the drop is created, the advancing contact angle; once the system has reached equilibrium, the static contact angle; and as the drop is

withdrawn, the receding contact angle. The contact angle, θ, is related to interfacial tension, γ, by Young's equation, such that

$$\gamma^{ns} - \gamma^{ws} = \gamma^{nw} cos(\theta) \tag{2.1}$$

where s is the solid phase, n is the NAPL phase, and w is the aqueous phase. Water-wet materials have contact angles less than 90°, and oil-wet materials have contact angles greater than 90° [17]. The transition from water to oil wet is referred to as intermediate wetting, the range for which is generally considered to be between 62 and 133° [105].

Films at the NAPL-aqueous phase interface appear to strongly influence contact angle measurements. In Powers et al. [130], equilibrium contact angle measurements for coal tar on quartz were attempted, but not reported, due to the presence of films interfering with these measurements. Barranco and Dawson [15] measured static, advancing and receding contact angles for solutions of varying pH, from 3.4–12.4. The static and advancing contact angles were almost constant and below 20°, indicating a water-wet system. However, the receding contact angles varied with pH, averaging approximately 175°, from pH 3.4–6.7; steadily decreasing, from pH 6.7–8; and averaging approximately 10°, from pH 8.0 and above. When the receding contact angle indicated oil-wet conditions, a film was also present on the surface of the tar, which adhered strongly to the quartz surface. Zheng et al. [170] also measured receding contact angles and showed similar changes in wettability with pH, as well as with increasing asphaltene concentration.

2.5.4 Capillary Pressure

The contact angle and the IFT both affect the mobility of NAPL through porous media. The relationship is expressed quantitatively at the microscale using the Laplace equation, which relates the capillary pressure, P_c, to the IFT and contact angle as

$$P_c = \frac{2\gamma^{nw}\cos\,\theta}{r}, \tag{2.2}$$

where r is the average radius of curvature [31]. For many environmentally relevant NAPLs such as, PCE and TCE, P_c is controlled primary by the IFT. For tars, the IFT is much lower, and the contact angle or wettability is likely to also play an important role in the P_c [15, 170].

The work of adhesion has also been used to understand the relative importance of IFT and wettability, which, in this case, is the work required to separate the NAPL from the solid and is given by [96]

$$W^{ns} = \gamma^{nw}(1 - \cos\,\theta). \tag{2.3}$$

Dong et al. [33] concluded that W^{ns} was driven primarily by the coal tar-IFT rather than contact angle; however, their assessment was based on the static contact angle, which indicated water to weakly-water wetting behavior. As discussed in § 2.5.3 the static and receding contact angles are very different in tar systems. In Dong et al. [33], photographs of both static and receding NAPL drops are provided. While the static case has a contact angle $< 90°$, the receding case has a contact angle $> 90°$,

indicating oil wetting behavior.

2.6 Process Modeling

In order to understand the risks posed by tars in the subsurface, we must be able to estimate the dissolution of individual chemical species. This requires an understanding of both equilibrium concentrations and the amount of time required to reach equilibrium, or the rate of mass transfer. Because the individual species in tars have different solubilities, the overall chemical composition of the NAPL phase can change over time. This can lead to instabilities in tar mixtures, such that some compounds may begin to precipitate within the NAPL phase. The following sections describe the approaches taken in the literature to model these processes.

2.6.1 Equilibrium Dissolution

In general, the aqueous phase concentration for an individual chemical species in equilibrium with tar will be less than the solubility for the pure species; however, the exact relationship between aqueous and tar phase concentrations is not completely understood. Some researchers have described the equilibrium dissolution from a NAPL phase empirically using a partition coefficient, K_{nw_i}, defined as

$$K_{nw_i} = \frac{C_i^n}{C_{ei}^a} \tag{2.4}$$

where C_i^n is the concentration of the i^{th} species in the NAPL phase and C_{ei}^a is the equilibrium concentration of the i^{th} species in the aqueous phase [81, 38]. A common

approach in environmental chemistry is to relate a compound's octanol-water partition coefficient, K_{ow}, to the partition coefficient in a more complicated NAPL [144]. Endo and Schmidt [38] developed the following regression equation for coal tar-water systems from a survey of literature data

$$\log K_{nw_i} = 1.16 \log K_{ow_i} - 0.19. \tag{2.5}$$

Using this relationship, we can estimate the $\log K_{nw}$ for any chemical that has a known $\log K_{ow}$; however, this approach does not account for the variability among tars that may affect partitioning.

A more rigorous approach to predicting equilibrium concentrations based in thermodynamics is Raoult's law [144]. This approach relates C_{ei}^a to the species' subcooled pure liquid solubility, S_i, and mole fraction in the nonaqueous phase, χ_i^n, such that

$$C_{ei}^a = \chi_i^n S_i. \tag{2.6}$$

By definition, the mole fraction for the i^{th} species is the ratio of the moles of i, m_i, to the total number of moles. Since the entire composition of these complex mixtures is not known, the mole fraction is typically calculated as follows,

$$\chi_i^n = \frac{m_i}{\sum_{i=1}^{n} m_i} = \frac{C_i^n \times \overline{Mw}}{10^6 \times Mw_i}, \tag{2.7}$$

using the concentration of species i in the NAPL phase, C_i^n (mg/kg); the molecular

weight of the species, Mw_i; and the average molecular weight of the NAPL, $\overline{Mw}$. The subcooled pure liquid solubility is determined by

$$S_i = \frac{C_{si}^a}{(f^S/f^L)_i}, \tag{2.8}$$

where C_{si}^a is the solubility in the aqueous phase of the single species i neglecting composition effects and $(f^S/f^L)_i$ is the solid to liquid fugacity ratio. For compounds that are liquids at ambient conditions, $(f^S/f^L)_i$ is one, reducing Raoult's law to

$$C_{ei}^a = \chi_i^n C_{si}^a. \tag{2.9}$$

Theoretically, a compound in a NAPL mixture consisting of like compounds, should adhere to Raoult's law. If a compound is in a mixture of compounds with very different properties, deviations from ideal behavior can occur [144]. In a non-ideal mixture, C_{ei}^a is expressed as

$$C_{ei}^a = \gamma_i^n \chi_i^n C_{si}^a, \tag{2.10}$$

where γ_i^n is the activity coefficient for species i in the NAPL phase.

In Figure 2.2, we plotted experimentally determined values for C_{ei}^a versus predicted values calculated based on Raoult's law for several tar samples. Predicted values for C_{ei}^a require the $\overline{Mw}$ for the NAPL phase. The traditional method of determining $\overline{Mw}$ is vapor pressure osmometry (VPO), which can be prone to error due to high solids content and viscosity [22]. In Figure 2.2, predicted values were calculated using either experimentally determined $\overline{Mw}$ (Figure 2.2a) or best fit values for $\overline{Mw}$ using

the method described by Brown et al. [22] (Figure 2.2b). Brown et al. [22] concludes that using fitted values for $\overline{Mw}$ is more appropriate given the ultimate use of the data (i.e., predicting C_{ei}^{a} using Raoult's law). While this may be true, several chemicals in Figure 2.2 continue to have deviations from the ideal prediction exceeding a factor of 2, even when the fitted $\overline{Mw}$ is used.

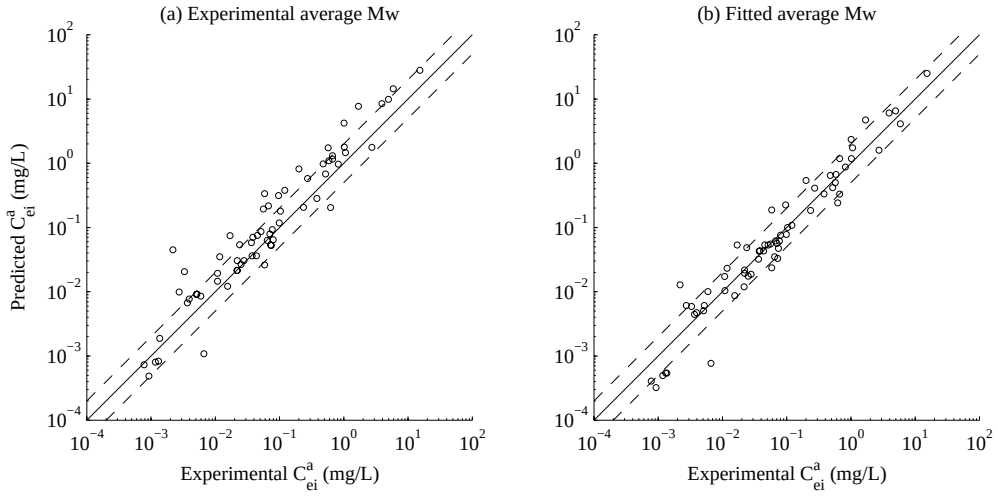

Figure 2.2: Comparison of experimental and predicted C_{ei}^{a}. Predicted values were calculated based on Raoult's law using either experimentally determined $\overline{Mw}$ (a) or fitted $\overline{Mw}$ (b). Values for C_{ei}^{a} were determined by Lee et al. [81] for samples in the EPRI survey [41]. The solid line corresponds to an ideal mixture. Dashed lines correspond to concentrations that deviate from the ideal by a factor of 2.

Deviations from Raoult's law could be due to non-ideal behavior, analytical limitations, or uncertainty in chemical properties. Thermodynamic modeling has been conducted to estimate activity coefficients for several tars, including the Stroudsburg tar [124]. MAHs generally had activity coefficients slightly less than 1 (e.g., 0.8), and most PAHs had activity coefficients at or near 1. Their analysis did not include tars

with more polar constituents (e.g., phenols), which are more likely to deviate from Raoult's law [39]. In terms of analytical methods, the analysis of PAHs is generally considered somewhat standard; however, special care must be taken to quantify accurately individual compounds in complex mixtures [142]. Measuring aqueous phase concentrations of PAHs can also be confounded by losses in sample preparation, including volatilization, photodegradation, and sorption. Finally, there is also some uncertainty due to chemical properties, such as the subcooled liquid solubility [122].

Higher molecular weight PAHs, such as benzo(a)pyrene, are a particular concern from a risk perspective due to their relatively high toxicity and possible increased mole fraction as tar ages [123]; however, little data is available to evaluate the dissolution behavior of these compounds. The range of molecular weights for all the priority pollutant PAHs is from 128–278 g/mol, with benzo(a)pyrene having a molecular weight of 252 g/mol. In Lee et al. [81], equilibrium aqueous phase concentrations were reported for compounds with a molecular weight up to 228 g/mol. In Brown et al. [22] close inspection of data plots reveal that equilibrium aqueous phase concentrations were not determined for PAHs with a molecular weight $>$ 202 g/mole. Though not explicitly discussed by either author, it is likely that the aqueous phase concentrations of higher molecular weight compounds were less than the analytical detection limit. In Lee et al. [81], the most significant deviations from Raoult's law were for the highest molecular weight compound measured, benzo(a)anthracene (i.e., 228 g/mol), such that measured concentrations were consistently less than expected. These deviations were attributed to analytical limitations [81].

2.6.2 Mass Transfer

Mass transfer from a NAPL to an aqueous phase is generally described by a linear driving force model of the following form

$$\overset{in\rightarrow ia}{M} = \epsilon^{na} k_{ai} (C^a_{ei} - C^a_i) \tag{2.11}$$

where C^a_i is the aqueous phase concentration, k_{ai} is a mass transfer coefficient, and ϵ^{na} is the specific interfacial area between the NAPL and aqueous phases [102]. Since the interfacial area is typically unknown, mass transfer is often characterized in terms of the lumped mass transfer rate coefficient

$$K_{ai} = \epsilon^{na} k_{ai}. \tag{2.12}$$

For single species NAPLs, a considerable body of work exists on determining the parameters affecting the mass transfer rate in porous media. Due to the complex nature of these systems, several empirical relationships have been derived to predict mass transfer using non-dimensional parameters [102, 47, 66, 129, 76]. Though these empirical relationships may successfully predict mass transfer for a set of experimental data, mass transfer is fundamentally a function of the microscale morphology and topology of the NAPL-aqueous phase interface, and several other properties. Recently, microscale simulations have been successfully used to predict macroscale mass transfer; however, there is considerable work that needs to be done for a complete understanding of this complicated process [116].

For multi-species NAPLs such as tars, mass transfer is further complicated by several factors. One obvious complication is that the composition of the NAPL itself can change over time. Changing composition may affect other physical parameters such as viscosity and density. Within the NAPL phase, varying rates of molecular diffusion or diffusional drag of individual species may limit dissolution and lead to changes in NAPL composition in both space and time [102, 64, 21]. Our ability to understand mass transfer is also limited by uncertainties in the equilibrium concentration and possible deviations from Raoult's law. Finally, the changing composition of tars may also lead to some species precipitating within the NAPL phase (See §2.6.3).

For tars, few experiments have been conducted to determine mass transfer rates. In flow-through and batch mass transfer experiments using coal tar imbibed into a porous medium consisting of small diameter silica particles, the lumped mass transfer coefficients for naphthalene and phenanathrene decreased over a two to three hour time frame [132, 48, 133]. This decrease was speculated to be a result of interfacial films forming at the water-NAPL interface; however, experiments with larger diameter glass beads and coal tar globules did not exhibit the same behavior [48, 133].

Some evidence suggests that the mass transfer coefficient may not vary much between different PAHs. Mass transfer coefficients were determined for various synthetic mixtures of toluene and eight PAHs with molecular weights from 128–202 g/mol [107]. The coefficients varied from 0.8×10^{-3}–3.0×10^{-3} cm/s. Mass transfer coefficients also tended to increase for high molecular weight compounds, yet this increase was attributed partly to analytical artifacts. In the synthetic mixtures, the mole fraction

of naphthalene was varied from 0.0–0.25 while the mass transfer coefficient remained essentially the same. No experiments were identified that determined mass transfer coefficients for higher molecular weight PAHs in tar, such as benzo(a)pyrene.

2.6.3 Precipitation of PAHs

Raoult's law has been used to predict the precipitation from tar NAPLs with some limited success. As pure compounds, many of the PAHs in tars are solids at ambient conditions. As tars age, we expect that the more soluble components will be preferentially depleted, resulting in increased mole fractions of other components. As derived by Peters et al. [122], components of ideal liquid mixtures will be stable when

$$\chi_i^n \leq (f^S/f^L)_i. \tag{2.13}$$

Peters et al. [122] compared mole fractions in a solid and liquid tar; in the solid tar, mole fractions of several PAHs exceeded $(f^S/f^L)_i$. To more definitely determine whether or not ideal behavior was likely for PAH mixtures, solid-liquid equilibria were evaluated for binary, ternary, and quaternary mixtures using naphthalene, 2-methylnaphthalene, acenaphthene, phenanthrene [122, 125]. While ideal behavior was observed for naphthalene and acenaphthene, phenanthrene and 2-methylnaphthalene appeared to co-precipitate even when solubility theory indicated only one should be forming a solid phase. Given the large number of compounds in tars, there is clearly much more work that needs to be done to understand this phenomena.

2.7 Remediation and Modeling

There is now a clear understanding that simple pump-and-treat approaches do not provide effective and efficient solutions for remediating FMGP sites. The methods currently used to remediate these sites can be grouped into three general categories: source-zone removal, including excavation and hauling; source-zone containment, including capping, slurry walls, sheet piling, and in-situ stabilization; and source-zone treatment, including thermal treatment, chemical treatment, and biodegradation [100]. For all of these methods, the overall goal is to reduce the mass flux from the source zone.

In terms of tar DNAPLs that have migrated into the saturated zone, excavation is not typically a viable option. At large sites, it is often possible to pump and remove the free-phase DNAPL directly [160]; however, a considerable amount of mass can be left behind as trapped residual. Much effort has been focused on the use of flushing solutions intended to facilitate DNAPL removal, such as hot water and polymers [160]. Initially developed for the petroleum industry, these methods can successfully remove large amounts of mass. For example, hot water injection resulted in the recovery of 1500 gallons of tar at the Stroudsburg, PA FMGP site [72]. For slow moving tar plumes, removing free-phase DNAPL can also reduce the potential for further migration.

In general, these techniques still tend to leave behind a substantial amount of entrapped residual material. Often additional efforts are necessary to reduce the mass flux from the residual phase to the mobile dissolved phase [160]. It is also believed

that at many sites that the majority of the tar mass is present as entrapped residual [94]. Mass removal of residual DNAPL may be achieved through mobilization or dissolution using cosolvents and surfactants. Chemical and biological treatment may also be applied. For single component NAPLs, a considerable amount of experimental work has been conducted to understand the effectiveness of these techniques at a variety of scales. For one-dimensional column experiments with relatively high residual saturations, the total mass removed is often greater than 90% [145]. In larger three-dimensional experiments with lower residual saturations, the total mass removed is typically much less, ranging from approximately 30–90% [145].

The number of controlled experiments with tar DNAPLs is much more limited but provides some perspective regarding the difficulty of removing these mixtures. In Table 10, several small-scale laboratory experiments that used tar DNAPLs are summarized. Two of these experiments were conducted with high starting residual saturations that are more likely to be encountered in tar pools [65, 49]. In both experiments, flushing solutions were tested under varying conditions of wettability. Under oil-wet conditions, the residual saturations after flushing ranged from 35–47%. Under water-wet conditions, the residual saturations were further reduced but still remained anywhere from 20–30%. Though mass flux was not determined in these experiments, it is clear from experimental results using single component DNAPLs that residual saturation must be reduced much further to achieve a meaningful reduction in mass flux [145].

In Table 10, an experiment is also summarized that used a cosolvent to enhance

the dissolution of a tar DNAPL in a one-dimensional column [140]. In this case, the starting residual saturation corresponded more closely to an entrapped DNAPL. The goal of this experiment was to remove the DNAPL constituents at the same rate. After 40 pore volumes, tar mass was still leaching from the column and the DNAPL remaining in the column appeared to have a much higher viscosity then the starting material. Though mass fluxes were not determined for individual chemicals, the researchers concluded that components where not dissolving at the same rates.

Table 2.10: Experimental assessments of tar DNAPL remediation approaches

Source	Methods	Result
Roy et al. [140]	Several 1-D columns packed with sand. Contaminated with Stroudsburg FMGP tar from 4–25% res. sat. Flushed with 80% n-butylamine.	Large amount of tar removed in the first 2 PV. Tar removal reduced to approx. constant value after ∼10 PV. Tar still leaching after 40 PV.
Hugaboom and Powers [65]	Three 1-D columns packed with sand. Contaminated with Pennsylvania FMGP tar at ∼87% res. sat. Flushed with water at varying pH to control wettability.	Reduced res. sat. after flushing under oil-wet conditions (pH=4.7) to 47%, water-wet conditions (pH=7.2 or 9.9) to ∼30%.
Giese and Powers [49]	Several 1-D columns packed with sand. Contaminated with either of two synthetic NAPLs having varying viscosity (10 or 20 cP) at 75% res. sat. Wettability was altered using varying concentrations of dodecylamine. Flushed with either water or polymer solutions.	Results similar for both NAPLs. Res. sat. reduced in water-wet systems to ∼20% regardless of flushing solution. In oil-wet systems, reduced to ∼45% using water flushing, ∼35% using polymer solutions with $\kappa \approxeq 1$, ∼20% using polymer solutions with κ=0.1.
Dong et al. [33]	2-D tank was packed with sand contaminated using tar from a FMGP in the United Kingdom. Tank was flushed with increasing concentrations of a poloxamine block copolymeric surfactant.	Tanks were assessed visually. Flushing with a 1% polymer solution mobilized the coal tar downward.

PV=pore volumes. κ=tar viscosity/polymer viscosity.

At sites where using chemical or physical means to remove tar is not possible, natural attenuation has become an important remedial option. Processes that contribute to natural attenuation include: dilution, dissolution, sorption, precipitation, volatilization, biodegradation, and abiotic degradation. Of these, biodegradation is

the primary mechanism for natural attenuation of PAHs [88]. The ability for microorganisms to degrade PAHs has been well documented [106, 28, 14]. It is also well documented that the presence of PAH degrading microorganisms is most likely to occur at locations of long-term persistent contamination [28]. Not surprisingly, the presence of PAH degrading microorganisms has been confirmed at several FMGP sites [88, 13, 164, 32].

For remediation via natural attenuation to be a viable option, there is often an emphasis on both confirming current attenuation of contaminants and understanding the length of time required for these processes. Thus, it is important to understand the factors controlling the biodegradation rate and considerable work is still required to understand the complex nature of this process [28, 14]. For example, most historic studies of biodegradation used pure cultures and single compounds. Thus, there is a need to understand the biodegradation of mixtures using native cultures [28, 14]. Though there has been limited study on the biodegradation of high molecular weight PAHs, it is known that biodegradation rates tend to decrease with increasing molecular weight [62, 28, 14].

One of the challenges with demonstrating natural attenuation for tars is that dissolution of individual compounds varies both spatially and temporally. This phenomena has been well documented in a long-term field study using an emplaced, immobile creosote source zone consisting of 74 kg of DNAPL premixed with sand [45]. Though creosote is a distillation product of coal tar and does not contain as wide a molecular weight distribution as coal tar, it has the same multi-component nature as other

FMGP tars. The dissolution of compounds from creosote to groundwater was found to qualitatively agree with Raoult's law for 9 out of 11 compounds analyzed. Specifically, the most soluble compounds (e.g., phenol) were first to appear in groundwater and were no longer detected after a few hundred days. Compounds with intermediate solubility (e.g., naphthalene) continued to increase in concentration up to 3,000 days, after which time concentrations began to decrease. The groundwater concentrations of the compounds with the lowest solubility continued to increase after 5,000 days. For each compound analyzed, the extent and concentration of the dissolved phase plume was much less than the Raoult's law prediction, which was attributed mostly due to biotransformations.

For most FMGP sites, we would expect much larger amounts of DNAPL to have been either leaked or disposed of over time when compared to the field study described above. At a FMGP site in Germany, innovative field techniques were used to define the extent and distribution of DNAPL mass, which was closely connected to local changes in heterogeneity [32]. From this analysis, it was determined that the plume contained 188 tons of DNAPL within a 50 by 100 meter footprint. Transport modeling was used to understand the time frame for natural attenuation. After 1,000 years, they estimated that 100% of the mass would be depleted for the high solubility compounds; 40%, for intermediate solubility compounds; and only 2% for the lowest solubility compounds. Thus, for sites with large amounts of subsurface tar DNAPLs, the highest molecular weight PAHs may not begin to dissolve for several hundred years.

Field-scale modeling assessments, like the one described above, are important

tools in understanding the time scales involved for natural attenuation to occur, along with the impacts further source reduction would have on that time scale. However, the uncertainty involved in such long-term estimates along with the complexity of the system being modeled cannot be overstated. The development of multiphase, multicomponent models is a substantial area of research in terms of appropriately describing these complex physical phenomena, as well as, achieving numerically accurate and computationally efficient implementations [103]. Even in the case of single component models, determining source-zone mass flux has proven to be difficult [145].

In the case of multicomponent tar DNAPLs, we are faced with further layers of complexity, including the changing composition of the DNAPL in space and time and changes in system wettability. In current modeling efforts, simplifying assumptions are often required due to lack of data or computational limitations. For example, D'Affonseca et al. [32] modeled two chemicals individually and all other chemicals were modeled using three representative chemicals. Over the long time scales that these DNAPLs exist, there is likely to be a dynamic relationship between the mobilization of DNAPL and the changing composition of DNAPL due to dissolution and precipitation. DNAPL aging will certainly increase density, possibly causing tars with near-neutral density to sink further over time. To date, there have been several efforts to model the dynamics of multicomponent dissolution [123, 80, 37], as well as investigations related to the migration of tar DNAPLs [68]. Little work has been done to understand the relationship between the two.

We also have almost no information on how tars might change spatially across a

given site. This could be important as some tars migrate over long distances. An area of active research in the petroleum industry is related to understanding the compositional changes in crude oils as they migrate. Asphaltenes are believed to interact with the solid phase resulting in a chromatographic separation of compounds [82, 84, 79, 86, 149, 16]. In fact, investigations are on-going in the petroleum literature on how to use this phenomenon as a way of tracking the movement of crude oil [82, 84, 79, 86, 149, 16]. Given the enhanced concentration of asphaltenes in tars, it seems possible that the movement of tar could result in similar changes in composition.

2.8 Conclusions

Gas manufacturing was a dominant industry throughout the U.S. and Europe for over a century. Decades have passed since the recognition that tars at FMGPs are potential sources of groundwater contamination; still, significant gaps exist in our fundamental understanding of the environmental processes that govern their movement and dissolution. Without this fundamental knowledge, it is impossible to build reliable mechanistic models to assess DNAPL migration and dissolution. We are also restricted in our ability to design and implement new remediation strategies.

Considering the published literature of the last half of the 20th century, in some respects, our knowledge of the composition and properties of these tars has progressed little, and may even have been lost. Early in the history of gas manufacturing, the complex nature of tars was well recognized and widely studied, along with the influence of the type of gas manufacturing, operating conditions, and raw materials.

We believe historic data is especially useful if we are able to connect tars at FMGPs to the original manufacturing process. Wider recognition of the influence of the tar origin on composition may provide future researchers an additional means of understanding the considerable variability among tar samples.

Given the variability in tar composition and properties, there is a clear need to study the properties of a wider range of tars (e.g., contact angles, IFT, wettability). This is especially needed to enhance our understanding of interfacial phenomena, which plays such a key role in the fate of subsurface tars. To date, the tars that have been studied in relation to interfacial phenomena are likely water-gas tars. In coal tars, the presence of phenolic compounds could have a significant impact on interfacial phenomena.

Though some methods of characterizing the bulk properties of mixtures are still used today (e.g., SARA analysis), current analysis of tars tend to focus more on particular chemicals or groups of chemicals. Clearly, this focus is driven partly by regulation but also by continued analytical limitations. Especially notable is a lack of data on the high molecular weight PAHs in studies of equilibrium dissolution, mass transfer, and biodegradation. These compounds are also typically drivers in risk assessments; thus, an accurate understanding of their behavior is critical to assessing the future risk from FMGPs.

In general, we believe that there is a need to view these complex mixtures in a more holistic manner. On one end of the spectrum, we have studies of mass transfer and biodegradation that consider a relatively small group of PAHs. On the other

end, we have studies on enhanced remediation that make no attempt to quantify the impact on individual components and consider only the total removal of NAPL mass. In particular, we believe there should be less emphasis on the average molecular weight as a means of characterizing these mixtures. More emphasis on determining the entire molecular weight distribution is needed, along with an understanding of how this distribution changes with NAPL aging.

Interestingly, both data and modeling indicate that subsurface tars at FMGPs have aged little. Compositional data also seem to contradict our understanding of aging described by Raoult's law. Specifically, it is noteworthy that naphthalene, the most abundant and most soluble PAH in unweathered samples, is still the most abundant compound in some of the most weathered samples reported in the literature. This apparent discrepancy could be due to diffusional limitations within the DNAPL phase associated with increasing viscosity.

Improving our understanding of the factors governing the long-term fate of these complex mixtures, improves our decision making ability with regard to remedial options. A sound understanding of interfacial phenomena is especially critical for developing better methods for source-zone remediation. Understanding the potential benefits of further source-zone remediation along with the viability of natural attenuation is directly linked to this fundamental understanding, which is critical to developing better mechanistic models.

CHAPTER 3

COSOLVENT FLUSHING FOR THE REMEDIATION OF PAHS FROM FORMER MANUFACTURED GAS PLANTS

P.S. Birak[1], A.P. Newman[2], S.D. Richardson[3] S.C. Hauswirth[4], J.A. Pedit[5], M.D. Aitken, and C.T. Miller

3.1 Abstract

Cosolvent flushing is a technique that has been proposed for the removal of hydrophobic organic contaminants in the subsurface. Cosolvents have been shown to dramatically increase the solubility of such compounds compared to the aqueous solubility; however, limited data are available on the effectiveness of cosolvents for field-contaminated media. In this work, we examine cosolvent flushing for the removal of polycyclic aromatic hydrocarbons (PAHs) in soil from a former manufactured gas plant (FMGP). Batch studies were used to determine the relationship between the soil-cosolvent partitioning coefficient (K_i) and the volume fraction of cosolvent (f_c). Using methanol at an f_c of 0.95, column studies were conducted at varying length scales, ranging from 11.9 to 110 cm. Removal of PAH compounds was determined as a function of pore volumes (PVs) of cosolvent flushed. Despite using a high f_c, rate and chromatographic effects were observed in all the columns. PAH effluent

[1]Responsible for small column experiments, modeling, data analysis, and manuscript preparation.
[2]Responsible for large column experiment.
[3]Responsible for analysis of soil samples and large column set-up.
[4]Responsible for analysis and fractionation of soil extracts.
[5]Provided expertise in column design, tracer tests, and modeling.

concentrations were modeled using a common two-site sorption model. Model fits were improved by using MeOH breakthrough curves to determine fitted dispersion coefficients. Fitted mass-transfer rates were two to three orders of magnitude lower than predicted values based on published data.

3.2 Introduction

The manufacture of gas from coal and oil was widespread throughout the U.S. and Europe during the 1800s to mid 1900s. In the U.S. alone, there are an estimated 33,000 to 50,000 former manufactured gas plants (FMGPs) and related sites, which are suspected of having soil and groundwater contamination. The most common contaminant is tar, a by-product of the manufacturing process [152].

FMGP tars are complex mixtures of mostly organic compounds. Though the exact chemical composition is still unknown and varies from site to site, tars contain a large percentage of PAHs, including several carcinogens [153]. In most tars, naphthalene (NAP), a two-ring PAH, is the most abundant individual compound, accounting for as much as 15% of tar mass [18]. As the number of rings increases, concentrations in tar generally decrease. For example, benzo(a)pyrene (BaP), a five-ring PAH, is usually less than 1% of tar mass [18].

In the subsurface, tars are long-term sources of soil and groundwater contamination. When released to soil, tars migrate vertically. Once they encounter the water table, tars may sink further as they are dense, non-aqueous phase liquids (DNAPLs). Tar-contaminated systems can become oil-wet, resulting in soil and sand grains being

coated with tar [15, 130]. PAHs dissolve from the DNAPL phase into bulk groundwater slowly because of low aqueous solubilities [94].

Tar composition and properties are altered over time as tars age. Lower molecular weight (MW) compounds, such as NAP, are depleted first, primarily due to dissolution [94]. Over time, the mole fractions of higher MW PAHs increase, along with their aqueous-phase concentrations [123]. This results in a chromatographic effect occurring down-gradient of tar-contaminated zones, as compounds are eluted at varying time-scales. Over time, dissolution can result in tars becoming increasingly viscous, and they may ultimately become solids or semi-solids [121].

Cosolvent flushing is a technique that has been proposed for the removal of hydrophobic organic contaminants in the subsurface. Cosolvents can markedly increase the solubility of compounds, such as PAHs. This relationship has been found to follow a log-linear equation, such that

$$\log C_i^{sat} = \log C_{iw}^{sat} + \sigma_i f_c \tag{3.1}$$

where C_i^{sat} is the solubility in a cosolvent for species i, C_{iw}^{sat} is the solubility in water, σ_i is the cosolvency power, and f_c is the cosolvent volume fraction [162]. In soils, cosolvents reduce the equilibrium partition coefficient, such that

$$\log K_i = \log K_{iw} - \alpha\sigma_i f_c \tag{3.2}$$

where K_i is equilibrium partition coefficient between the cosolvent and soil (L^3/M),

K_{iw} is the equilibrium partitioning coefficient between water and soil (L^3/M), and α is an empirical constant that accounts for sorbent-alcohol interactions [135, 159].

Cosolvents have also been found to reduce mass transfer rates. Brusseau et al. [25] and Bouchard [20] conducted column experiments to examine this relationship using breakthrough curves of PAHs in the presence of methanol (MeOH) at varying f_c. The initial condition was a column packed with uncontaminated Eustis sand saturated with a MeOH cosolvent solution. They pumped solutions with a known PAH concentration and the same f_c present in the column. Effluent concentrations were simulated using a two-site sorption model where one fraction of the mass was assumed to remain in equilibrium and the remaining fraction was rate-limited, such that

$$R_i \frac{\partial C_i}{\partial t} = -v \frac{\partial C_i}{\partial x} + D \frac{\partial^2 C_i}{\partial x^2} - \frac{\rho_b}{\theta} \frac{\partial S_{2i}}{\partial t} \tag{3.3}$$

$$\frac{\partial S_{2i}}{\partial t} = k_i[(1 - F_i) K_i C_i - S_{2i}] \tag{3.4}$$

$$R_i = \frac{\rho_b}{\theta} K_i F_i + 1 \tag{3.5}$$

$$S_i = S_{1i} + S_{2i} \tag{3.6}$$

where R_i is the retardation factor, C_i is the concentration in the aqueous phase (M/L^3), S_i is the solute mass ratio in soil (M/M), S_{1i} is a solute-solid mass ratio assumed to be in equilibrium (M/M), S_{2i} is a solute-solid mass ratio that is rate-limited (M/M), v is the linear pore velocity (L/T), D is the hydrodynamic dispersion

coefficient (L^2/T), ρ_b is the bulk density (M/L^3), θ is the porosity (L^3/L^3), k_i is the mass transfer rate ($1/T$), and F_i is the mass fraction of the solid phase assumed to always be in equilibrium with the aqueous phase.

The model was fit to determine values for k_i and F_i. For individual PAHs, correlations were found between k_i and f_c, such that

$$\log k_i = \log k_{iw} - \phi_i f_c \tag{3.7}$$

where k_{iw} is the mass transfer rate in a pure aqueous phase ($1/T$), and ϕ_i is a constant [25]. Data from multiple chemicals were used to develop a more general relationship between the rate and the partitioning coefficient

$$\log k_i = \tau \log K_i + b. \tag{3.8}$$

Brusseau et al. [25] reported a τ of -0.61 and b of 0.79 based on data for NAP and phenanthrene (PHE), where k_i is in hrs^{-1}. Bouchard [20] included additional PAHs and reported a value for τ of -0.91 and for b of 0.47. In addition, Brusseau et al. [25] found that F_i was lower as the cosolvent fraction increased, but was unable to develop a relationship to predict F_i based on other parameters.

Augustijn et al. [12] used the two-site model to simulate column desorption experiments. In these experiments, the initial condition was an aqueous solution containing either NAP or PHE in equilibrium with Eustis sand. Cosolvent solutions were then pumped through the columns and the effluent concentrations measured over time.

They modeled the system using the rate constants from Brusseau et al. [25] and found that model predictions generally agreed with experimental data.

A limitation of these previous modeling studies is that they all relied on single-solute systems of artificially contaminated media. Thus, the effects of aging and the complexity of contaminant mixtures were not considered. In terms of PAHs, previous studies have also tended to use compounds that have relatively low MW when compared to the entire suite of 16 U.S. EPA priority pollutant PAHs that are of concern from a risk perspective. These studies were also all conducted at the same length scale of approximately 5 cm. It has been well documented that remediation efficiency diminishes with length scale [145].

Few studies have been conducted to examine the removal of PAHs from field soils. Using an FMGP soil, Chen et al. [29] conducted column experiments and flushed 10 PVs of MeOH or ethanol (EtOH) at an f_c of 0.85 in 5.5-cm columns. Percent removal was lowest for the high MW compounds. For example, the percent removal for NAP was 67.9% using MeOH and 69.9% using EtOH. For BaP, removal was 42.3% using MeOH and 27.3% using EtOH. Since these results were not modeled, mass transfer rates were not reported. Kilbane [75] conducted batch experiments with an aged FMGP soil and removal rates were near 100% using pure ethanol, suggesting that it may be possible to achieve higher removal percentages by using a higher f_c.

The overall goal of this work was to evaluate the use of alcohol flushing for the remediation of field-contaminated and aged soils typical of FMGPs. The specific objectives were: (1) to investigate the remediation of aged, field-contaminated solid

materials from FMGPs using cosolvent flushing; (2) to observe the effects of system hydrodynamic characteristics on remediation efficiency; (3) to evaluate the presence and importance of mass transfer limitations as a function of solute properties; and (4) to assess the adequacy of a commonly posited model for field-contaminated systems.

3.3 Materials and Methods

3.3.1 Field Samples

Field samples were collected from a FMGP site in Salisbury, North Carolina. The highest PAH concentrations were detected in boreholes located between the former retort house and tar well. Soil samples were collected from this region at a depth of approximately 1.2 m and stored in sealed buckets at 4°C prior to processing. No free liquid-phase tar was observed in the field soil.

The field soil was screened through a 10-mm wire screen to break up large aggregates and remove rocks, brick fragments, and other debris. The screened soil was thoroughly mixed to create a homogeneous soil stock. The homogenized soil was then mixed with sterile 40/50-grade silica sand (Accusand, Unimin Corporation, Le Sueur, MN) at a 1:1 mass ratio to allow flow through packed columns with a sufficiently small pressure gradient.

Properties of soil mixture are given in Table 3.1. The soil organic carbon (OC) totaled 8.3%; however, the total extractable organic matter (TEOM) was 0.64%. The TEOM was determined gravimetrically from the soil extracts as described in §3.3.2. It is important to note that these data are based on a few samples; however, the

difference between the %OC and the %TEOM is consistent with other analyses of aged tar-contaminated soil. Specifically, most of the organic matter in similar soils has been identified as a heavy non-extractable fraction, believed to be the result of tar aging [53].

Table 3.1: Properties of the soil mixture

Property	n	Mean	SD	Method
% Sand	1	82.9		D422-63, ASTM [9]
% Silt	1	13.8		D422-63, ASTM [9]
% Clay	1	3.3		D422-63, ASTM [9]
% Moisture content	6	7.50	0.01	D2216-98, ASTM [10]
pH	3	7.56	0.11	D4972-01, ASTM [8]
Particle density (g/cm^3)	3	2.62	0.04	D854-92, ASTM [11]
% Inorganic carbon (IC)[a]	6	7.0	1.6	Lukasewycz and Burkhard [91]
% Organic carbon (OC)[a]	3	8.3	1.2	Lukasewycz and Burkhard [91]
% Total extractable organic matter (TEOM) [a]	15	0.64	0.10	See §3.3.2

[a] Dry mass basis.

3.3.2 Analytical Methods

PAH Analysis

PAHs were isolated from the soil mixture using a two-step solvent extraction procedure. Five-gram (wet wt.) aliquots of the soil mixture were extracted using 20 ml of dichloromethane-acetone (1:1, v/v). Sodium sulfate (6–7 g) was added to each extraction vial to absorb residual water, and three to six 5-mm diameter glass beads were added to each vial to improve soil-solvent mixing. Anthracene-d_{10} was used as an internal standard (Restek, Bellefonte, PA) to evaluate analytical recovery. Vials were sealed with Teflon-lined screw caps, vigorously shaken for 24 hr, and centrifuged for 15 min at 3,500 rpm (1,800 G). The supernatant was removed and the extraction was repeated. The extracts from each step were combined and stored in the dark at

4°C prior to analysis.

Sample extracts were analyzed using a Waters (Milford, MA) HPLC equipped with a 10-cm, 3-μm particle size Supelcosil^{TM}LC-PAH column (Sigma-Aldrich, St. Louis, MO), a fluorescence detector, and HPLC grade solvents. Over the course of the column experiments, two HPLC methods were used as a result of improvements to the analysis. Method I was a 20-min instrument method with a starting mobile phase of acetonitrile-water (60:40, v/v). Method II was a 45-min instrument method with a starting mobile phase of acetonitrile-water (55:45, v/v), which improved peak separation. In both methods, acetonitrile was increased linearly to 100% over the course of each run. External calibration standards were prepared from a PAH analyte mixture (SPEX Certiprep CLPS-B, Metuchen, NJ). Of the 16 U.S. EPA priority pollutant PAHs, two PAHs were not quantified, acenaphthylene, which does not fluoresce, and indeno[1,2,3-cd]pyrene, which had concentrations too low to detect.

TEOM Analysis

Field soil extracts were fractionated to better understand the overall composition of the TEOM. First, soil was screened through a 2-mm wire mesh and extracted with dichloromethane and acetone, as described above. To precipitate the asphaltene fraction, n-pentane was added to the extracts at a ratio of 40 mL per mL of extract. Samples were vacuum-filtered through 0.2-μm pore-size nylon filters. The precipitate was dried under nitrogen and weighed. To determine what is referred to as the "neutral" fraction, the filtrate was passed through a solid-phase extraction column

containing 2 g of Florisil, dried under nitrogen and weighed. Finally, the sample mass retained on the column was eluted using toluene-acetone (1:1, v/v), which was also dried under nitrogen. This fraction is referred to as the "polar" fraction. A Hewlett-Packard 5890 gas chromatograph, coupled with a Hewlett-Packard 5971 quadrapole mass spectrum detector was used for the semi-quantitative analysis of the neutral fraction.

Density Measurements

Density was measured in batch extracts and column effluent samples using an Anton Paar density meter (Model DMA 48) calibrated at 22°C, the average temperature in the laboratory. These density measurements were converted to methanol f_c using empirical data. In MeOH:water solutions, converting between density and volume fraction is complicated by the fact that volume is not conserved. As published data were not found for 22°C, density was measured in solutions of known MeOH f_c (Fisher, ACS Certified) and distilled-deionized water (DD) with mass fractions from zero to one. For each solution, the f_c was calculated from the MeOH mass fraction, ω, and measured solution density, ρ, as

$$f_c = 1.266\omega\rho \tag{3.9}$$

These data are provided in Table 3.2 and were in excellent agreement with data published at other temperatures [50]. A piecewise cubic Hermite interpolating polynomial was generated from the data using MATLAB's pchip function. Since column studies

used simulated groundwater, we confirmed that this relationship held for cosolvent mixtures using simulated groundwater as well. For samples with unknown MeOH concentration, the polynomial was evaluated to convert measured ρ to f_c.

Table 3.2: Density as a function of ω and f_c at 22°C (n=3)

		ρ	
ω	f_c	Mean	Stdev
0.000	0.000	0.9977	0.0002
0.040	0.050	0.9906	0.0001
0.080	0.101	0.9842	0.0004
0.165	0.204	0.9710	0.0002
0.253	0.308	0.9578	0.0003
0.345	0.414	0.9426	0.0002
0.441	0.519	0.9254	0.0003
0.441	0.519	0.9254	0.0003
0.543	0.624	0.9052	0.0003
0.648	0.726	0.8819	0.0001
0.759	0.826	0.8552	0.0001
0.877	0.919	0.8244	0.0001
0.938	0.964	0.8074	0.0001
1.000	1.000	0.7898	0.0003

3.3.3 Batch Experiments

Batch experiments were conducted to determine the relationship between K_i and f_c. The batch experiments were performed using f_c values of 0 to 1 in increments of 0.1, and at an f_c of 0.95. Batch experiments were conducted in triplicate for each f_c. Approximately 3 g of the soil mixture was added to 20 mL of MeOH solution in a centrifuge vial and shaken for 48 hr. Vials were centrifuged for 15 min at 3,500 rpm (1,800 G). The cosolvent was decanted and analyzed for PAHs as described in §3.3.2 to determine the concentration of PAHs in the cosolvent (C_i^{eq}). The total starting solute masses in the soil mixture (M_{0i}) were determined by extracting the remaining mass of PAH as described in §3.3.2 and adding to the mass removed from the cosolvent.

The K_i was calculated as follows

$$K_i = \frac{M_{0i} - C_i^{eq} V}{C_i^{eq} M_s}, \tag{3.10}$$

where M_s is the dry mass of the soil mixture and V is the volume of the cosolvent solution.

3.3.4 Column Experiments

For each column, the same general experimental procedure was followed: (1) determination of the dispersion coefficient using a tracer test, (2) flushing with a MeOH solution at an f_c of 0.95 under density stable conditions, (3) collection and analysis of effluent samples, and (4) analysis of the soil after flushing. The design parameters of the columns are given in Table 3.3.

Table 3.3: Column apparatus and conditions during cosolvent flushing experiments

	C1	C2	C3	C4
Mass of soil mixture (kg)	0.160	13.4	0.170	0.082
Total height (cm)	22.2	110	21.3	11.9
Inner diameter (cm)	2.5	9.83	2.5	2.5
Porosity, θ	0.401	0.417	0.382	0.397
Linear pore velocity, v (cm/day)	24.2	109	25.5	24.7
Mean residence time (day)	0.92	1.0	0.84	0.48
Hydrodynamic dispersion coefficient, D (cm^2/day)	–	4,680	22.3	29.9
Peclet number	–	2.56	24.4	9.83

For C1, C3, and C4, a glass column was equipped with stainless steel end caps and tubing. The columns were wet packed over a 10 g bed of 30/40 Accusand. The soil mixture was then introduced in 0.5 cm lifts, each lift followed by either slight vibration (using a pneumatic vibrator) or tapping of the column walls. Gentle stirring was also used to remove entrained air bubbles and to ensure amalgamation of the lift layers.

In C4 only, the column was also topped with an additional layer of Accusand. This layer was added so the column could be flipped 180° post colsolvent flushing and prior to flushing with water; thus, we were able to maintain a density stable front without reversing the direction of flow. A syringe pump was used to maintain flow through the columns (Harvard Apparatus; Model 44).

For C2, a 110-cm column was constructed out of 10.2-cm outer diameter stainless steel pipe. Three evenly-spaced sampling ports were located at 30, 55, and 80 cm below the column top. The column was wet-packed over a 5-cm bed of oven-dried, autoclaved 30/40 Accusand sand. The soil mixture was introduced in 3 to 5 cm lifts followed by vibration of the column walls (using a pneumatic vibrator) and gentle stirring. A stainless steel single-piston metering pump (Eldex Laboratories, Inc., Napa, CA) was used to maintain flow. This column was one of several constructed for studying biological and chemical treatment of soil. Further detail on the column design can be found in Richardson et al. [139].

Prior to alcohol flushing, the columns were equilibrated with a simulated groundwater solution, based on historical groundwater ion concentrations near Salisbury, North Carolina [56]. This solution was prepared by adding 1.83 g $CaCl_2{\cdot}2H_20$, 1.01 g $MgSO_4{\cdot}7H_20$, 2.19 g $NaHCO_3$, 1 mL of 8.77 g/L KCl solution, and 1 ml of 1 N H_2SO_4 to 20 L of sterile-filtered DI water. For C2 only, the column operated continuously for approximately 11 months prior to cosolvent flushing. Soil samples were analyzed for PAHs immediately before cosolvent flushing to assess the loss of PAH mass during the equilibration period.

Tracer Tests

Tritium was used as a conservative tracer to determine the hydrodynamic dispersion coefficient, D, by fitting breakthrough curves to the advection-dispersion equation. A 16 nCi/mL tracer solution was prepared by combining a stock solution of tritiated water with simulated groundwater. Effluent samples were collected in glass scintillation vials, combined with a scintillation cocktail (Fisher Scientific SX23-5), and analyzed on a Packard Tri-Carb Liquid Scintillation Analyzer (Meriden, CT; Model 1900 TR).

In C2, approximately 0.5 PVs of tritiated groundwater was pumped into the column, followed by continuous flushing with non-tritiated groundwater. For C2, the tracer test was run soon after the column was prepared, prior to the equilibration period and alcohol flushing. In C3 and C4, the tritiated groundwater was pumped through the columns until complete breakthrough was observed (approximately two PVs), followed by continuous pumping of non-tritiated groundwater. A tracer test was not run on column C1, though we would expect the dispersion coefficient to be similar to column C3.

Cosolvent Flushing

In Table 3.4, the flushing strategy for each column is provided. In three of the columns, flow was halted during cosolvent flushing to test for rate effects. In C3 and C4, the time for the stop flow was increased after rate effects were observed in C1. During flushing, effluent samples were collected in glass vials equipped with PTFE-lined screw caps. In the smaller scale experiments (C1, C3, C4), effluent was

continuously collected. Sample vials were initially changed hourly during C1 and C3, and every half-hour during C4. In the largest column (C2), the samples were collected intermittently on an hourly basis, with 10 ml of effluent collected during each sampling event. In all the columns, the time between samples was increased as the change in concentrations decreased.

Table 3.4: Comparison of cosolvent flushing experiments

	C1	C2	C3	C4
Total PVs Flushed	10.6	11.9	12.1	3.8
PVs Prior to Stop	6.2	–	5.6	3.8
Stop Time	2 d	–	2 wk	4 d

Effluent samples were collected in vials pre-filled with acetonitrile for all the columns except C4, for which samples were collected in MeOH. Effluent samples were analyzed for PAHs using HPLC as described in §3.3.2. Most samples required further dilution prior to HPLC analysis. Because the concentrations of individual PAHs increased rapidly during cosolvent flushing, it was necessary to change the dilution factor between samples, periodically causing some PAHs to fall near or below the quantification limit. In C4, two or three different dilution factors were used for each sample to ensure concentrations above the detection limit. Density was also measured in C4. Since the amount of MeOH pre-added to each vial was known, the estimated MeOH concentration was corrected for the pre-added MeOH.

After cosolvent flushing, the columns were flushed with water for two to three PVs. In C4, the water flush began immediately after the stop flow and the column was rotated 180°, such that the flow direction was maintained along with a density stable front. For this column only, effluent samples were collected during the water

flush and a complete breakthrough curve could be determined for MeOH.

Post-flushing Soil Analysis

The column soil was extracted as described in §3.3.2. For the experiments conducted in the glass columns (C1, C3, C4), the soil was removed and divided into four layers along the length of the column. Each section was homogenized and a portion was used for moisture content analysis. For C2, soil samples were taken immediately before and after alcohol flushing from each of the three soil sampling ports. A portion of these samples was also used to determine the moisture content. All samples were analyzed in triplicate for PAHs.

In the glass column experiments, the final mean soil concentration was calculated as a weighted average of the concentration in each layer. In C2, the final mean soil concentrations were calculated by taking the mean of the concentrations from each sampling port. The initial concentrations were estimated by summing the mass remaining post-flushing with the mass removed during flushing, which was determined by integrating the effluent concentrations with respect to the volume flushed using the trapezoidal rule.

Modeling of Cosolvent Flushing

A code was written in Matlab to solve the two-site model (Eqn 3.3–3.6). Advection, dispersion and desorption were solved numerically using a finite-difference alternating-split-operator approach. Advection was solved explicitly using MUSCL as described

in Farthing and Miller [43] and dispersion was solved implicitly using a centered-difference formula. For the cosolvent flushing, desorption was solved for each node using an ODE solver (Matlab, ode15s). Experimental data were fit using the trust-region-reflective lease-squares algorithm (Matlab, lsqcurvefit).

3.4 Results

3.4.1 Soil Analysis

The PAH mass ratios in the soil mixture are presented in Table 3.5. The wide range of values demonstrates the heterogeneity of the mixtures and the distribution of PAH mass ratios suggests that the tar is highly weathered. In unweathered tar samples, NAP is typically the most prevalent PAH [18]. For this soil, PHE was present at the highest mass ratio. The relatively low mass ratios of NAP are consistent with other analyses of highly weathered tar-contaminated soils [89], although the soil processing methods in the current study could have also lead to additional losses of NAP by volatilization.

In addition to quantifying individual compounds, soil extracts (i.e., TEOM) were fractionated into asphaltenes, polar compounds, and neutral compounds. These data are presented in Table 3.6. This analysis revealed that 46% of the TEOM was in either the asphaltene or polar fraction. The neutral fraction was further analyzed by GC-MS. The GC-MS data were used to conduct a semi-quantitative analysis of the neutral fraction based on relative peak area. Based on this analysis, the U.S. EPA priority pollutant PAHs contributed to 24% of the total peak area. The most

Table 3.5: PAH mass ratios in the soil mixture (mg PAH/kg dry) (n=33)

Chemical	Abbreviation	MW	mean[a]	range
2 Rings				
Naphthalene	NAP	128	9.5 ± 1.5	4.5 – 25.6
3 Rings				
Acenaphthene	ACE	152	11.9 ± 1.0	8.4 – 20.1
Fluorene	FLE	166	9.5 ± 0.7	6.6 – 15.8
Phenanthrene	PHE	178	129 ± 11	73 – 254
Anthracene	ANT	178	10.5 ± 0.8	6.0 – 17.4
4 Rings				
Fluoranthene	FLA	202	25.2 ± 1.8	15.6 – 39.5
Pyrene	PYR	202	40.9 ± 2.8	25.5 – 65.5
Benzo[a]anthracene	BaA	228	13.8 ± 1.1	8.9 – 22.3
Chrysene	CHR	228	14.0 ± 1.3	9.1 – 22.7
5 Rings				
Benzo[b]fluoranthene	BbF	252	6.9 ± 0.6	4.1 – 13.2
Benzo[k]fluoranthene	BkF	252	4.2 ± 0.4	2.3 – 8.3
Benzo[a]pyrene	BaP	252	13.5 ± 1.5	8.1 – 28.5
Dibenzo[ah]anthracene	DBA	278	1.0 ± 0.2	0.6 – 3.1
6 Rings				
Benzo[ghi]perylene	BgP	276	5.3 ± 0.6	2.8 – 10.9
Total PAHs			295 ± 12	

[a] Confidence interval is the 95th percentile around the mean.

prominent group of compounds were the methylphenanthrenes, which accounted for 40% of the total peak area. The remaining peak area consisted of a large number of much smaller peaks that were typically 1% or less of the total peak area.

Table 3.6: Fractionation of TEOM from field soil, n=3

Fraction	Mean	SD	RSD
Asphaltenes	25.4	0.7	0.027
Polar compounds	20.8	1.9	0.089
Neutral compounds	45.0	1.4	0.030

3.4.2 Batch Experiments

The batch data were used to determine the cosolvent partition coefficient, K_i, for f_c ranging from 0 to 1. In Figure 3.1, log K_i is plotted as a function of f_c for PHE and BaP. As shown in Figure 3.1, the K_i sometimes spanned as much as an order of mag-

nitude for a given f_c, while the high MW PAHs were often below the quantification limit for the low f_c batch tests. Regardless, the data were well fit by the log-linear model (Eq 3.2), for which the coefficients and corresponding R^2 values are provided in Table 3.7.

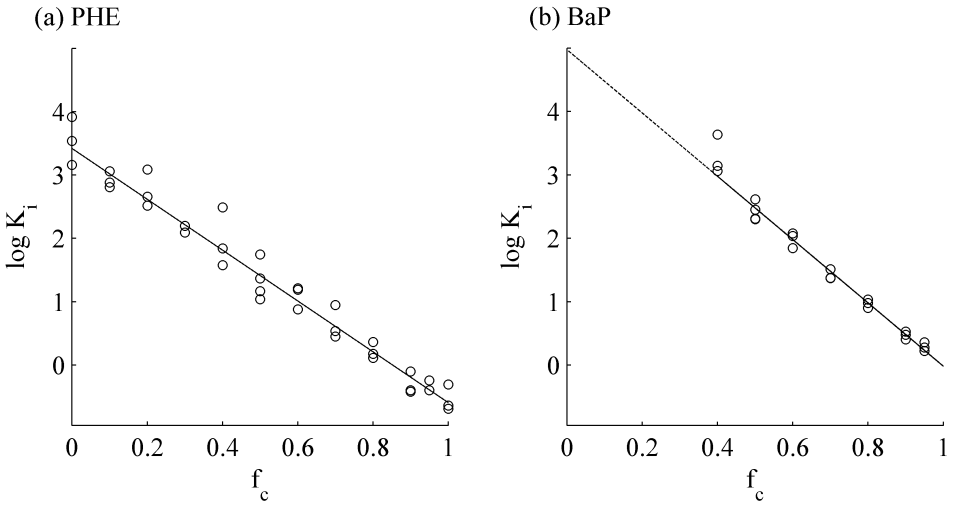

Figure 3.1: Least-square fits to batch data using the log-linear model (Eqn. 3.2) for PHE and BaP. The dashed line represents values extrapolated beyond the experimental data.

3.4.3 Tracer Tests

A standard advective-dispersive model was fit to the tracer test data. Results are given in Table 3.3 for all the columns and plots are given in Figure 3.2a and 3.3a for C2 and C4. All the data were well fit by the advective-dispersive model.

The tracer data were used to predict the MeOH f_c in the cosolvent flushing experiment in C2. In Figure 3.2b, the modeled f_c is compared to estimates based on the mass and volume of each sample. This is a relatively imprecise method but does

Table 3.7: Least-squares coefficients, log K_{iw} and $\alpha\sigma_i$, for predicting log K_i as a function of f_c (Eq 3.2).

PAH	log K_{iw}	$\alpha\sigma_i$	R^2	n	Range of f_c
2 Rings					
NAP	3.3 ± 0.3	2.8 ± 0.5	0.909	30	0.2 – 1
3 Rings					
ACE	2.7 ± 0.3	3.1 ± 0.4	0.919	36	0 – 1
FLE	2.9 ± 0.2	3.1 ± 0.4	0.940	36	0 – 1
PHE	3.5 ± 0.2	4.2 ± 0.3	0.970	36	0 – 1
ANT	3.3 ± 0.2	3.4 ± 0.3	0.968	36	0 – 1
4 Rings					
FLA	3.7 ± 0.3	4.3 ± 0.4	0.965	33	0.1 – 1
PYR	4.0 ± 0.3	4.9 ± 0.4	0.973	30	0.2 – 1
BaA	4.5 ± 0.3	5.0 ± 0.4	0.979	30	0.2 – 1
CHR	4.6 ± 0.4	5.2 ± 0.5	0.961	30	0.2 – 1
5 Rings					
BbF	5.0 ± 0.5	5.2 ± 0.6	0.966	23	0.4 – 1
BkF	4.6 ± 0.3	4.7 ± 0.4	0.981	22	0.5 – 1
BaP	5.2 ± 0.4	5.3 ± 0.5	0.974	22	0.4 – 0.95
DBA	5.8 ± 0.8	6.1 ± 0.9	0.967	16	0.6 – 1
6 Rings					
BgP	5.2 ± 0.4	5.0 ± 0.5	0.978	20	0.4 – 0.95

provide some indication that the MeOH concentrations are reasonably estimated using the dispersivity from the tracer tests, although there does appear to be slightly sharper breakthrough of MeOH as compared to the conservative tracer.

For C4, the density was measured in the effluent samples, providing a more precise estimate of f_c. In this case, the dispersion data from the conservative tracer did not provide a good fit to these data. In addition, the breakthrough-curve for MeOH was not symmetric; thus, the up and down portion were fit separately and are given in Figure 3.3b. Though fitting the up and down portion of the curve was an improvement, the MeOH data still deviated from the advection-dispersion model.

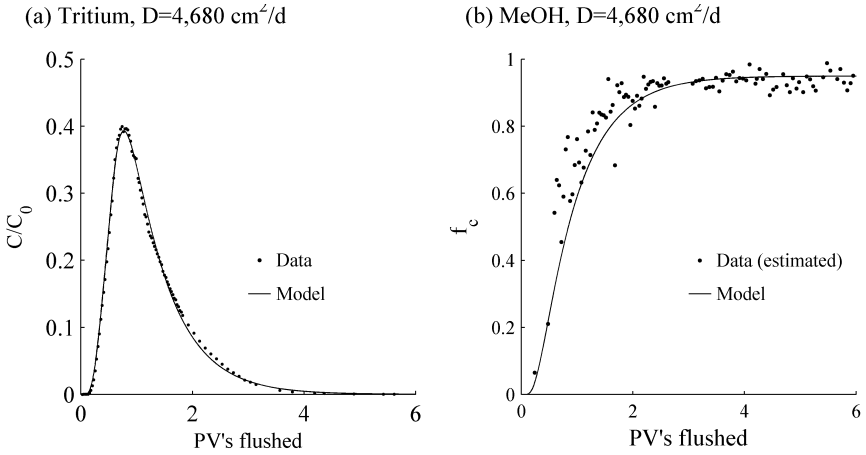

Figure 3.2: Tritium and MeOH concentration as a function of PVs flushed in C2 (110 cm). The dispersivity from the tracer test was used to estimate the methanol f_c.

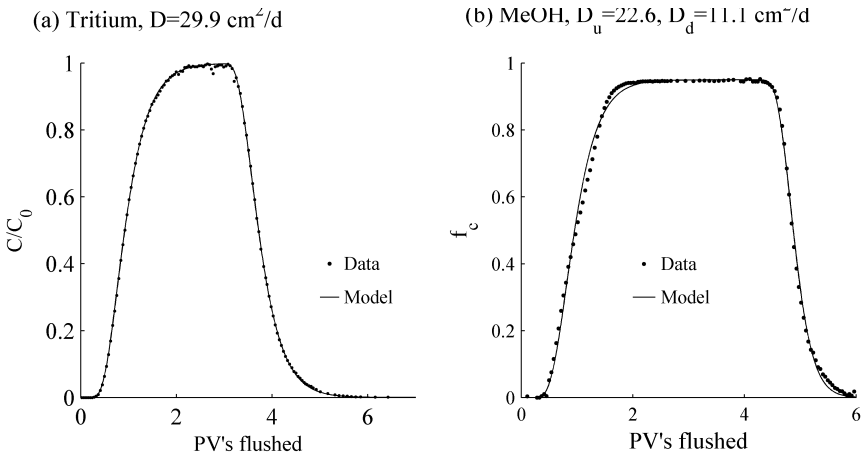

Figure 3.3: Tritium and MeOH concentration as a function of PVs flushed in C4 (11.9 cm). The MeOH data was fit separately to determine the dispersion coefficient during the breakthrough and elution portions of the curve.

3.4.4 Column Flushing Experiments

Cosolvent flushing was found to significantly reduce the mass of PAHs in all the column experiments. Figure 3.4 compares the pre- and post-flushing soil mass ratios in C1 and C2. Values are shown for the 10 PAHs that were consistently quantifiable during these experiments. The pre-flushing mass ratios are estimated as described in §3.3.4 and are in reasonable agreement with measurements from the soil mixture. We also did not find any significant difference in the mass ratios measured immediately before flushing. The post-flushing mass ratios are average values measured along the extent of the column. Based on the 10 PAHs in Figure 3.4, the PAH mass was reduced 93% in C1 and 95% in C2.

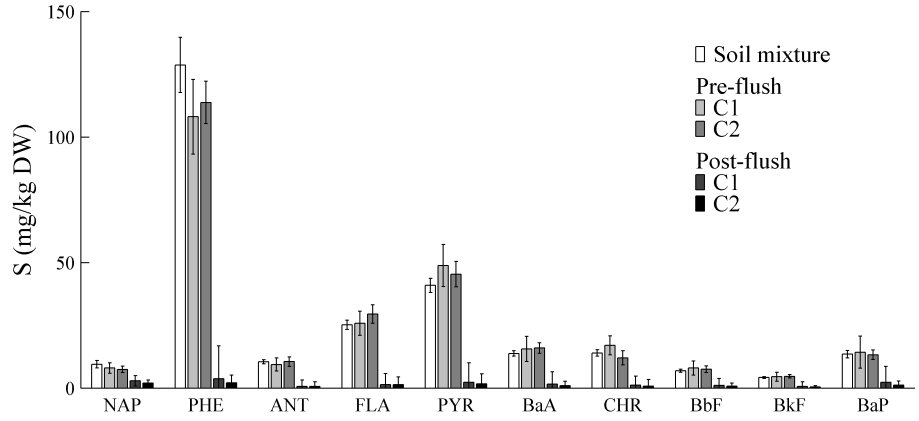

Figure 3.4: Comparison between soil mass ratios pre- and post-flushing in columns C1 (22.2 cm) and C2 (110 cm). The pre-flushing mass ratios compare favorably to the mass ratios in the original soil mixture.

Although the total PAH mass removed was similar between C1 and C2, achieving the same amount of mass removal in C2 required more PVs of cosolvent flushed as compared to C1. In Figure 3.5, the cumulative fraction of mass removed is plotted for the first 10 PVs flushed. The number of PVs required to remove 50% of the PAH mass was 1.8 in C1 and 3.9 in C2, while 90% removal required 6.5 in C1 and 9.5 in C2.

We also found that individual compounds eluted over different time scales. In Figure 3.5, the cumulative mass removed for individual compounds is plotted. These curves are grouped by the number of rings for a given PAH. For the most part, the three, four, and five-ring PAHs eluted in order of decreasing solubility. Interestingly, NAP eluted last, despite having the highest solublity. Also, NAP was the only compound to show a slight increase in concentration at the stop flow in C1.

In C3 and C4, longer stop flows were allowed and rate effects were more clearly observed. In these experiments, all the PAHs in Table 3.5 were quantifiable. The total PAH mass was reduced 89% in C3 and 81% in C4. In Figure 3.6, the cumulative mass removal is plotted for C3 and C4. During the stop in flow, NAP had the most significant increase in relative mass removed followed by the three and four-ring PAHs. The five and six-ring PAHs had relatively small increases in concentrations that are not visible on this scale.

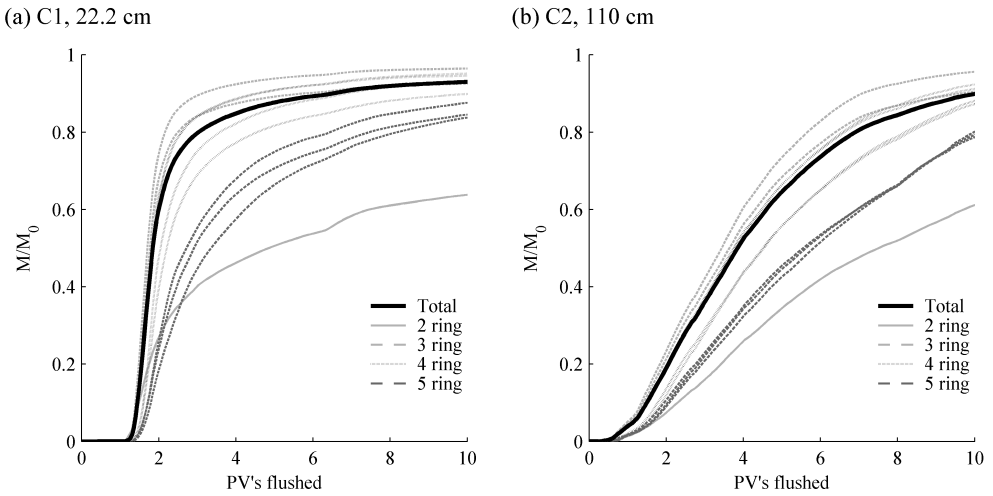

Figure 3.5: PAH mass removal as a function of PV in columns C1 and C2 after flushing 10 PVs of cosolvent (MeOH $f_c = 0.95$) for the 10 PAHs noted in Fig 3.4.

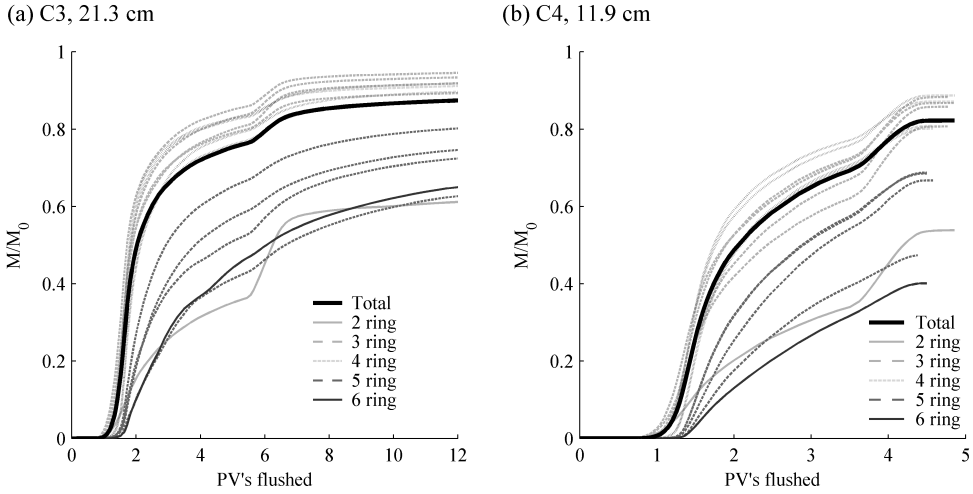

Figure 3.6: PAH mass removal as a function of PV in columns C3 and C4 during cosolvent flushing (MeOH $f_c = 0.95$) for the 14 PAHs in Table 3.5. Flow was stopped at 5.6 PVs in C3 and 3.8 PVs in C4. In C4, the column was flushed with water immediately after the stop flow, while C3 was flushed with additional cosolvent.

3.4.5 Modeling

The two-site model was used to simulate the concentrations eluting from the columns. A series of simulations was conducted to determine the need for fitting various parameters: (1) assuming equilibrium (i.e., F_i=1), (2) fitting F_i and calculating the rate k_i using Eq 3.8 and coefficients from Bouchard [20], (3) fitting F_i and k_i, and (4) fitting F_i, k_i, and the two parameters required to calculate K_i (i.e., K_{iw} and $\alpha\sigma_i$). The model fits were very sensitive to the steep gradients during the flow of MeOH into and out of the column; thus, we did not include concentrations during the first PV, or after PV 4.8 in C4, in the data used for fitting.

When using an equilibrium only assumption, the model predicted the concentrations dropping much too fast and did not predict increased concentrations during the stop flows. Using calculated rate constants and fitting F_i, we saw limited improvement to the model fits compared to the equilibrium assumption, indicating that the rates were likely too high. When fitting both k_i and F_i, we were able to better capture the tails and predict the increase after the stops; however, the peak concentrations were often underestimated. When fitting the four parameters, F_i, k_i, K_{iw} and $\alpha\sigma_i$, we were better able to capture both the tails and predict the peak concentrations. The fitted parameter values along with the L_2 norm of the error are provided in Table 3.8.

The parameters in Table 3.8 data were used to model the effluent concentrations and are compared to the data in Figure 3.7, 3.8, and 3.9 for columns C2, C3 and C4, respectively. In general, the model provided a good fit to the experimental data. For C2, the concentrations were well predicted throughout the experiment for most

Table 3.8: Fitted parameter values and the L_2 norm of the error.

Column	PAH	log K_{iw}	$\alpha\sigma_i$	F_i	k_i (day^{-1})	L_2
C2	NAP	3.01	3.26	0.063	0.145	0.94
	PHN	3.28	4.50	0.071	0.537	1.16
	ANT	3.12	3.72	0.280	0.843	1.36
	FLA	3.49	4.57	0.106	0.434	0.94
	PYR	3.73	5.23	2.1E-05	0.390	0.91
	BaA	4.25	5.35	0.074	0.274	0.82
	CHR	4.29	5.45	4.7E-03	0.294	0.92
	BbF	4.49	5.77	0.037	0.172	0.92
	BkF	4.30	5.17	0.044	0.188	0.92
	BaP	4.81	5.74	0.033	0.179	1.06
C3	NAP	3.01	3.26	0.267	0.039	3.07
	ACE	2.38	3.31	0.726	0.353	2.56
	FLU	2.67	3.52	0.638	0.374	1.00
	PHN	3.28	4.16	0.681	0.370	1.05
	ANT	3.12	3.72	0.736	0.355	1.36
	FLA	3.45	4.27	0.735	0.315	1.38
	PYR	3.72	4.52	0.724	0.292	1.36
	BaA	4.42	5.03	0.709	0.315	1.28
	CHR	4.96	5.58	0.716	0.341	1.31
	BbF	4.54	4.83	0.581	0.188	1.63
	BkF	4.88	5.17	0.723	0.043	1.43
	BaP	5.56	5.74	0.620	0.033	1.19
	DBA	5.77	5.72	0.421	0.028	1.35
	BgP	5.58	5.45	0.462	0.020	1.89
C4	NAP	3.01	3.26	0.137	0.271	1.10
	ACE	2.38	3.28	0.483	0.515	0.49
	FLU	2.67	3.47	0.375	0.480	0.54
	PHN	3.28	4.25	0.520	0.512	0.66
	ANT	3.12	3.72	0.368	0.418	0.83
	FLA	3.45	4.40	0.567	0.439	0.74
	PYR	3.72	4.78	0.649	0.523	0.82
	BaA	4.67	5.35	0.541	0.288	1.25
	CHR	4.96	5.67	0.546	0.316	1.26
	BbF	5.39	5.77	0.368	0.395	1.59
	BkF	4.84	5.17	0.423	0.359	1.50
	BaP	5.48	5.79	0.308	0.453	1.70
	DBA	5.02	5.18	0.373	0.162	1.03
	BgP	5.55	5.50	0.210	0.356	1.61

chemicals and the average L_2 norm of the error was 0.99. For C3, the average L_2 norm of the error was higher at 1.6. This experiment included a stop flow. For most of the PAHs, the model consistently was unable to fit the concentrations immediately prior to the stop in flow. The model also tended to predict higher concentrations in the effluent after the stop flow. In C4, the average L_2 norm was 1.08, similar to C2; however, considerably better fits were obtained for the lower MW PAHs. The average L_2 error was 0.63 for the two-ring PAHs and 1.45 for the five ring PAHs.

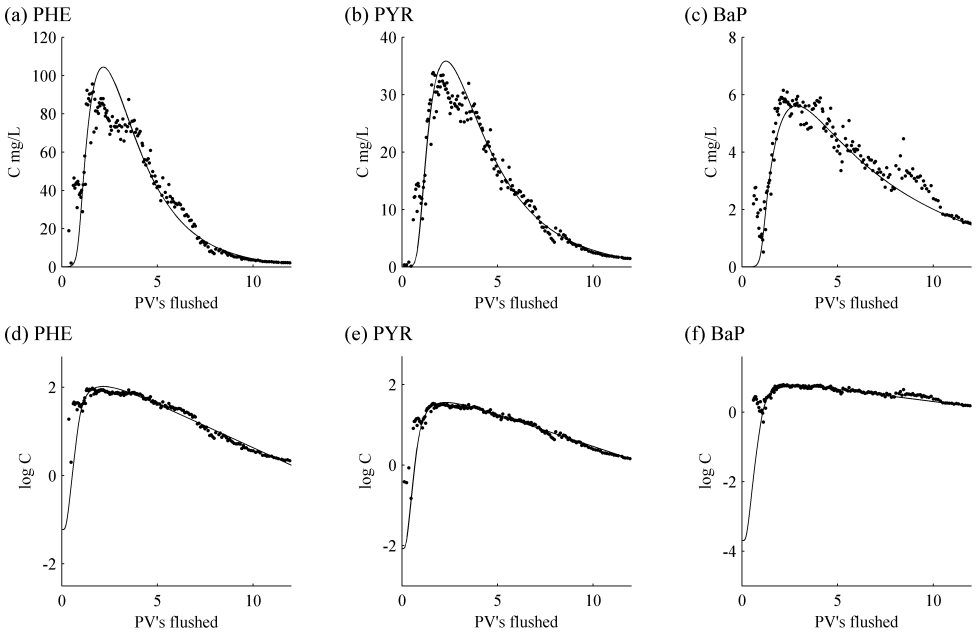

Figure 3.7: Modeled effluent concentrations compared to data from C2.

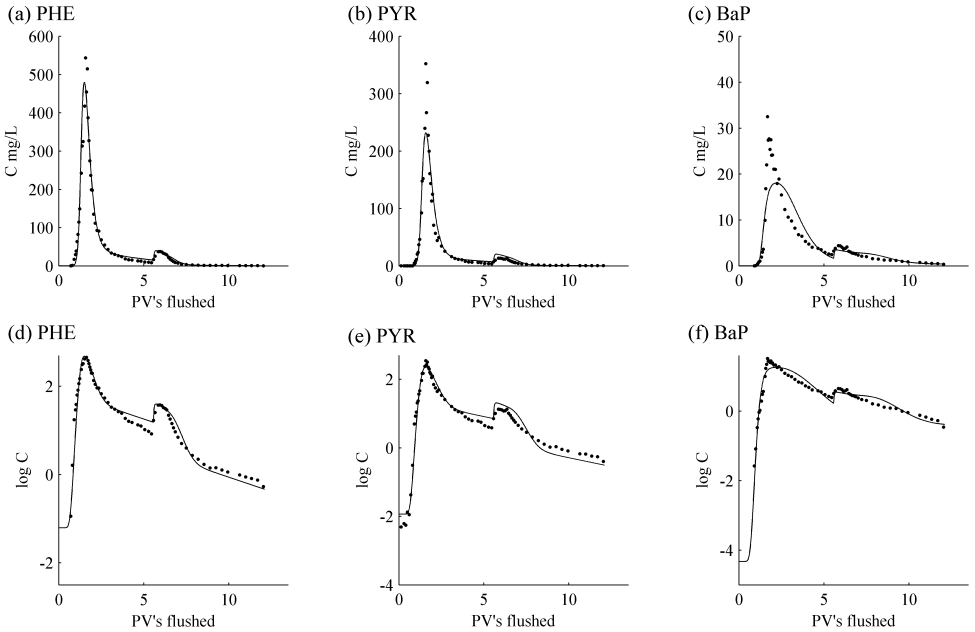

Figure 3.8: Modeled effluent concentrations compared to data from C3.

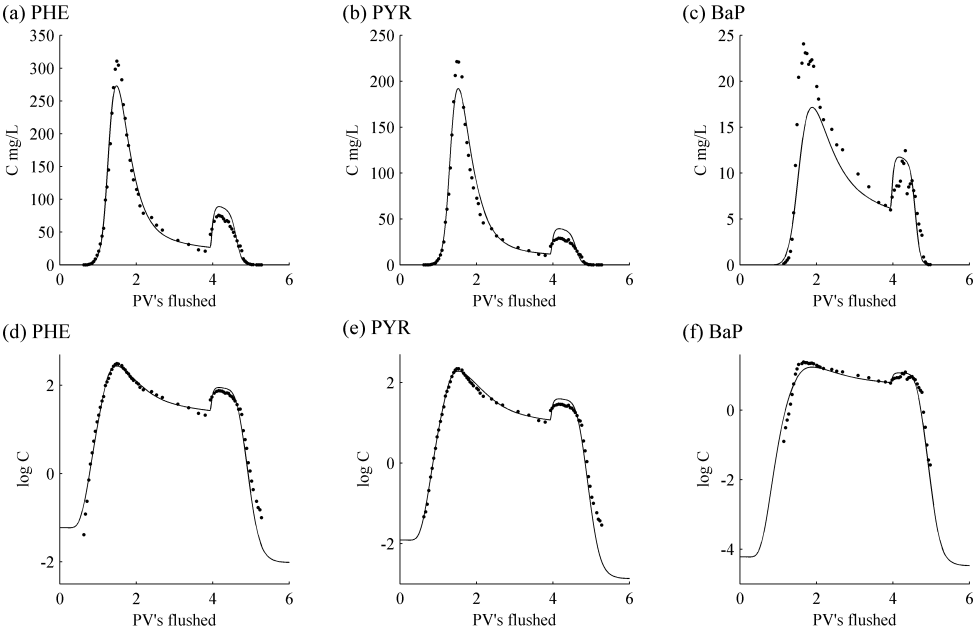

Figure 3.9: Modeled effluent concentrations compared to data from C4.

In Figure 3.10a and 3.10b, the fitted values for K_{iw} and $\alpha\sigma_i$ are plotted for each of the columns and compared to the values from the batch experiments. For most of the two-, three-, and four-ringed compounds, there was excellent agreement between the fitted values across the columns. For these compounds, the fitted values of K_{iw} tended to be lower than the batch data, while the values of $\alpha\sigma_i$ tended to be higher. This trend was less evident for the five- and six-ringed compounds, for which there was a lot more scatter in the data.

In Figure 3.10c and 3.10d, the fitted values for F_i and k_i are plotted. F_i did not show any trend across chemicals but varied between the columns. The average value for F_i was 0.068 in C2, 0.63 in C3, and 0.48 in C4. For the rate constant, the values tended to be higher for the three- and four-ringed PAHs; however, there was a lot of scatter in the data.

3.5 Discussion

In this work, we investigated the remediation of field-contaminated media from a FMGP using cosolvent flushing. These experiments were conducted in systems with varying hydrodynamic characteristics. Specifically, the longest column, C2, had much greater dispersivity than the smaller columns, which is likely due to increased heterogeneity in the column packing. The increase in dispersivity with length scale is a well-documented phenomena that is generally attributed to increased heterogeneity [46]. We found that remediation was less efficient in the largest column (e.g., 110 cm), such that more PVs were needed for the same amount of PAH removed.

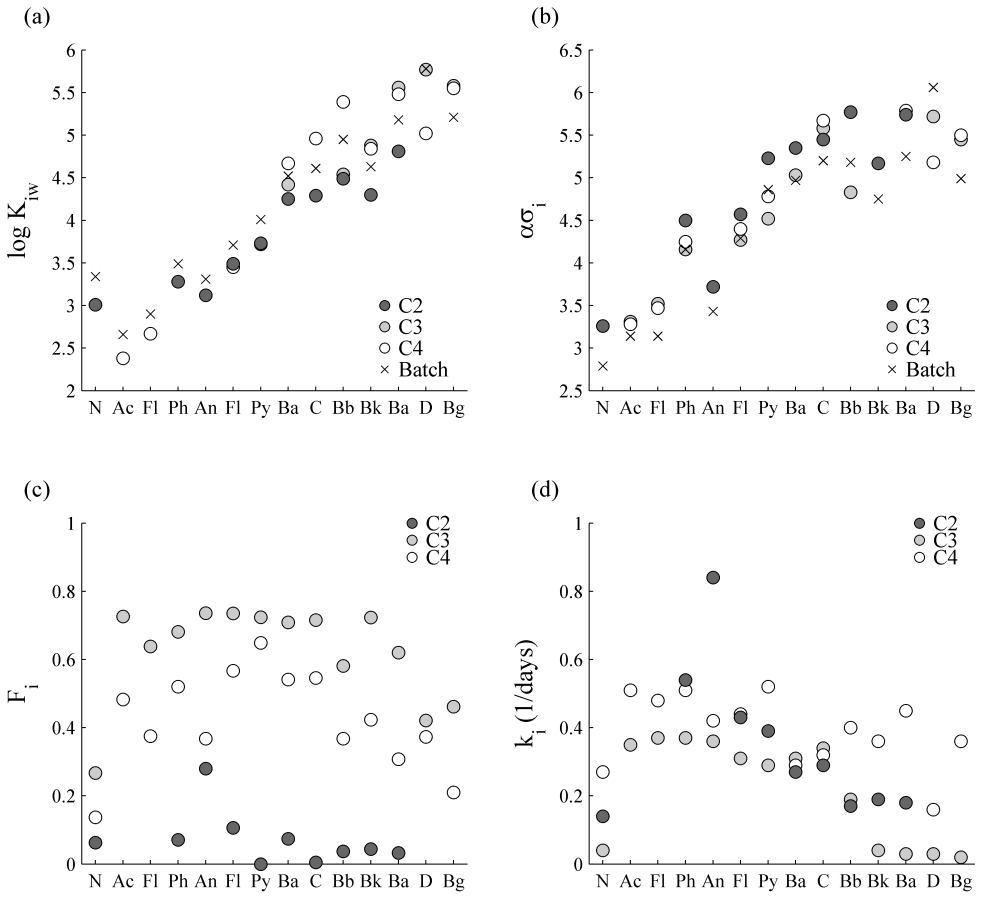

Figure 3.10: Fitted parameter values.

Though the 110 cm column is still relatively small when compared to field scale, the results from this column provide a better indication of the efficiency of cosolvent flushing in field-scale systems.

Results from other studies have suggested that using a high f_c would eliminate rate and chromatographic effects [25, 12, 20]. The results here suggest that this is not the case for field contaminated soil. When flow was temporarily halted, we found rate effects to be present in all the small columns. NAP in particular appeared to be highly rate-limited, despite being the most soluble PAH considered. Other than NAP, we also found that the most soluble PAHs tended to elute before the least soluble, higher MW PAHs. The chromatographic effects were most prominent in the largest column.

Experimental data were fit using a two-site model. In general, the model provided a reasonable fit to the experimental data. As reported previously, the model was found to be extremely sensitive to the equilibrium partition coefficient, K_i, [20], and even small changes in this parameter could provide significant improvements to the model fits. The values for K_i were estimated as a function of K_{iw} and $\alpha\sigma_i$. During the model fitting, the values for K_{wi} and $\alpha\sigma_i$ were constrained by the 99% confidence interval of the predicted values based on the batch tests. In batch tests, many of the high-MW PAHs were below the quantification limit for low values of f_c. These compounds also tended to have the most error in the model fits. Using improved analytical methods for batch tests may provide better data, which would further improve model fits.

Values for K_i are also a function of f_c, which varied over the course of the exper-

iment as MeOH displaced the water in the column. Following Augustijn et al. [12], we initially used the dispersivity from a conservative tracer to model the cosolvent breakthrough curve. In column C4, we measured density of the effluent and found evidence of sharpening of the cosolvent front, consistent with other miscible displacement studies [58]. In addition to sharpening of the MeOH front, we also found that the MeOH breakthrough curve deviated from the advection-dispersion equation. It is not clear if this deviation is caused by instabilities that developed despite the stable displacement or due to interactions between MeOH and the soil organic matter. In past studies, MeOH has been shown to impact the sorptive properties of natural organic matter [19]. More work is need to understand how MeOH may be interacting with the organic phase in FMGP soils. Because the concentrations of PAH are a small fraction of the total organic matter, we do not expect the average molecular weight to vary greatly during cosolvent flushing.

Raoult's Law can be used to account for compositional changes during tar dissolution Peters et al. [123]. Estimating equilibrium concentrations according to Raoult's Law would require an estimate of the amount of tar mass remaining on the soil, which would be difficult to ascertain given the degree of aging. Rather than estimating equilibrium concentrations, we based these concentrations on measured values for K_i determined from batch studies. Given Raoult's Law, K_i may vary with composition when the average molecular weight changes. Because the concentrations of PAH are a small fraction of the total organic matter, we do not expect the average molecular weight to vary greatly during cosolvent flushing.

Parameter values for F_i and k_i were determined by fitting the model to experimental data. In previous studies, F_i was shown to decrease to near zero as f_c increased [25, 12]. In this work we used a very high f_c, and yet the best fit value for F_i was over 0.4 for most of the chemicals in the smaller columns. Similar to other studies, we did not see any trend for F_i between chemicals; however, we did see a difference in the F_i between systems with varying hydrodynamic characteristics. Specifically, we found that F_i decreased as the dispersion coefficient increased.

Unlike past studies, we did not find a strong correlation between k_i and K_i, according to Eq 3.8. In Figure 3.11, we compare rate constants determined for the aged-FMGP soil to values calculated using Eq 3.8. The rate constants for the aged soil were approximately two to three orders of magnitude less than values based on artificially contaminated sand. Other studies have found these relationships provided a good fit to experimental data [12]; however, previous studies replicated the experimental set-up used to derive the k_i and K_i relationship, using single-solute systems, $\sim$5-cm columns, and relatively high flow rates. As noted by Augustijn et al. [12], high flow rates were necessary to induce rate effects. They also noted that rate effects diminished with higher f_c. In this study, flow rates were much slower and we used a higher f_c, yet we still observed rate effects in all our column experiments.

Although the model provided a reasonable fit to the data, the fitted parameters do not necessary reflect the physical phenomena of the system. Others have shown that as f_c increases, the value for k_i increases and the value for F_i decreases [25, 12]. This is somewhat counterintuitive. As k_i increases, the effluent concentrations approach

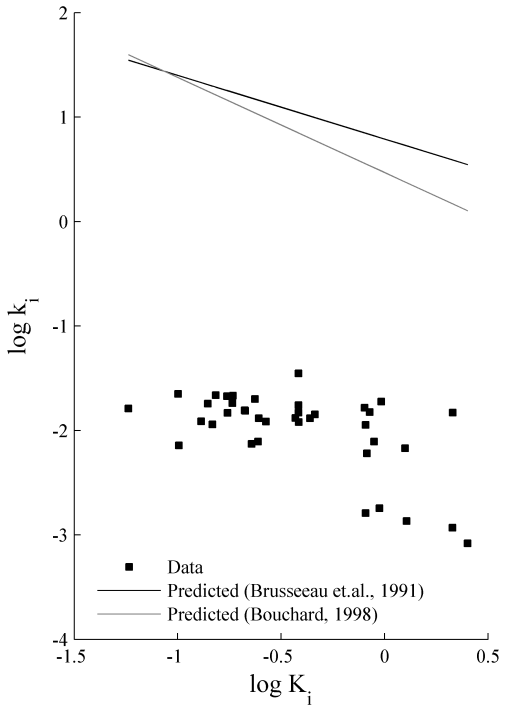

Figure 3.11: Relationship between the mass transfer rate, log k_i, and the partition coefficient, log K_i (f_c=0.95). The k_i data are for the FMGP soil (Table 3.8) and were converted to units of hr^{-1} to compare with predicted values from Eq 3.8, which were based on artificially contaminated sands.

the model prediction of the equilibrium only assumption, $F_i = 1$. We found that using values for k_i predicted from Eq 3.8 resulted in the model being completely insensitive to the chosen value for F_i. We believe better modeling approaches are needed in which the model parameters have a well-defined physical meaning.

It is also important to recognize that this model is a simplification of a very complex system, especially in terms of the nature of the organic phase. In our analysis, we only monitored PAH concentrations, but we would expect other compounds to also be removed during flushing. In other words, we not only have desorption of PAHs from the organic phase, but the organic phase is itself undergoing some degree of dissolution. We do not know how the other components of the organic phase (e.g., polar compounds and asphaltenes) are impacted by cosolvent flushing. Improvements can be gained from a better understanding of this dissolution process. Future models may also be improved by explicit consideration of the flow equation to account for the non-ideal flow behavior of MeOH during cosolvent flushing.

3.6 Conclusion

These results illustrate the importance of using field samples in order to understand the complexity of contaminant behavior in environmental systems. We found previous conclusions and relationships developed based on artificially contaminated sands did not translate to the field-contaminated soil used in this study. Existing relationships to predict mass transfer rates were incapable of simulating the desorption from field contaminated media. Though we significantly reduced the chromatographic effect, we

still found that compounds were removed over varying time scales, particularly in the largest column. In evaluating cosolvent flushing, it is extremely important to consider compounds on an individual basis, particularly for higher MW compounds that can drive human health risk. Interestingly, NAP was also extremely recalcitrant despite being the most soluble PAH, which was also contrary to results based on artificially contaminated media.

Cosolvent flushing has the potential to remove large quantities of contaminant mass with a minimum number of PVs, compared to water flushing alone. For a particular site, the appropriateness of cosolvent flushing will be dependent on a number of factors including site heterogeneity and the particular remediation goal. Regardless, removing all of the contaminant mass is likely to be an unachievable goal even when using a high cosolvent fraction. Batch and column studies can be used to understand how a particular media will respond to a given remediation technology, such as cosolvent flushing. Improvement to models will aid our ability to evaluate the effectiveness of cosolvent flushing over temporal and spatial scales and provide reasonable estimates of the number of PVs required for a given remediation goal.

CHAPTER 4

THE EFFECT OF TEMPERATURE AND CHEMICAL COMPOSITION ON THE VISCOSITY AND DENSITY OF COMPLEX TAR MIXTURES

P.S. Birak[1], S.C. Hauswirth[2], and C.T. Miller

4.1 Abstract

Tars are a by-product of gas manufacturing that are present in the subsurface at many former manufactured gas plants (FMGPs). Viscous tars are generally slow-moving in the subsurface and difficult to recover under ambient conditions. Thermal treatment can be used to lower tar viscosity. To accurately predict the removal of tar during thermal treatment, viscosity-temperature correlations are needed. For this work, tar samples were obtained from eight wells at two FMGPs. The tars were analyzed to determine the concentration of monocyclic aromatic hydrocarbons (MAHs) and polycyclic aromatic hydrocarbons (PAHs). Viscosity and density were measured from 5 to 70°C. Tar composition and properties varied spatially across both sites, illustrating the importance of considering tar heterogeneity. The density and viscosity data were fit to standard equations and coefficients were determined for predicting these data given reference values. Density data were well fit using a linear correlation to temperature and a constant coefficient across all the tars.

[1]Responsible viscosity measurements, data analysis, and manuscript preparation.
[2]Responsible for analysis PAHs, MAHs, and asphaltenes.

The commonly used Andrade equation was not valid for predicting tar viscosity as a function of temperature because the activation energy for viscous flow was not constant over the temperature range. Instead, the data were well-fit to the Vogel-Fulcher-Tammann-Hesse equation, which is commonly used for glasses. The deviation from the Andrade equation was directly correlated to sample density. Empirical equations were developed to predict viscosity as a function of temperature using both a reference density and viscosity.

4.2 Introduction

From the early 1800s to the mid 1900s, the U.S. EPA estimates that between 36,000 to 55,000 gas plants and related sites existed in the U.S. prior to the widespread use of natural gas [154]. Though the type of gas produced varied regionally and over time, three gas manufacturing processes were dominant in the U.S.: water gas, coal gas, and oil gas [57, 108, 54, 18]. The by-products from these operations varied, but all produced large quantities of tar [18]. Though sometimes used as fuel or sold to tar refineries, tar has also contaminated soils and groundwater through leaking tanks and intentional disposal.

Tars produced at FMGPs are a complex mixture of mostly aromatic, organic compounds. The exact chemical composition of tars is not known but includes volatile monocyclic aromatic compounds MAHs, semi-volatile polycyclic aromatic compounds PAHs, and an essentially non-volatile pitch fraction [18]. Though sparingly soluble, the dissolution of these compounds from tar to groundwater may pose a risk to human

health [95]. The composition of tar across a given site is also likely to vary given the changes in tar manufacturing over time; however, limited data have been published on the heterogeneity of tar for a given site [18].

Tars in the subsurface are classified as dense non-aqueous phase liquids (DNAPLs). Though the exact distribution of tars in the subsurface is a function of complex capillary history and interfacial phenomena, these materials tend to migrate downward when released to the saturated zone. In some cases, large volumes of subsurface tar have resulted in horizontal movement of a tar plume over some confining layer. The first site to receive emergency funding under U.S. EPA's Superfund program was a FMGP in Stroudsburg, PA [95]. At this site, a slow moving tar plume was contaminating a nearby creek, posing a direct risk to human health and the environment.

Unfortunately, detecting the migration of tar DNAPLs is difficult due to the slow moving nature of these plumes. One of the key properties required to predict flow is the viscosity, or resistance to flow. Mathematically the dynamic viscosity is defined as

$$\eta = \frac{\tau}{\dot{\gamma}} \tag{4.1}$$

where η is the viscosity, τ is the applied shear stress, $\dot{\gamma}$ is the resulting shear rate [51]. When the viscosity is constant over a range of shear stresses for a given temperature, the liquid is considered Newtonian.

It is widely recognized that increasing temperatures will decrease viscosity. One of the most widely used equations to correlate viscosity with temperature is an

Arrhenius-type equation, commonly referred to as the Andrade equation, where

$$\ln \eta = A + B\frac{1}{T}. \tag{4.2}$$

Values for A and B can be determined from a plot of $\ln(\eta)$ versus $1/T(\mathrm{K})$ [51]. For many liquids, the slope of this line, B, is a constant, which can be interpreted as the activation energy for viscous flow, E_a, divided by the ideal gas constant, R. In currently available multiphase modeling software (e.g., UTCHEM-9.0 [131]) this relationship is used to calculate the viscosity as a function of temperature given a known value at a reference temperature, such that

$$\eta = \eta_r \exp\left[B\left(\frac{1}{T} - \frac{1}{T_r}\right)\right]. \tag{4.3}$$

Thermal treatment of FMGP sites has become increasingly attractive for increasing the ability to pump tars O'Carroll and Sleep [115]; yet, limited data are available on the variability of tar viscosity with temperature. Birak and Miller [18] compiled data on the viscosity of tars at 35°C but found limited data at other temperatures relevant to subsurface systems or for elevated temperatures. Kong [77] measured the viscosity for three FMGP tars from at 20, 30, 40 and 50°C. These data were well fit by Eqn 4.2; however, plots of the data on a log scale revealed some curvature over this limited temperature range. For large temperature ranges, this equation may not hold.

The overall goal of this work is to advance understanding of the physicochemical

characteristics of tars from FMGPs. The specific objectives of this work are the following: (1) to measure the density and viscosity of tars as a function of temperature; (2) to determine an appropriate equation of state for tar density; (3) to determine a functional relationship that describes tar viscosity; and (4) to determine the change in physicochemical properties as a function of location and field site to assess variability.

4.3 Experimental section

4.3.1 Tar Sampling

Subsurface tar samples were obtained from wells at two FMGPs: one in Portland, Maine and the other in Baltimore, Maryland. From the Portland site, tar samples were obtained from five wells in August 2006. The site consists of inland and shoreline parcels of land. Two adjacent wells were located on the inland parcel, closest to the presumed location of tar disposal (P1, P2). Approximately 700 ft away, three wells were sampled from the shoreline parcel (P3, P4, P5) near an intermittent seep of tar into the Fore River, which is believed to be the result of subsurface tar migration. P3 was located ∼130 feet from the river bank. P4 and P5 were adjacent to one another and located ∼65 feet from the river bank. From the Baltimore site, one well was sampled in May of 2007 (B1). B1 was re-sampled in July 2009 along with two additional wells: one less than 50 ft away from B1 (B2) and another ∼1,000 ft away (B3). Samples from B1 and B2 were from a tar pool resting on a confining layer, near a former tar disposal pit. B3 was located near a former tar injection well. All samples were stored at 4°C prior to sampling and analysis.

4.3.2 Sample Characterization

Quantification of MAHs and PAHs was conducted on a Hewlett-Packard 5890 II GC equipped with a flame-ionization detector (FID). The column used was a 30 m Equity-5 (95%methyl- 5%phenyl-methylsiloxane) capillary column with an ID of 0.25 mm and a 0.5 μm film thickness. The analysis was divided into two runs, the first for compounds with boiling points up to 150°C (MAHs) and the second for compounds with boiling points from 150°C to about 500°C (PAHs).

For all runs, the chromatographic conditions were as follows: injector 300°C, detector 310°C, constant helium carrier flow of 1 mL per minute, and splitless injection. For the MAH analysis the oven was programmed as follows: initial temperature 30°C, hold 4 minutes, increase at 2°C per minute to 40°C, hold 2 minutes, increase at 7°C per minute to 80 °C, hold 5 minutes, then increase at 70°C per minute to 315°C. For the PAH analysis, the oven was programmed as follows: initial oven temperature 40°C, hold 2 minutes, increase linearly at 4°C per minute to 310°C, hold 5 minutes.

MAH analyses were conducted by first sonicating the tar sample with n-pentane for 10 minutes, then filtering with a 0.2 μm PTFE syringe filter. Fluorobenzene was used as the internal standard. The PAH analysis was conducted using the same method as the MAH analysis, except that a 3:1 n-hexane/acetone mixture was used as the solvent. Internal standards were added to span a wide range of molecular weights. Specifically, 2-fluorobiphenyl, 1,8-dimethylnaphthalene, 4,4'-dimethylbiphenyl, m-terphenyl, 2,2'-binaphthalene, and perylene were selected because they were commercially available and, with the exception of perylene, do not coelute with compounds

in the sample. The area under the perylene peak was corrected by using the area relative to benzo[a]pyrene determined from a non-spiked sample.

Asphaltenes are were determined as the mass of tar that is insoluble in n-pentane. Others investigating FMGP tars have typically used ASTM D2007 to separate asphaltenes [119, 15, 167]. Briefly, with this method n-pentane is added to the sample at a 10:1 ratio, the mixture is warmed, stirred, settled for 30 min, and filtered. An improved asphaltene method was developed based on combining several techniques described in the literature, which included extended precipitation times [148], the use of a sonication bath [4], and reprecipitation from toluene [146]. Specifically, asphaltene concentration was determined by adding 60 mL of n-pentane to 1.5 g of tar, sonicating for 15-minutes, and settling for 24 hours. The liquid portion was decanted through a vacuum filtration apparatus with a 0.2-m nylon filter. The precipitate remaining in the flask was dissolved in toluene at a ratio of 10 mL per gram of solid, and sonicated until the solids were completely dissolved. The asphaltenes were then reprecipitated by adding n-pentane at a ratio of 50 mL per mL of toluene-asphaltene, allowed to settle for 30 minutes, and vacuum filtered using the same filter as was used in the first stage. The flask and precipitate were rinsed with an additional 200 mL of n-pentane and dried under vacuum and weighed. This analysis was conducted for each of the samples in triplicate.

Density was measured using an Anton Paar density meter (Model DMA 48). Rheological measurements were made using a stress controlled rotational rheometer (TA Instruments, Model AR-G2) equipped with a 40-mm cone and plate. A Peltier

plate was used to control the temperature. Measurements were made from 5 to 70°C with a shear rate of 5 s^{-1} for the lower viscosity fluids, and a shear rate as low as 0.1 s^{-1} for the more viscous samples. Though some shear thinning behavior was observed in these fluids at low shear rates, the shear rate selected for the temperature curves was well within a region where viscosity was no longer varying.

4.3.3 Standard Materials

Three viscosity standards were obtained to span the range of viscosity in the tar samples (Cannon Instrument company, Standards N10, S60, and S600). The N10 and S60 standards are both highly-refined mineral oils, which are straight-chained hydrocarbons. S600 is a poly-alpha-olefin. The standards were used both to validate the methodology for the rheometer and also to provide an example of a less chemically complex mixture as compared to the FMGP tars. A commercially available coal tar was also analyzed (Fisher Scientific).

4.4 Results

4.4.1 Composition

Table 4.1 provides a summary of the chemical characterization of FMGP tars and the commercial coal tar. Concentrations were summed by number of rings. Though not provided in Table 4.1, the concentrations from multiple samples from the same well were very similar. As shown in Table 4.1, the concentrations taken from the same well, but two years apart, were also very similar. In terms of variability across a given

site, concentrations varied little between wells that were essentially co-located, while concentrations varied considerably between wells that were further apart.

4.4.2 Density and Viscosity

The density and viscosity at 20°C is provided in Table 4.1. For the Portland samples, the upland wells were more dense and had a higher viscosity than the shoreline wells. The Baltimore samples were all more dense and more viscous than any of the Portland samples. Well B3 contained the most viscous tar, while the coal tar was the most dense sample.

Over the temperature range considered, we found that tar densities varied linearly with temperature. Given density at a reference temperature, this relationship can be described by

$$\rho = \rho_r + \beta_1(T - T_r). \tag{4.4}$$

Density data were fit to Equation 4.4 and a least-squares regression resulted in a best fit value for β_1 of -0.00071922 (R^2=0.9972), where T is in Kelvin. The measured versus the predicted values for density are plotted in Figure 4.1 and show excellent agreement between the two.

Viscosity data were initially fit using the Andrade equation and a reference temperature of 20°C (Eqn. 4.3). A plot of the measured viscosity compared to the predicted values is given in Figure 4.2. The equation was unable to capture the complete set of data, particularly at the lowest and highest temperatures considered. Errors in the viscosity ranged from 14% to 45% at 5°C and from 9% to 33% at 70°C.

Table 4.1: Characterization of FMGP tars and a commercial coal tar

	Portland, 2006					Baltimore, 2007	Baltimore, 2009			Coal Tar
	P1	P2	P3	P4	P5	B1	B1	B2	B3	
	MAH and PAH Concentrations (mg/kg)									
1 ring	14.9	21.6	22.5	21.6	21.6	3.5	5.2	5.0	4.7	1.40
2 rings	115	128	164	168	173	150.4	145	134	115	117
3 rings	44.3	44	49	50	50.9	51.3	52	49	31.4	82
4 rings	19.7	19.0	17.7	16.6	16.4	24.0	24.2	22.5	11.1	43
5 rings	7.2	6.0	6.0	5.5	5.0	9.7	10.2	9.5	3.8	17.7
6 rings	3.2	2.7	2.48	2.17	1.84	3.4	3.9	3.7	1.38	6.6
Total	204	222	261	264	268	242	240	223	167	268
Asphltenes, % mass	16.7%	17.0%	13.6%	12.8%	12.5%	16.8%	16.1%	15.2%	23.0%	17.4%
Density at 20°C (g/ml)	1.0666	1.0674	1.0681	1.0611	1.0609	1.0911	1.0869	1.0895	1.1239	1.1632
Viscosity at 20°C (mPa·s)	66.8	58.9	39.4	31.4	27.0	143	146	172	2170	271

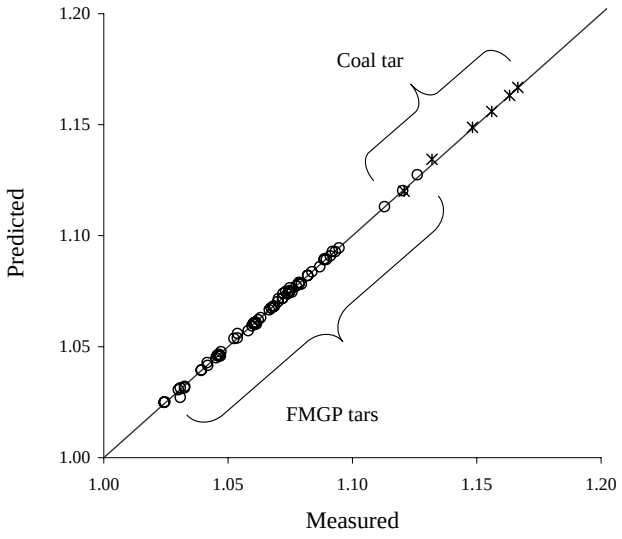

Figure 4.1: Measured compared to predicted density (g/ml), T = 278-343 K

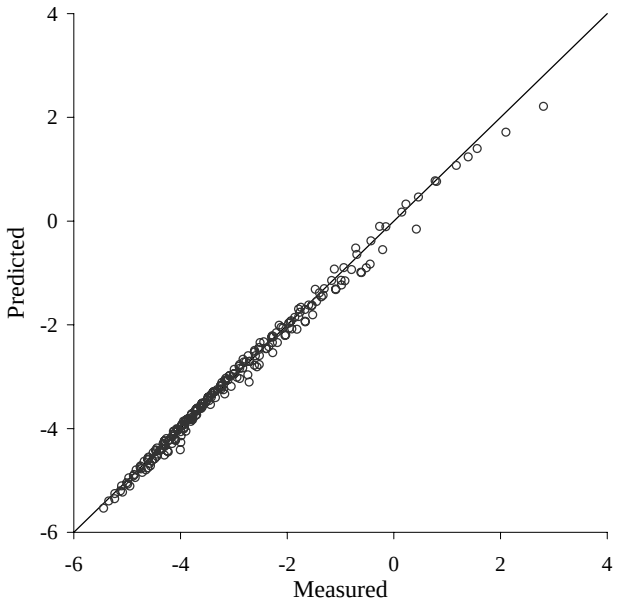

Figure 4.2: Measured compared to predicted natural log viscosity (Pa s) using the Andrade equation, T = 278-343 K

An improved fit to viscosity versus temperature was found by using the Vogel-Fulcher-Tamlen-Hesse (VFTH) equation [109] where

$$\log \eta = A + B\frac{1}{T - C}. \tag{4.5}$$

Specifically, the viscosity data were fit using a reference temperature of 20°C and the following equation

$$\eta = \eta_r \exp\left[B\left(\frac{1}{T - C} - \frac{1}{T_r - C}\right)\right]. \tag{4.6}$$

Unlike the density correlation, which had a single coefficient for all samples, the coefficients required to predict viscosity varied between the samples. A least-squares analysis was used to determine whether or not any additional correlations could be used to predict the coefficients B and C. Correlations were significant when $p<0.05$. C was positively correlated with the density. The viscosity standards had the lowest densities and the lowest values for C. Using a reference temperature of 20°C, C was correlated to density, such that

$$C = 189\rho_r \tag{4.7}$$

where the R^2 was 0.9327. B was found to depend on both sample density and viscosity as

$$B = 1120 - 731\rho_r + 101\eta_r \tag{4.8}$$

where the R^2 was 0.9888.

In Figure 4.3, a plot is provided of measured viscosity compared to predicted using

Equations 4.6, 4.7, and 4.8. In this case, over 85% of the predicted values were within 5% of the measured values. Errors in the viscosity ranged from -4% to 5% at 5°C and from -13% to 13% at 70°C.

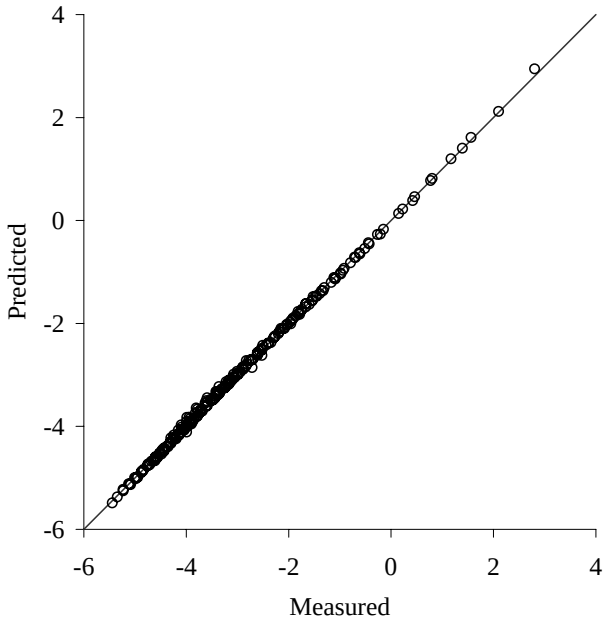

Figure 4.3: Measured compared to predicted natural log viscosity (Pa s) using the VFTH equation, T = 278-343°K

4.5 Discussion

To date, limited data have been published on the variability of FMGP tars spatially and temporally. Though still a relatively small sample size, our data show the importance of characterizing the spatial variability of tars for a given site. We also found that tars from the same well and co-located wells do not vary greatly. This suggests that sampling efforts should focus on delineating the extent of tar contamination and

sampling at locations across tar plumes to better understand the variability of tar at a given site.

Though tar plumes are generally slow moving, many sites are located near water bodies. One might expect tars that have migrated to appear more aged since they presumably have been in the subsurface longer, resulting in higher density and viscosity tars. For tars from the Portland site, we found the tars closest to the water body to be less dense and less viscous than tars located in upland wells. This could be evidence of a change in tar composition with migration distance. Such changes in multi-component NAPL composition are well documented for petroleum migration [83, 78, 85]. Given the complex histories at FMGP sites, more data are needed to better understand whether or not this type of phenomena is possible over the spatial and temporal scales relevant to tar migration.

When modeling the movement of NAPLs, current models assume that viscosity behaves according to the Andrade equation. In Figure 4.4, our relationship is compared to relationships from Kong [77], which were determined over a smaller temperature range and used the Andrade equation. Though Kong [77] found that this relationship was a reasonable approximation over this temperature range, these equations predict a much sharper decrease in viscosity above 50°C compared to using the VFTH equation. At higher temperatures, the VFTH equation predicted that the rate of viscosity reduction decreases as temperature continues to be increased. Understanding this limitation is important for designing efficient thermal remediation approaches.

Thermal treatment can also modify the tar remaining in the subsurface post-

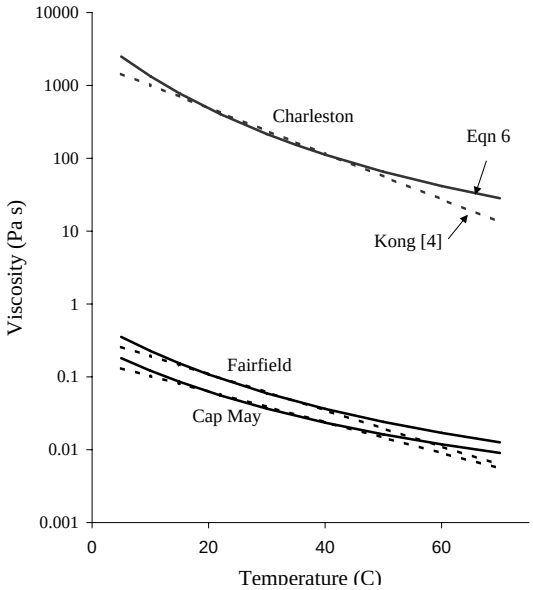

Figure 4.4: Predicted viscosity compared to relationships from Kong [77] for three FMGP tars.

treatment. By potentially stripping the lower molecular weight compounds, tar viscosity can be dramatically increased, decreasing the potential for further migration. Additional work is needed to understand how the composition of tars many be altered during thermal treatment and what temperatures are needed to affect this change.

Tars from FMGP's are likely to continue to persist for many decades to come. Thermal treatment of tars is a means of reducing tar viscosity and increasing the ability to pump tars. The work here provides an improvement over existing relationships between viscosity and temperature that can be used in models to predict tar mobilization. More work is needed to fundamentally understand how viscosity is impacted by tar composition to gain a better mechanistic understanding of the factors affecting tar viscosity.

CHAPTER 5

CONCLUSION

The overall objective of this work has been to conduct research that will lead to more effective and efficient remediation approaches for tars in the subsurface at FMGPs. Tars at FMGPs have received less attention in the scientific literature than other environmentally relevant DNAPLs, despite the large number of contaminated sites and potential impact on human heath and the environment. The research conducted for this dissertation provides a considerable advancement to the understanding of these complex mixtures. A focus of this work has been to improve our knowledge of the factors controlling the fate and distribution of tars at FMGPs and to contribute to the advancement of in-situ remediation technologies. To provide a realistic understanding of these sources, an emphasis has been placed on the use of field samples, rather than using artificially contaminated media or synthetic mixtures of chemicals.

In the course of this research, three papers have been written to complete this dissertation. The first paper was a critical review of the literature that detailed the gaps in our current knowledge that contribute to our limited ability to model the movement of FMGP tars and to develop new remediation techniques. The second paper was a laboratory study that evaluated the use of cosolvent flushing for the remediation of contaminated soil at FMGPs. The third paper characterized tars obtained from two FMGPs and developed equations to predict density and viscosity

as a function of temperature. A summary of the findings from each paper is provided below, along with recommendations for further research.

For the first paper, considerable effort was taken to consolidate and compare data from historical accounts of tar properties and composition. These historic documents provided a wealth of data on how the composition and properties of tars varied over time and were highly dependent on the gas manufacturing process. In more recent literature, FMGP tars are commonly referred to as coal tars, despite the fact that the physical properties of these tars indicate that they are probably water-gas tars. True coal tars contain acidic compounds that are likely to play a key role in affecting interfacial phenomena and are lacking in water-gas tars.

The first paper concluded that significant gaps exist in our fundamental understanding of the environmental processes that govern tar movement and dissolution. Key parameters such as IFT have only been studied for a small number of tar samples that have relatively low density and viscosity. Processes such as dissolution, mass transfer, and biodegradation have yet to be studied for high molecular weight compounds, which are typically risk drivers. One significant hurdle to progress is our continued limitation in understanding the composition of these materials. Our ability to predict relevant environmental properties will likely be greatly enhanced by a more complete understanding of tar composition.

The objective of the second paper was to examine the ability of cosolvent flushing to remediate an aged soil from an FMGP in Salisbury, N.C. This work extended prior cosolvent flushing studies that used 5-cm columns packed with artificially con-

taminated sands. Relationships based on these small-scale systems were unable to predict contaminant behavior in the more complex systems studied here, which used a field sample in column experiments at varying lengths from 15 to 100 cm. In the Salisbury soil, fitted mass transfer rates were two to three orders of magnitude lower than predicted using relationships derived from single-solute systems in artificially contaminated sands.

Compared to using a "pump and treat" approach to remediating a contaminated FMGP soil, cosolvent flushing was able to remove large amounts of contaminant mass in a relatively short time frame; however, further study is needed to better understand the mechanisms controlling the effectiveness of these approaches in the field. In modeling the removal of PAHs during cosolvent flushing, the consistent deviation of NAP from trends that held for other PAHs points to a need for a better understanding of tar aging. In addition, this work was limited to one-dimensional systems. It has been shown that remediation efficiency typically decreases with increasing scale and dimensionality [145]. Further studies should consider two- and three-dimensional systems.

The objective of the third paper was to develop relationships for predicting the density and viscosity of FMGP tars as a function of temperature. Though the understanding that viscosity decreases with temperature is a well-known phenomena, little data were available in the literature to confirm the exact relationship for tars. This work confirmed that the relationship between viscosity and temperature for these complex mixtures did not conform to the Andrade equation that is typically assumed

in modeling environmental systems. Rather, the VFTH equation was found to provide a good fit to experimental data. The equations developed here will be useful for modeling the removal of tars due to thermal treatment.

Future work is needed to better understand the effectiveness of thermal treatment in the field. This type of treatment can certainly aid in the removal of tars by decreasing viscosity, but a potential negative side effect is that subsurface zones that were not previously contaminated could become coated with tar residual. Removing heavily contaminated tar zones could also increase the permeability through source zones, increasing downgradient aqueous-phase concentrations. Future work is also needed to expand the temperature range considered to allow for prediction of removal at temperatures above 70°C. The cone and plate configuration used in this work has a limited temperature range, but other rheological apparatus, such as a concentric cylinder, can be used to expand this range.

This work also concluded that tar composition and properties varied considerably across a given site. In one case, this was likely a function of changes in the source of the tar or the process used to generate gas, which varied over the lifetime of many sites. In another case, the tar is believed to be moving in the subsurface and changes in the tar suggest a chromatographic separation within the tar phase. Regardless of whether or not the variability in tars is a function of the complex site history or a function of changes during tar migration, it is clear that tar plumes need to be delineated to the extent possible, not only to determine the boundary of the plume, but also to determine the compositional changes throughout the plume that may

impact tar mobility.

Tars from FMGPs are likely to persist for many decades, if not centuries, to come. A classic example is the FMGP in Stroudsburg, NC. From 1982 to 2001, this site was on EPA's National Priorities List of the nations most contaminated sites. In 2007, a new tar seep was found in McMichael Creek, prompting additional remedial actions. Clearly, there is a need for FMGPs to be monitored and remediated, particularly when there is a potential for off-site tar migration. Although the research conducted for this dissertation makes several important contributions to this field, additional work is needed to further our understanding of these complex mixtures. Ultimately, models are required that can aid decision-makers in assessing and eliminating the risk of these chemicals in the environment through new remediation approaches.

BIBLIOGRAPHY

[1] H. Abraham. Determination of bituminous substances including asphalts tars and pitches. In W. W. Scott, editor, *Standard methods of chemical analysis: A manual analytical methods and general reference for the analytical chemist and for the advanced student*, volume II, pages 1289–1327. D. Van Norstrand Company, New York, 1922.

[2] Herbert Abraham. *Asphalts and allied substances: Their occurrence, modes of production, uses in the arts, and methods of testing*, volume 2 of *Industrial Raw Materials*. Van Nostrand, Princeton, N.J., 1961.

[3] W.G. Adam. *Coal tar distillation and its products and gas liquor and ammonium sulphate*, volume 12 of *Modern Science Memoirs*. John Murray, London, 1932.

[4] H. Alboudwarej, J. Beck, W. Y. Svrcek, H. W. Yarranton, and K. Akbarzadeh. Sensitivity of asphaltene properties to separation techniques. *Energy & Fuels*, 16(2):462–469, 2002.

[5] W. M. Alley. Tracking us groundwater – reserves for the future? *Environment*, 48(3):10–25, 2006.

[6] W. M. Alley, T. E. Reilly, and O. L. Franke. Sustainabiliy of ground-water resources. Technical report, U.S. Geological Survey Circular 1186, 1999.

[7] American Gas Association. *Gas engineers handbook; fuel gas engineering practices*. Industrial Press, New York, NY, 1965.

[8] ASTM. Standard test method for pH of soils, D4972–01. In *Annual Book of ASTM Standards*, volume 4.08. American Society for Testing and Materials, Philadelphia, PA, 2001.

[9] ASTM. Standard test method for particle-size analysis of soils, D422–63. In *Annual Book of ASTM Standards*, volume 4.08, pages 10–17. American Society for Testing and Materials, Philadelphia, PA, 1999.

[10] ASTM. Standard test method for laboratory determination of water (moisture) content of soil and rock by mass, D2216–98. In *Annual Book of ASTM Standards*, volume 4.08, pages 190–194. American Society for Testing and Materials, Philadelphia, PA, 1999.

[11] ASTM. Standard test method for specific gravity of soil solids by water pycnometer, D854–92. In *Annual Book of ASTM Standards*, volume 4.08. American Society for Testing and Materials, Philadelphia, PA, 1999.

[12] D. C. M. Augustijn, R. E. Jessup, P. S. C. Rao, and A. L. Wood. Remediation of contaminated soils by solvent flushing. *Journal of Environmental Engineering*, 120(1):42–57, 1994.

[13] C. Bakermans, A. M. Hohnstock-Ashe, S. Padmanabhan, P. Padmanabhan, and E. L. Madsen. Geochemical and physiological evidence for mixed aerobic and anaerobic field biodegradation of coal tar waste by subsurface microbial communities. *Microbial Ecology*, 44(2):107–117, 2002.

[14] S. M. Bamforth and I. Singleton. Bioremediation of polycyclic aromatic hydrocarbons: current knowledge and future directions. *Journal of Chemical Technology and Biotechnology*, 80(7):723–736, 2005.

[15] F. T. Barranco and H. E. Dawson. Influence of aqueous ph on the interfacial properties of coal tar. *Environmental Science & Technology*, 33(10):1598–1603, 1999.

[16] T. P. Bastow, B. G. K. van Aarssen, G. E. Chidlow, R. Alexander, and R. I. Kagi. Small-scale and rapid quantitative analysis of phenols and carbazoles in sedimentary matter. *Organic Geochemistry*, 34(8):1113–1127, 2003.

[17] J. Bear. *Dynamics of Fluids in Porous Media*. Dover Publications, Inc., New York, 1972.

[18] P. S. Birak and C. T. Miller. Dense non-aqueous phase liquids at former manufactured gas plants: Challenges to modeling and remediation. *Journal of Contaminant Hydrology*, 105(3–4):81–172, 2009.

[19] D. C. Bouchard. Cosolvent effects on sorption isotherm linearity. *Journal of Contaminant Hydrology*, 56(3-4):159–174, 2002.

[20] D. C. Bouchard. Sorption kinetics of PAHs in methanol-water systems. *Journal of Contaminant Hydrology*, 34(1-2):107–120, 1998.

[21] P. P. Brahma and T. C. Harmon. The effect of multicomponent diffusion on NAPL dissolution from spherical ternary mixtures. *Journal of Contaminant Hydrology*, 67(1-4):43–60, 2003.

[22] D. G. Brown, L. Gupta, H. K. Horace, and A. J. Coleman. Raoult's law-based method for determination of coal tar average molecular weight. *Environmental Toxicology and Chemistry*, 24(8):1886–1892, 2005.

[23] D. G. Brown, L. Gupta, T. H. Kim, H. K. Moo-Young, and A. J. Coleman. Comparative assessment of coal tars obtained from 10 former manufactured gas plant sites in the eastern United States. *Chemosphere*, 65(9):1562–1569, 2006.

[24] R.L. Brown and R.D. Howard. Indene and styrene – constituents of carbureted water-gas tar. *Ind. Eng. Chem.*, 15(11):1147, 1923.

[25] M. L. Brusseau, A. L. Wood, and P. S. C. Rao. Influence of organic cosolvents on the sorption kinetics of hydrophobic organic chemicals. *Environmental Science & Technology*, 25(5):903–910, 1991.

[26] J. S. Buckley and J. X. Wang. Crude oil and asphaltene characterization for prediction of wetting alteration. *Journal of Petroleum Science and Engineering*, 33(1-3):195–202, 2002.

[27] C.J. Castaneda. *Invisible fuel : manufactured and natural gas in America, 1800-2000*. Twayne's evolution of modern business series. Twayne, New York, 1999.

[28] Carl E. Cerniglia. Biodegradation of polycyclic aromatic hydrocarbons. *Biodegradation*, 3:351–368, 1992.

[29] C. S. Chen, P. S. C. Rao, and J. J. Delfino. Oxygenated fuel induced cosolvent effects on the dissolution of polynuclear aromatic hydrocarbons from contaminated soil. *Chemosphere*, 60(11):1572–1582, 2005.

[30] Conservation Foundation, National Groundwater Policy Forum. Groundwater protection. Technical report, Conservation Foundation, Washington, D. C., 1987.

[31] A. T. Corey. *Mechanics of immiscible fluids in porous media*. Water Resources Publications, Highlands Ranch, CO, 3rd edition, 1994.

[32] Fernando M. D'Affonseca, Philipp Blum, Michael Finkel, Reiner Melzer, and Peter Grathwohl. Field scale characterization and modeling of contaminant release from a coal tar source zone. *Journal of Contaminant Hydrology*, 102 (1-2):120–139, 2008.

[33] J. F. Dong, B. Chowdhry, and S. Leharne. Investigation of the wetting behavior of coal tar in three phase systems and its modification by poloxamine block copolymeric surfactants. *Environmental Science & Technology*, 38(2):594–602, 2004.

[34] C. R. Downs and A. L. Dean. Study of the composition of water gas tar. *Ind. Eng. Chem.*, 6(5):366–370, 1914.

[35] C. Drummond and J. Israelachvili. Fundamental studies of crude oil-surface water interactions and its relationship to reservoir wettability. *Journal of Petroleum Science and Engineering*, 45(1-2):61–81, 2004.

[36] S. T. Dubey and P. H. Doe. Base number and wetting properties of crude oils. *SPE Reservoir Engineering*, 8(3):195–200, 1993.

[37] C. Eberhardt and P. Grathwohl. Time scales of organic contaminant dissolution from complex source zones: coal tar pools vs. blobs. *Journal of Contaminant Hydrology*, 59(1-2):45–66, 2002.

[38] S. Endo and T. C. Schmidt. Prediction of partitioning between complex organic mixtures and water: Application of polyparameter linear free energy relationships. *Environmental Science & Technology*, 40(2):536–545, 2006.

[39] S. Endo, W. J. Xu, K. U. Goss, and T. C. Schmidt. Evaluating coal tar-water partitioning coefficient estimation methods and solute-solvent molecular interactions in tar phase. *Chemosphere*, 73(4):532–538, 2008.

[40] Robert Eng. *Survey of town gas and by-product production and locations in the U.S. (1880-1950)*. Prepared by Radian Corporation. Prepared for U.S. EPA, Air and Energy Engineering Research Laboratory, Research Triangle Park, North Carolina, 1985. EPA 600-7-85-004.

[41] EPRI. *Chemical and physical characteristics of tar samples from selected manufactured gas plant (MGP) sites*. Electric Power Research Institute, Palo Alto, Calif., 1993. TR-102184.

[42] T. G. Fan and J. S. Buckley. Rapid and accurate SARA analysis of medium gravity crude oils. *Energy & Fuels*, 16(6):1571–1575, 2002.

[43] M. W. Farthing and C. T. Miller. A comparison of high-resolution, finite-volume, adaptive-stencil schemes for simulating advective-dispersive transport. *Advances in Water Resources*, 24(1):29–48, 2000.

[44] J. C. Fetzer and J. R. Kershaw. Identification of large polycyclic aromatic-hydrocarbons in a coal-tar pitch. *Fuel*, 74(10):1533–1536, 1995.

[45] M. Fraser, J. F. Barker, B. Butler, F. Blaine, S. Joseph, and C. Cooke. Natural attenuation of a plume from an emplaced coal tar creosote source over 14 years. *Journal of Contaminant Hydrology*, 100(3-4):101–115, 2008.

[46] L. W. Gelhar, C. Welty, and K. R. Rehfeldt. A critical review of data on field-scale dispersion in aquifers. *Water Resources Research*, 28(7):1955–1974, 1992.

[47] J. T. Geller and J. R. Hunt. Mass-transfer from nonaqueous phase organic liquids in water-saturated porous-media. *Water Resources Research*, 29(4):833–845, 1993.

[48] S. Ghoshal, A. Ramaswami, and R. G. Luthy. Biodegradation of naphthalene from coal tar and heptamethylnonane in mixed batch systems. *Environmental Science & Technology*, 30(4):1282–1291, 1996.

[49] S. W. Giese and S. E. Powers. Using polymer solutions to enhance recovery of mobile coal tar and creosote DNAPLs. *Journal of Contaminant Hydrology*, 58 (1-2):147–167, 2002.

[50] B Gonzalez, N. Calvar, E. Gomez, and A. Dominguez. Density, dynamic viscosity, and derived properties of binary mixtures of methanol or ethanol with water, ethyl acetate, and methyl acetate at t = (293.15, 298.15, and 303.15) k. *J. of Chem. Thermodynamics*, 39:1578–1588, 2007.

[51] J. W. Goodwin and R. W. Hughes. *Rheology for Chemists*. The Royal Society of Chemistry, Cambridge, 2000.

[52] GRI. *Wastes and Chemicals of Interest*, volume 1 of *Management of manufactured gas plant sites*. Gas Research Institute, Chicago, Ill., 1987.

[53] F. Haeseler, D. Blanchet, V. Druelle, P. Werner, and J. P. Vandecasteele. Analytical characterization of contaminated soils from former manufactured gas plants. *Environmental Science & Technology*, 33(6):825–830, 1999.

[54] M. J. Hamper. Manufactured gas history and processes. *Environmental Forensics*, 7(1):55–64, 2006.

[55] W.E Hanson. Nomenclature and terms. In A.J. Hoiberg, editor, *Bituminous materials: asphalts, tars, and pitches*, volume 1 of *Asphalts Tars and Pitches*, pages 1–24. Interscience Publishers, New York, 1964.

[56] S. L. Harden, M. J. Chapman, and D. A. Harned. Characterization of groundwater quality based on a regional geologic setting in the Piedmont and Blue Ridge Physiographic Provinces, North Carolina. Technical Report 2009-5149, U.S. Geological Survey, 2009.

[57] S. M. Harkins, R. S. Truesdale, R. Hill, P. Hoffman, and S. Winters. *U.S. Production of Manufactured Gases: Assessment of Past Disposal Practices*. Prepared by Research Triangle Institute. Prepared for Hazardous Waste Engineering Research Laboratory, U.S. Environmental Protection Agency, Cincinnati, OH, 1988. EPA 600-2-88-012.

[58] T. C. Harmon, T. J. Kim, B. K. Dela Barre, and C. V. Chrysikopoulos. Cosolvent-water displacement in one-dimensional soil column. *Journal of Environmental Engineering-Asce*, 125(1):87–91, 1999.

[59] A. W. Hatheway. Estimated number of manufactured gas and other coal-tar sites in the United States. *Environmental & Engineering Geoscience*, 3(1):141–142, 1997.

[60] A. W. Hatheway. Geoenvironmental protocol for site and waste characterization of former manufactured gas plants; worldwide remediation challenge in semivolatile organic wastes. *Engineering Geology*, 64(4):317–338, 2002.

[61] P. V. Hemmingsen, A. Silset, A. Hannisdal, and J. Sjoblom. Emulsions of heavy crude oils. I: Influence of viscosity, temperature, and dilution. *Journal of Dispersion Science and Technology*, 26(5):615–627, 2005.

[62] S. E. Herbes. Rates of microbial transformation of polycyclic aromatic-hydrocarbons in water and sediments in the vicinity of a coal-coking waste-water discharge. *Applied and Environmental Microbiology*, 41(1):20–28, 1981.

[63] E. H. Hill, M. Moutier, J. Alfaro, and C. T. Miller. Remediation of dnapl pools using dense brine barrier strategies. *Environmental Science & Technology*, 35 (14):3031–3039, 2001.

[64] H. Y. N. Holman and I. Javandel. Evaluation of transient dissolution of slightly water-soluble compounds from a light nonaqueous phase liquid pool. *Water Resources Research*, 32(4):915–923, 1996.

[65] D. A. Hugaboom and S. E. Powers. Recovery of coal tar and creosote from porous media: The influence of wettability. *Ground Water Monitoring and Remediation*, 22(4):83–90, 2002.

[66] P. T. Imhoff, P. R. Jaffe, and G. F. Pinder. An experimental-study of complete dissolution of a nonaqueous phase liquid in saturated porous-media. *Water Resources Research*, 30(2):307–320, 1994.

[67] P. T. Imhoff, S. N. Gleyzer, J. F. McBride, L. A. Vancho, I. Okuda, and C. T. Miller. Cosolvent enhanced remediation of residual reuse nonaqueous phase liquids - experimental investigation. *Environmental Science & Technology*, 29 (8):1966–1976, 1995.

[68] R. E. Jackson, V. Dwarakanath, J. E. Ewing, and J. Avis. Migration of viscous non-aqueous phase liquids (NAPLs) in alluvium, Fraser River lowlands, British Columbia. *Canadian Geotechnical Journal*, 43(7):694–703, 2006.

[69] S. S. Johansen, A. B. Hansen, and H. Mosbaek. Method development for trace analysis of heteroaromatic compounds in contaminated groundwater. *Journal of Chromatography A*, 738(2):295–304, 1996.

[70] D. N. Johnson, J. A. Pedit, and C. T. Miller. Efficient, near-complete removal of dnapl from three-dimensional, heterogeneous porous media using a novel combination of treatment technologies. *Environmental Science & Technology*, 38(19):5149–5156, 2004.

[71] J. C. Johnson, S. B. Sun, and P. R. Jaffe. Surfactant enhanced perchloroethylene dissolution in porous media: The effect on mass transfer rate coefficients. *Environmental Science & Technology*, 33(8):1286–1292, 1999.

[72] Jr. Johnson, L. A. and L. J. Fahy. *In situ treatment of manufactured gas plant contaminated soils demonstration program*, volume DOE/MC/30127–5783. U.S. Department of Energy, 1997.

[73] W. P. Johnson and W. W. John. Pce solubilization and mobilization by commercial humic acid. *Journal of Contaminant Hydrology*, 35(4):343–362, 1999.

[74] A. M. Kharrat, J. Zacharia, V. J. Cherian, and A. Anyatonwu. Issues with comparing SARA methodologies. *Energy & Fuels*, 21(6):3618–3621, 2007.

[75] J. J. Kilbane. Extractability and subsequent biodegradation of PAHs from contaminated soil. *Water Air and Soil Pollution*, 104(3–4):285–304, 1998.

[76] T. J. Kim and C. V. Chrysikopoulos. Mass transfer correlations for nonaqueous phase liquid pool dissolution in saturated porous media. *Water Resources Research*, 35(2):449–459, 1999.

[77] L. Kong. Characterization of mineral oil, coal tar and soil properties and investigation of mechanisms that affect coal tar entrapment in and removal from porous media. 2004.

[78] S. R. Larter, B. F. J. Bowler, M. Li, M. Chen, D. Brincat, B. Bennett, K. Noke, P. Donohoe, D. Simmons, M. Kohnen, J. Allan, N. Telnaes, and I. Horstad. Molecular indicators of secondary oil migration distances. *Nature*, 383(6601): 593–597, 1996.

[79] S. R. Larter, B. F. J. Bowler, M. Li, M. Chen, D. Brincat, B. Bennett, K. Noke, P. Donohoe, D. Simmons, M. Kohnen, J. Allan, N. Telnaes, and I. Horstad. Molecular indicators of secondary oil migration distances. *Nature*, 383(6601): 593–597, 1996.

[80] K. Y. Lee. Modeling long-term transport of contaminants resulting from dissolution of a coal tar pool in saturated porous media. *Journal of Environmental Engineering-ASCE*, 130(12):1507–1513, 2004.

[81] L. S. Lee, P. S. C. Rao, and I. Okuda. Equilibrium partitioning of polycyclic aromatic-hydrocarbons from coal-tar into water. *Environmental Science & Technology*, 26(11):2110–2115, 1992.

[82] M. Li, S. R. Larter, and D. Stoddart. Liquid chromatographic separation schemes for pyrrole and pyridine nitrogen aromatic heterocycle fractions from crude oils suitable for rapid characterization of geochemical samples. *Analytical Chemistry*, 64:7337–1344, 1992.

[83] M. Li, S. R. Larter, and Y. B. Frolov. Adsorptive interactions between petroleum nitrogen compounds and organic/mineral phases in subsurface rocks as models for compositional fractionation of pyrrolic nitrogen compounds in petroleum during petroleum migration. *Journal of high resolution chromatography*, 17:203–236, 1994.

[84] M. Li, S. R. Larter, and Y. B. Frolov. Adsorptive interactions between petroleum nitrogen compounds and organic/mineral phases in subsurface rocks as models for compositional fractionation of pyrrolic nitrogen compounds in petroleum during petroleum migration. *Journal of high resolution chromatography*, 17:203–236, 1994.

[85] M. Li, H. Yao, L. D. Stasiuk, M. G. Fowler, and S. R. Larter. Effect of maturity and petroleum expulsion on pyrrolic nitrogen compound yields and distributions in duvernay formation petroleum source rocks in central alberta, canada. *Organic Geochemistry*, 26(11-12):731–744, 1997.

[86] M. Li, H. Yao, L. D. Stasiuk, M. G. Fowler, and S. R. Larter. Effect of maturity and petroleum expulsion on pyrrolic nitrogen compound yields and distributions in duvernay formation petroleum source rocks in central alberta, canada. *Organic Geochemistry*, 26(11-12):731–744, 1997.

[87] X. K. Li and O. T. Li. Rheological properties and carbonization of coal-tar pitch. *Fuel*, 75(1):3–7, 1996.

[88] James W. Lingle and Kevin L. Brehm. Application of source removal and natural attenuation remediation strategies at mgp sites in wisconsin. *Remediation Journal*, 13(4):29–39, 2003.

[89] L. H. Liu, S. Endo, C. Eberhardt, P. Grathwohl, and T. C. Schmidt. Partition behavior of polycyclic aromatic hydrocarbons between aged coal tar and water. *Environmental Toxicology and Chemistry*, 28(8):1578–1584, 2009.

[90] J. T. Londergan, H. W. Meinardus, P. E. Mariner, R. E. Jackson, C. L. Brown, V. Dwarakanath, G. A. Pope, J. S. Ginn, and S. Taffinder. Dnapl removal from a heterogeneous alluvial aquifer by surfactant-enhanced aquifer remediation. *Ground Water Monitoring and Remediation*, 21(4):57–67, 2001.

[91] M. T. Lukasewycz and L. P. Burkhard. Complete elimination of carbonates: A critical step in the accurate measurement of organic and black carbon in sediments. *Environmental Toxicology and Chemistry*, 24(9):2218–2221, 2005.

[92] G. Lunge. *Coal-tar and ammonia*. Gurney and Jackson, London, 1916.

[93] R. G. Luthy, A. Ramaswami, S. Ghoshal, and W. Merkel. Interfacial films in coal-tar nonaqueous-phase liquid water-systems. *Environmental Science & Technology*, 27(13):2914–2918, 1993.

[94] R. G. Luthy, D. A. Dzombak, C. A. Peters, S. B. Roy, A. Ramaswami, D. V. Nakles, and B. R. Nott. Remediating tar-contaminated soils at manufactured gas plant sites. *Environmental Science & Technology*, 28(6):266A–276A, 1994.

[95] R. G. Luthy, D. A. Dzombak, C. A. Peters, S. B. Roy, A. Ramaswami, D. V. Nakles, and B. R. Nott. Remediating tar-contaminated soils at manufactured-gas plant sites. *Environmental Science & Technology*, 28(6):A266–A276, 1994.

[96] C Mack. Phyiscal chemistry. In A.J. Hoiberg, editor, *Bituminous materials: asphalts, tars, and pitches*, volume 1 of *Asphalts Tars and Pitches*, pages 25–121. Interscience Publishers, New York, 1964.

[97] A. A. MacKay and P. M. Gschwend. Enhanced concentrations of PAHs in groundwater at a coal tar site. *Environmental Science & Technology*, 35(7): 1320–1328, 2001.

[98] L. K. MacKinnon and N. R. Thomson. Laboratory-scale in situ chemical oxidation of a perchloroethylene pool using permanganate. *Journal of Contaminant Hydrology*, 56(1-2):49–74, 2002.

[99] Alex Mayer and S. Majid Hassanizadeh. *Soil and groundwater contamination: nonaqueous phase liquids*. Water resources monograph, 17. American Geophysical Union, Washington, D.C., 2005.

[100] T. F. McGowan, B. A. Greer, and M. Lawless. Thermal treatment and non-thermal technologies for remediation of manufactured gas plant sites. *Waste Management*, 16(8):691–698, 1996.

[101] D. McNeil. The physical properties and chemical structure of coal tar pitch. In A.J. Hoiberg, editor, *Bituminous materials: asphalts, tars, and pitches*, volume 1 of *Asphalts Tars and Pitches*, pages 139–216. Interscience Publishers, New York, 1964.

[102] C. T. Miller, M. M. Poirier-McNeill, and A. S. Mayer. Dissolution of trapped nonaqueous phase liquids: Mass transfer characteristics. *Water Resources Research*, 26(11):2783–2796, 1990.

[103] C. T. Miller, G. Christakos, P. T. Imhoff, J. F. McBride, J. A. Pedit, and J. A. Trangenstein. Multiphase flow and transport modeling in heterogeneous porous media: challenges and approaches. *Advances in Water Resources*, 21(2):77–120, 1998.

[104] T.J. Morgan, A. George, D.B. Davis, A.A. Herod, and R. Kandiyoti. Optimization of 1H and 13C NMR methods for structural characterization of acetone and pyridine soluble/insoluble fractions of a coal tar pitch. *Energy Fuels*, 22 (3):1824–1835, 2008.

[105] N. R. Morrow. Capillary-pressure correlations for uniformly wetted porous-media. *J. Can. Pet. Technol.*, 15(4):49–69, 1976.

[106] J.G. Mueller, P.J. Chapman, and P.H. Pritchard. Creosote-contaminated sites: Their potential for bioremediation. *Environmental Science & Technology*, 23 (10):1197–1201, 1989.

[107] S. Mukherji, C. A. Peters, and W. J. Weber. Mass transfer of polynuclear aromatic hydrocarbons from complex DNAPL mixtures. *Environmental Science & Technology*, 31(2):416–423, 1997.

[108] B. L. Murphy, T. Sparacio, and W. J. Shields. Manufactured gas plants – processes, historical development, and key issues in insurance coverage disputes. *Environmental Forensics*, 6(2):161–173, 2005.

[109] M.L.F. Nascimento and C. Aparicio. Data classification with the Vogel-Fulcher-Tammann-Hesse viscosity equation using correspondence analysis. *Physica B-Condensed Matter*, 398(1):71–77, 2007.

[110] E. C. Nelson, S. Ghoshal, J. C. Edwards, G. X. Marsh, and R. G. Luthy. Chemical characterization of coal tar-water interfacial films. *Environmental Science & Technology*, 30(3):1014–1022, 1996.

[111] NIOSH. *Criteria for a Recommended Standard: Occupational Exposure to Coal Tar Products*. U.S. Dept. of Health, Education, and Welfare, Public Health Service; Center for Disease Control; National Institute for Occupational Safety and Health, Cincinnati, 1977.

[112] NIST. *Certificate of Analysis, Standard Reference Material 1597a, Complex Mixture of Polycyclic Aromatic Hydrocarbons from Coal Tar*. National Institute of Standards & Technology, Gaithersburg, MD, 2006. Publication No. 78-107.

[113] M. Novotny, J. W. Strand, S. L. Smith, D. Wiesler, and F. J. Schwende. Compositional studies of coal-tar by capillary gas chromatography-mass spectrometry. *Fuel*, 60(3):213–220, 1981.

[114] NRC. *Contaminants in the subsurface: Source zone assessment and remediation*. National Research Council, Committee on Source Removal of Contaminants in the Subsurface, National Academies Press, Washington, D.C., 2005.

[115] D. M. O'Carroll and B. E. Sleep. Hot water flushing for immiscible displacement of a viscous NAPL. *Journal of Contaminant Hydrology*, 91(3-4):247–266, 2007.

[116] C. Pan, E. Dalla, D. Franzosi, and C. T. Miller. Pore-scale simulation of entrapped non-aqueous phase liquid dissolution. *Advances in Water Resources*, 30(3):623–640, 2007.

[117] W. E. Pereira, C. E. Rostad, J. R. Garrbarino, and M. F. Hult. Groundwater contamination by organic bases derived from coal-tar wastes. *Environmental Toxicology and Chemistry*, 2:283–294, 1983.

[118] C. A. Peters and R. G. Luthy. Coal-tar dissolution in water-miscible solvents: Experimental evaluation. *Environmental Science & Technology*, 27(13):2831–2843, 1993.

[119] C. A. Peters and R. G. Luthy. Coal tar dissolution in water-miscible solvents: Experimental evaluation. *Environmental Science & Technology*, 27:2831–2843, 1993.

[120] C. A. Peters and R. G. Luthy. Semiempirical thermodynamic modeling of liquid-liquid phase equilibria: Coal tar dissolution in water-miscible solvents. *Environmental Science & Technology*, 28(7):1331–1340, 1994.

[121] C. A. Peters, S. Mukherji, C. D. Knightes, and J. W. J. Weber. Phase stability of multicomponent NAPLs containing PAHs. *Environmental Science & Technology*, 31(9):2540–2546, 1997.

[122] C. A. Peters, S. Mukherji, C. D. Knightes, and W. J. Weber. Phase stability of multicomponent NAPLs containing PAHs. *Environmental Science & Technology*, 31(9):2540–2546, 1997.

[123] C. A. Peters, C. D. Knightes, and D. G. Brown. Long-term composition dynamics of PAH-containing NAPLs and implications for risk assessment. *Environmental Science & Technology*, 33(24):4499–4507, 1999.

[124] C. A. Peters, S. Mukherji, and W. J. Weber. UNIFAC modeling of multicomponent nonaqueous phase liquids containing polycyclic aromatic hydrocarbons. *Environmental Toxicology and Chemistry*, 18(3):426–429, 1999.

[125] C. A. Peters, K. H. Wammer, and C. D. Knightes. Multicomponent NAPL solidification thermodynamics. *Transport in Porous Media*, 38(1-2):57–77, 2000.

[126] P.F. Phelan and E.O Rhodes. Road tars and tar paving. In A.J. Hoiberg, editor, *Bituminous materials: asphalts, tars, and pitches*, volume 3 of *Coal Tars and Pitches*, pages 411–531. Interscience Publishers, New York, 1966.

[127] H. C. Porter. *Coal Carbonization*. American Chemical Society Monograph Series. J. J. Little & Ives Company, New York, 1924.

[128] D. L. Poster, M. M. Schantz, L. C. Sander, and S. A. Wise. Analysis of polycyclic aromatic hydrocarbons (PAHs) in environmental samples: a critical review of gas chromatographic (GC) methods. *Analytical and Bioanalytical Chemistry*, 386(4):859–881, 2006.

[129] S. E. Powers, L. M. Abriola, and Jr. Weber, W. J. An experimental investigation of nonaqueous phase liquid dissolution in saturated subsurface systems: transient mass transfer rates. *Water Resources Research*, 30(2):321–332, 1994.

[130] S. E. Powers, W. H. Anckner, and T. F. Seacord. Wettability of NAPL-contaminated sands. *Journal of Environmental Engineering - ASCE*, 122(10): 889–896, 1996.

[131] Reservoir Engineering Research Program. UTCHEM-9.0, A three-dimensional chemical flood simulator. Volume II: Technical documentation. Technical report, Reservoir Engineering Research Program,Center for Petroleum and Geosystems Engineering,The University of Texas at Austin, Austin, Texas, 2000.

[132] A. Ramaswami, S. Ghoshal, and R. G. Luthy. Mass transfer and biodegradation of PAH compounds from coal tar. *Water Science and Technology*, 30(7):61–70, 1994.

[133] A. Ramaswami, S. Ghoshal, and R. G. Luthy. Mass transfer and bioavailability of PAH compounds in coal tar NAPL-slurry systems. 2. experimental evaluations. *Environmental Science & Technology*, 31(8):2268–2276, 1997.

[134] A. Ramaswami, P. K. Johansen, M. Isleyen, A. R. Bielefeldt, and T. Illangasekare. Assessing multicomponent DNAPL biostabilization. I: Coal tar. *Journal of Environmental Engineering-ASCE*, 127(12):1065–1072, 2001.

[135] P. S. Rao, L. S. Lee, and R. Pinal. Cosolvency and sorption of hydrophobic organic chemicals. *Environmental Science & Technology*, 24(5):647–654, 1990.

[136] E.O Rhodes. The chemical nature of coal tar. In H.H. Lowry, editor, *Chemistry of coal utilization*, volume 2, pages 1287–1370. John Wiley & Sons, New York, 1945. (U.S.).

[137] E.O Rhodes. The history of coal tar and light oil. In A.J. Hoiberg, editor, *Bituminous materials: asphalts, tars, and pitches*, volume 3 of *Coal Tars and Pitches*, pages 1–31. Interscience Publishers, New York, 1966.

[138] E.O Rhodes. Water-gas tars and oil-gas tars. In A.J. Hoiberg, editor, *Bituminous materials: asphalts, tars, and pitches*, volume 3 of *Coal Tars and Pitches*, pages 33–55. Interscience Publishers, New York, 1966.

[139] S. D. Richardson, B. L. Lebron, C. T. Miller, and M. D. Aitken. Recovery of phenanthrene-degrading bacteria after simulated in situ persulfate oxidation in contaminated soil. *Environmental Science & Technology*, 45(2):719–725, 2011.

[140] S. B. Roy, D. A. Dzombak, and M. A. Ali. Assessment of in situ solvent extraction for remediation of coal tar sites: Column studies. *Water Environment Research*, 67(1):4–15, 1995.

[141] J. Schaerlaekens, J. Vanderborght, R. Merckx, and J. Feyen. Surfactant enhanced solubilization of residual trichloroethene: an experimental and numerical analysis. *Journal of Contaminant Hydrology*, 46(1-2):1–16, 2000.

[142] B. Schmid and J. T. Andersson. Critical examination of the quantification of aromatic compounds in three standard reference materials. *Analytical Chemistry*, 69(17):3476–3481, 1997.

[143] M. Schnarr, C. Truax, G. Farquhar, E. Hood, T. Gonullu, and B. Stickney. Laboratory and controlled field experiments using potassium permanganate to remediate trichloroethylene and perchloroethylene dnapls in porous media. *Journal of Contaminant Hydrology*, 29(3):205–224, 1998.

[144] R. P. Schwarzenbach, P. M. Gschwend, and D. M. Imboden. *Environmental Organic Chemistry*. John Wiley & Sons, Inc., Hoboken, New Jersey, 2003.

[145] K. Soga, J. W. E. Page, and T. H. Illangasekare. A review of NAPL source zone remediation efficiency and the mass flux approach. *Journal of Hazardous Materials*, 110(1–3):13–27, 2004.

[146] J. G. Speight. Petroleum asphaltenes part 1: Asphaltenes, resins and the structure of petroleum. *Oil & Gas Science and Technology*, 59(5):467–477, 2004.

[147] J. G. Speight. The chemical and physical structure of petroleum: effects on recovery operations. *Journal of Petroleum Science and Engineering*, 22(1-3): 3–15, 1999.

[148] J. G. Speight, R. B. Long, and T. D. Trowbridge. Factors influencing the separation of asphaltenes from heavy petroleum feedstocks. *Fuel*, 63:616–620, 1984.

[149] Paul Taylor, Steve Larter, Martin Jones, Jason Dale, and Idar Horstad. The effect of oil-water-rock partitioning on the occurrence of alkylphenols in petroleum systems. *Geochimica et Cosmochimica Acta*, 61(9):1899–1910, 1997.

[150] T.E. Thorpe. *A Dictionary of Applied Chemistry*. Longmans Green, London, 1912.

[151] R.N. Traxler. Rheology and rheological modifiers other than elastomers: structure and time. In A.J. Hoiberg, editor, *Bituminous materials: asphalts, tars, and pitches*, volume 1 of *Asphalts Tars and Pitches*, pages 143–211. Interscience Publishers, New York, 1964.

[152] U.S. EPA. Cleaning up the nation's waste sites: Markets and technology trends. Technical Report EPA/542/R-04/015, U.S. Environmental Protection Agency, Cincinnati, OH, 2004.

[153] U.S. EPA. Provisional guidance for quantitative risk assessment of polycyclic aromatic hydrocarbons. Technical Report EPA/600/R-93/089, U.S. Environmental Protection Agency, Washington, D. C., 1993.

[154] U.S. EPA. *Cleaning up the nation's waste sites: markets and technology trends*. United States Environmental Protection Agency, Office of Solid Waste and Emergency Response, Washington, DC, 2004. EPA 542-R-04-015.

[155] U.S. EPA Region 3. Brodhead creek, current site information. 2011. `http://www.epa.gov/reg3hwmd/npl/PAD980691760.htm`.

[156] J. F. Villaume. Coal tar wastes: Their environmental fate and effects. In S. K. Majumdar and E. W. Miller, editors, *Hazardous and Toxic Wastes: Technology, Management, and Health Effects*, pages 362–375. The Pennsylvania Academy of Science, 1984.

[157] J.M. Weiss. Specific gravity–its determination for tars, oils and pitches. *Ind. Eng. Chem.*, 7(1):21–24, 1915.

[158] J.M. Weiss and C. R. Downs. Some of the constituents of coke-oven tar. *Ind. Eng. Chem.*, 15(10):1022–1023, 1923.

[159] A. L. Wood, D. C. Bouchard, M. L. Brusseau, and P. S. Rao. Cosolvent effects on sorption and mobility of organic contaminants in soils. *Chemosphere*, 21 (4-5):575–587, 1990.

[160] W. J. Wu, M. Delshad, T. Oolman, and G. A. Pope. Remedial options for creosote-contaminated sites. *Ground Water Monitoring and Remediation*, 20 (2):78–86, 2000.

[161] X. Xie, N. R. Morrow, and J. S. Buckley. Contact angle hysteresis and the stability of wetting changes induced by adsorption from crude oil. *Journal of Petroleum Science and Engineering*, 33(1-3):147–159, 2002.

[162] S. H. Yalkowsky. Solubility and solubilization of nonelectrolytes; solubilization of drugs by cosolvents. In S. H. Yalkowsky, editor, *Techniques of Solubilization of Drugs*, pages 1–14;91–134. Marcel Dekker, Inc., New York, 1981.

[163] Y.G. Yanovsky, V.K. Zhdanyuk, V.A. Zolotarev, and G.V. Vinogradov. The peculiarities of the rheological behaviour of coal tars. *Rheologica Acta*, 27(3): 298–310, 1988.

[164] D. Zamfirescu and P. Grathwohl. Occurrence and attenuation of specific organic compounds in the groundwater plume at a former gasworks site. *Journal of Contaminant Hydrology*, 53(3-4):407–427, 2001.

[165] M. J. Zhang, S. D. Li, and B. J. Chen. Compositional studies of high-temperature coal-tar by GC/FTIR analysis of light oil fractions. *Chromatographia*, 33(3-4):138–146, 1992.

[166] M. J. Zhang, B. J. Chen, S. D. Shen, and S. Y. Chen. Compositional studies of high-temperature coal tar by g.c.–FT-i.r. analysis of middle oil fractions. *Fuel*, 76(5):415–423, 1997.

[167] J. Z. Zheng and S. E. Powers. Identifying the effect of polar constituents in coal-derived NAPLs on interfacial tension. *Environmental Science & Technology*, 37 (14):3090–3094, 2003.

[168] J. Z. Zheng and S. E. Powers. Organic bases in NAPLs and their impact on wettability. *Journal of Contaminant Hydrology*, 39(1-2):161–181, 1999.

[169] J. Z. Zheng and S. E. Powers. Identifying the effect of polar constituents in coal-derived NAPLs on interfacial tension. *Environmental Science & Technology*, 37 (14):3090–3094, 2003.

[170] J. Z. Zheng, J. H. Shao, and S. E. Powers. Asphaltenes from coal tar and creosote: Their role in reversing the wettability of aquifer systems. *Journal of Colloid and Interface Science*, 244(2):365–371, 2001.